

Fractonic Orders from Lattice Models and Field Theories

Thesis by
Xiuqi Ma

In Partial Fulfillment of the Requirements for the
Degree of
Doctor of Philosophy

The logo for the California Institute of Technology (Caltech), featuring the word "Caltech" in a bold, orange, sans-serif font.

CALIFORNIA INSTITUTE OF TECHNOLOGY
Pasadena, California

2023
Defended May 26, 2023

© 2023

Xiuqi Ma

ORCID: 0000-0001-8294-2277

All rights reserved

ACKNOWLEDGEMENTS

I am immensely grateful to my advisor, Xie Chen, for her guidance and encouragement throughout my PhD life. It has been a great pleasure learning from and collaborating with such an insightful physicist as her.

I would like to thank the members of my thesis defense committee for their support: Jason Alicea, David Hsieh and Yi Ni. I would also like to thank my collaborators for numerous inspirational discussions: Meng Cheng, Michael Hermele, Ho Tat Lam, Michael Levin, Ananth Malladi, John McGreevy, Wilbur Shirley, David Stephen, Zhenghan Wang and Zongyuan Wang.

I am lucky to have enjoyed my time at Caltech with many friends. I deeply appreciate the help, advice and company of all of them, especially: Xiang Li, Sizheng Ma, Bowen Yang, and Yida Li.

Finally, I am indebted forever to my family for making me who I am.

ABSTRACT

Fracton models are characterized by exotic features such as point-like excitations with restricted mobility, sub-extensive ground state degeneracy and UV/IR mixing. They have been studied previously using exactly solvable lattice models, higher rank gauge theories, etc. In an effort to classify fracton models into phases (i.e., fractonic orders), the so-called foliation structure has been introduced and shown to exist in many previously known models. A natural question then arises concerning the feasibility of the foliation paradigm in general. In this thesis, I study fracton models beyond the foliation paradigm and give simple diagnostics for the absence of a foliation structure. New notions of fractonic orders therefore need to be conceived, and I present such a conception which is a generalization of the foliation RG.

In Chapters 2 – 4, I introduce new fracton models obtained from infinite-component Chern-Simons (CS_∞) theories. By calculating observables such as ground state degeneracy and planon braiding statistics, I prove that most CS_∞ theories are not foliated. A CS_∞ theory can also be gapless with certain choices of parameters, and I show that such a theory is a stable gapless fracton model. Furthermore, I discuss topological features of a large subclass of gapless CS_∞ theories and present fully continuous effective field theories for this subclass.

In Chapters 5 – 6, I discuss a new notion of fractonic orders by studying the example of the Ising cage-net model. I begin by calculating the ground state degeneracy of the model, which shows that the model is not foliated. The calculation uses an operator algebra approach which relies only on intrinsic physical properties of the model rather than microscopic details, and I establish the framework of this approach conceptually and via examples. I then argue why this intrinsic approach, despite being a tool for calculation initially, may be a useful characterization of a fractonic order. Finally, I present a generalized foliation RG scheme, apply it to the Ising cage-net model, and discuss its limitations.

PUBLISHED CONTENT AND CONTRIBUTIONS

- [1] X. Chen, H. T. Lam, and X. Ma, “Gapless infinite-component Chern-Simons-Maxwell theories”, arXiv:2211.10458,
X.M. participated in the conception of the project, the theoretical analysis and the writing of the manuscript.
- [2] X. Chen, H. T. Lam, and X. Ma, “Ground state degeneracy of infinite-component Chern-Simons-Maxwell theories”, arXiv:2306.00291,
X.M. participated in the conception of the project, the theoretical analysis and the writing of the manuscript.
- [3] Z. Wang, X. Ma, D. T. Stephen, M. Hermele, and X. Chen, “Renormalization of Ising cage-net model and generalized foliation”, arXiv:2301.00103,
X.M. participated in the theoretical analysis.
- [4] X. Ma, A. Malladi, Z. Wang, Z. Wang, and X. Chen, “Ground state degeneracy of the Ising cage-net model”, Phys. Rev. B **107**, 085123 (2023),
X.M. participated in the conception of the project, the theoretical analysis and the writing of the manuscript.
- [5] X. Ma, W. Shirley, M. Cheng, M. Levin, J. McGreevy, and X. Chen, “Fractonic order in infinite-component Chern-Simons gauge theories”, Phys. Rev. B **105**, 195124 (2022),
X.M. participated in the theoretical analysis and the writing of the manuscript.

TABLE OF CONTENTS

Acknowledgements	iii
Abstract	iv
Published Content and Contributions	v
Table of Contents	v
Chapter 1: Introduction	1
Chapter 2: Periodic Chern-Simons theory	6
2.1 Review of Chern-Simons theory	6
2.2 Polynomial description	8
2.3 GSD: Non-degenerate case	8
2.4 Braiding statistics: Non-degenerate case	10
2.5 GSD: Degenerate case	13
2.6 Fusion group	20
2.7 Appendix: Determining K matrix from statistics	21
Chapter 3: Gapped infinite-component Chern-Simons theory	29
3.1 Foliation RG and foliated theories	30
3.2 Criterion for foliation and non-foliated theories	32
3.3 Lattice construction	36
Chapter 4: Gapless infinite-component Chern-Simons theory	47
4.1 Stability	48
4.2 Exotic one-form symmetry	49
4.3 Observables	54
4.4 Effective field theory	66
Chapter 5: GSD of fracton models: An operator algebra approach	68
5.1 Motivating example: The Ising cage-net model	70
5.2 The chiral Ising anyon model and operator algebra	73
5.3 Structure of semisimple algebra	77
5.4 The doubled Ising anyon model and condensation	79
5.5 The one-foliated Ising cage-net model and Cartan subalgebra	84
5.6 Tackling the Ising cage-net model	90
5.7 Trick or treat?	99
5.8 Appendix: Supplementary mathematics	103
Chapter 6: Generalized foliation	108
6.1 Generalized foliation via condensation	109
6.2 The doubled Ising anyon model and linear-depth circuit	109
6.3 Generalized foliation via planar linear-depth circuit	113
6.4 Feasibility for infinite-component Chern-Simons theory	118
Bibliography	121

Chapter 1

INTRODUCTION

Many-body systems are diverse and often messy. From Fe_3O_4 magnets painted in red and blue that we all played with at school, to superconducting coils buried in MRI machines, to lattice spin models that theorists write down on a piece of paper and hope to exist in reality, by far the most many-body systems are too complicated to understand completely. Nevertheless, certain common, macroscopic features of **classes** of systems can be understood. For example, Fe_3O_4 is ferromagnetic below temperature $T = 858\text{K}$ and paramagnetic above [1]. These two situations are referred to as two *phases* of Fe_3O_4 , and macroscopic magnetic properties of Fe_3O_4 samples in the same phase are the same qualitatively although different quantitatively. In general, two systems are said to be in the same phase if they have the same long-distance effective theory when zoomed sufficiently far out.

The process of zooming out on a system is achieved by the renormalization group (RG), which throws away short-distance details while keeping long-distance features. The result of RG is a flow in the parameter space of the system, and systems in the same phase flow to the same fixed point. For example, Fig. 1.1 shows the RG flow of the $d = 3$ Euclidean space scalar field theory [2]

$$S = \int d^3x \left[\frac{1}{2}(\nabla\phi)^2 + \frac{1}{2}m^2\phi^2 + \lambda\phi^4 \right]. \quad (1.1)$$

This RG flow has two stable fixed points, i.e., the upper infinity corresponding to the paramagnetic phase, and the lower infinity corresponding to the ferromagnetic phase. From this example, the following conclusions (known as *universality*) can be drawn which apply to most systems known to the condensed matter community:

1. The parameter space of a theory has finitely many stable fixed points under the RG flow, which are representatives of different phases.
2. Unless a theory is close to a phase transition, a small change in its parameters does not change which fixed point it flows to and hence its phase.

Universality is the reason why theorists can propose their lattice models, which are hugely simplified compared with the reality, and still be confident that the models can describe the macroscopic properties of Fe_3O_4 magnets or superconducting coils. In particular, Point 2 is also known as *UV/IR separation*. It states that the long-distance (IR) properties of a system are insensitive to short-distance (UV) details. From the perspective of the philosophy of science, UV/IR separation also implies, for

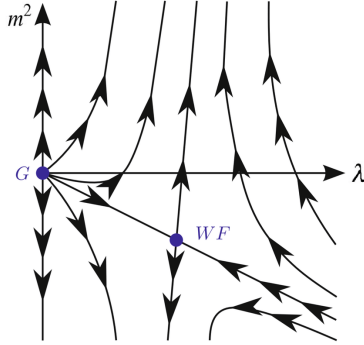


Figure 1.1: RG flow of the $d = 3$ Euclidean space scalar field theory (1.1). G is the Gauss fixed point (unstable), and WF is the Wilson-Fisher critical point (saddle point). Figure taken from Ref. [3].

example, that the study of seismic waves does not rely on and cannot reveal details of the Higgs boson mass in the standard model. This is our common sense.

It was therefore a surprise to the condensed matter community when such common sense was challenged by the discovery of fracton models. The first fracton model, known as the Chamon model, is an exactly solvable lattice spin model in $d = 3 + 1$ introduced in 2005 by Chamon [4] and later studied in detail by Bravyi, Leemhuis and Terhal [5]. This model was found to have some unusual properties. First, when placed on a 3-torus, its ground state degeneracy (GSD) grows exponentially with the linear system size. Equivalently, its GSD grows exponentially as one shrinks the lattice constant while holding the overall physical size of the system fixed. Since the GSD, which is literally the observable of the lowest energy, depends on the UV regulation, this model violates UV/IR separation and exhibits *UV/IR mixing*. Furthermore, the model hosts fractional excitations with restricted mobility, namely *planons*, which can only move within a plane, *lineons*, which can only move along a line, and *fractons*, which are completely immobile. The Chamon model is an example of *type-I* fracton models, where at least some of the fractional excitations have partial mobility.

In 2011, fracton models with even more unusual properties were constructed by Haah, known as the Haah codes [6]. In these models, there is no string-like logical operator, and all fractional excitations are fractons. Four fractons at the corners of a tetrahedron can move together by enlarging or shrinking the tetrahedron, and the creation operator of such a fracton quadrupole has the shape of a fractal (hence the name “fracton”). Due to this fractal geometry of operators, the GSD of a Haah code on a 3-torus fluctuates wildly as a function of the system size inside an exponential envelope [7]. The Haah codes are examples of *type-II* fracton models, where all fractional excitations are immobile.

Over the next few years, interest in fracton models grew in the condensed matter community, and more models were constructed with increasingly systematic methods. In 2016, Vijay, Haah and Fu introduced the X-cube model, a relatively simple exactly solvable model, by applying Wegner’s duality [8] on a plaquette Ising model with planar subsystem symmetries [9]. This duality is now more commonly known as gauging subsystem symmetries, and many more fracton models can be obtained this way [10, 11]. In 2017, Pretko pointed out that the restricted mobility of excitations in fracton models can be understood as a result of higher moment (for example, dipole) conservation laws, which often arise in higher rank gauge theories [12, 13]. It was then shown by Bulmash and Barkeshli [14], and independently by Ma, Hermele, and Chen [15] that certain higher rank gauge theories can give rise to gapped fracton models such as the X-cube model via the Higgs mechanism. Also in 2017, Ma, Lake, Chen and Hermele developed a coupled layer construction of fracton models via particle-loop condensation [16]. This approach was then adopted by Prem, Huang, Song and Hermele to construct the Ising cage-net model, which features intrinsic non-abelian lineons [17]. In 2020, Aasen, Bulmash, Prem, Slagle and Williamson proposed the defect network construction and used it to obtain previously known models such as the X-cube model and the Haah codes in a unified language [18].

The rapid expansion of the reservoir of fracton models calls for a classification of these models into phases, i.e., *fractonic orders*. In other words, an RG scheme for fracton models is needed. Conventional RG schemes are unsatisfactory, because they preserve all low-energy observables such as the GSD, and would therefore put the same fracton model of different system sizes into different phases. Instead, a coarser RG scheme is needed that is able to throw away part of the low-energy physics. It was for this purpose that Shirley, Slagle, Wang and Chen proposed *foliated* fractonic orders in 2018, where the foliation RG is allowed to perform local unitaries as well as add or remove decoupled $d = 2 + 1$ topological states [19]. This proposal generalizes the entanglement RG for topological order, which can perform local unitaries as well as add or remove decoupled product states [20]. With this generalization, the dependence of the GSD on the system size can be accounted for, and indeed many type-I fracton models are found to have foliated fractonic order. For example, the X-cube model is able to change its system size under the foliation RG [19], and it has the same foliated fractonic order as the semionic X-cube model [21] and the Majorana checkerboard model [22].

Foliation RG has found its success in many more type-I fracton models, and more distinct RG fixed points have been identified [23, 24]. It is then natural to question the generality of foliated fractonic orders. Are there type-I fracton models beyond the foliation paradigm? What are some simple diagnostics for the lack of a foliation

structure? How does one define phases for such models? In this thesis, I will address these questions, the first two to a relatively comprehensive level and the third only partially. The main tools that I will use are abelian Chern-Simons theory [25] and cage-net fracton models [17] on the physics side, as well as commutative and non-commutative algebra on the mathematics side. All discussions concerning the GSD of a model assume that the model is placed on a torus of the appropriate dimension. This thesis is organized as follows.

In Chapter 2, I review abelian Chern-Simons (CS) theory in $d = 2 + 1$, which is used later in Chapter 3 to construct type-I fracton models beyond foliation. I introduce a polynomial description for a periodic CS theory, i.e., one whose K matrix has translation symmetry along its diagonal. I then use this polynomial description to obtain a strong constraint for the fusion group of the theory, as well as calculate the GSD and braiding statistics when K is non-degenerate. The GSD calculation is trickier when K is degenerate, and I perform this calculation using a perturbative method [26]. Finally, I discuss how to construct a K matrix given the braiding statistics of abelian anyons, which is essentially a translation of Wall's theorem [27] into physics language.

In Chapter 3, I take the size of the K matrix of a periodic CS theory to infinity, obtaining an infinite-component Chern-Simons (CS_∞) theory. When the indices i and j of K_{ij} are viewed as living in a third spatial direction, the theory becomes a fracton model in $d = 3 + 1$ which hosts planons but not lineons or fractons. A CS_∞ theory can be gapped or gapless, and in this chapter I focus on the gapped case. I start by discussing the action of foliation on a K matrix, and then present examples of CS_∞ theories with/without a foliation structure. I also give a necessary condition for foliation in terms of the polynomial description in Chapter 2, and derive the corollary that most CS_∞ theories are not foliated. Moreover, a CS theory cannot be put on a lattice by naive discretization, and locality in the field theory does not manifestly correspond to locality in the underlying lattice model (if a lattice model exists). Therefore, I construct lattice models for gapped CS_∞ theories and discuss the spatial profiles of fractional excitations at the end of the chapter [28].

In Chapter 4, I turn to CS_∞ theories that are gapless. Despite the absence of a bulk gap, a gapless CS_∞ theory turns out to be stable. Interestingly, the theory has an exotic one-form symmetry, part of which is broken spontaneously. Furthermore, in a large subclass of gapless CS_∞ theories, the planon braiding phase depends only on the linking number of the planon trajectories (just like in gapped theories), which I show by explicit calculation of Wilson loop correlation functions. This calculation also reveals the spatial profiles of fractional excitations. Finally, I derive fully continuous low-energy effective theories for this subclass of gapless CS_∞ theories [29].

In Chapter 5, I introduce a method for calculating the GSD of a fracton model that uses intrinsic features of the model such as anyon fusion, braiding and quantum dimension, which I call the operator algebra approach. The original motivation of the operator algebra approach is to calculate the GSD of the Ising cage-net model, which is exactly solvable but fairly complicated. The idea is to describe the algebra A_0 of logical operators as a redundant, formal algebra A of operators quotiented by certain physically justified relations. Once the quotienting procedure is completed, the GSD is obtained from $\text{GSD}^2 = \dim(A_0)$. Since the operator algebra approach is intrinsic and does not rely on microscopic details, it is able to tackle topological or fracton models in any dimension that are not necessarily exactly solvable. I explain this approach both conceptually and through a series of examples of increasing complexity, and eventually calculate the GSD of the Ising cage-net model. The GSD formula (5.1) implies that the model is not foliated [30].

In Chapter 6, I discuss a generalized foliation RG scheme that works for the Ising cage-net model. This new RG scheme generalizes the original constant depth circuit to planar linear-depth circuit, which is equivalent to allowing boson condensation in the RG flow. I show the RG process on the Ising cage-net model step by step, and also prove that this RG does not work for certain CS_∞ theories. New notions of phases are therefore still to be invented [31].

Chapter 2

PERIODIC CHERN-SIMONS THEORY

Although the main topic of this thesis is fractonic orders, I begin my detailed discussions by reviewing the well-known TQFT of abelian Chern-Simons (CS) theory in $d = 2 + 1$. In particular, I consider those CS theories that are periodic (see definition in Section 2.2), which will be generalized in Chapter 3 into fracton models. I study basic properties of a periodic CS theory, namely GSD, braiding statistics and fusion group. Results about these properties will be used in later chapters.

The results in this chapter are based on Refs. [26, 28, 29].

2.1 Review of Chern-Simons theory

An abelian CS theory in $d = 2 + 1$ has Lagrangian

$$\mathcal{L} = -\frac{1}{4g^2} \sum_i F_{\mu\nu}^i F^{i,\mu\nu} + \frac{1}{4\pi} \sum_{ij} K_{ij} \epsilon^{\mu\nu\rho} A_\mu^i \partial_\nu A_\rho^j, \quad (2.1)$$

where A_μ^i are compact U(1) gauge fields labelled by $i = 1, \dots, N$, $F_{\mu\nu}^i$ are the field strengths of A_μ^i , g is the Maxwell coupling constant, and K is an integer symmetric matrix (known as “the K matrix”) [25]. The integrality of K is required by gauge invariance under a large gauge transformation. The indices i and j may be raised or lowered arbitrarily in this thesis for aesthetic reason. The classical equation of motion of the theory is solved by plane waves, and the spectrum has N branches

$$\omega_i^2 = k_x^2 + k_y^2 + \left(\frac{g^2}{2\pi} \lambda_i \right)^2, \quad (2.2)$$

where λ_i are the eigenvalues of K .

An important phenomenon in a CS theory is *flux-charge attachment*, which I explain now. Consider adding background charged matter with conserved current $J_e^{i,\mu}$ to the Lagrangian via the term $\sum_i A_\mu^i J_e^{i,\mu}$, where the subscript “e” stands for “electric”. The Gauss’s law of the theory is the equation of motion of A_0^i ,

$$J_e^{i,0} + \frac{1}{2\pi} \sum_j K^{ij} B_j = \frac{1}{g^2} \nabla \cdot \mathbf{E}^i, \quad (2.3)$$

where \mathbf{E} and B are the electric and magnetic fields, respectively. Suppose that the background charge is localized in the xy plane with total charge Q^i , and let

$$\Phi^i = \frac{1}{2\pi} \int dx dy B^i.$$

I will refer to Φ^i as the (total) flux of A_μ^i , where the factor of $1/2\pi$ is included to simplify many mathematical expressions. It turns out that the charge vector Q and the flux vector Φ satisfy the relation

$$Q = -K\Phi, \quad (2.4)$$

which makes the LHS of (2.3) integrate to 0 in the xy plane. This is necessary since otherwise, (2.3) implies that \mathbf{E} decays like r^{-1} , leading to an IR divergence in the energy of the field. The relation (2.4) will be used constantly throughout this thesis.

In addition to the electric $U(1)^N$ gauge symmetry, a CS theory also has a magnetic $U(1)^N$ global symmetry. The conserved current of the magnetic $U(1)^N$ symmetry is $J_m^{i,\mu} = \epsilon^{\mu\nu\rho} \partial_\nu A_\rho^i$, where the subscript ‘‘m’’ stands for ‘‘magnetic’’. In particular, the charge density $J_m^{i,0}$ of the conserved current is precisely the magnetic flux of A_μ^i , hence the name ‘‘magnetic symmetry’’.

In most sections of this chapter, the K matrix of a CS theory is assumed to be non-degenerate, i.e., $\det(K) \neq 0$. In this case, the spectrum (2.2) is gapped, the Maxwell term in (2.1) is irrelevant, and the theory is a TQFT at low energy. Non-degenerate CS theories give a complete characterization of $d = 2 + 1$ abelian topological orders [32]. For example, the $\nu = 1/3$ fractional quantum Hall state is described by $K = (3)$, a 1×1 matrix.

Apart from the precise form (2.2) of the spectrum, all low-energy physics of (2.1) is encoded in K . First, $\text{GSD} = |\det(K)|$. Second, an anyon in the theory is specified by its charge vector $Q \in \mathbb{Z}^N$, which is bound to a flux vector $\Phi = -K^{-1}Q$ due to flux-charge attachment. If the flux Φ of an anyon is integral, then the anyon as a symmetry charge of the magnetic $U(1)^N$ symmetry is not fractionalized, and thus can be created locally. Therefore, the distinct anyons of the theory form the fusion group $G = \mathbb{Z}^N / K\mathbb{Z}^N$. Here, the group elements are charge vectors, and the group operation (addition of vectors) corresponds to fusion of anyons. Finally, the braiding phase of two anyons $Q, Q' \in \mathbb{Z}^N / K\mathbb{Z}^N$ is $\exp(-2\pi i Q^T K^{-1} Q')$.

The K matrix of a CS theory is not necessarily unique. Consider new fields

$$\tilde{A}_\mu^i = \sum_j (W^{-1})^{ij} A_\mu^j \quad (2.5)$$

defined in terms of the original fields A_μ^i and an invertible matrix W . To make sure that the compact gauge fields A_μ^i and \tilde{A}_μ^i have the same periodicity, both W and W^{-1} must be integral. Equivalently,

$$W \in \text{GL}_N(\mathbb{Z}) = \{M \in \text{Mat}_N(\mathbb{Z}) : \det(M) = \pm 1\}.$$

The change of variables (2.5) yields a new K matrix $\tilde{K} = W^T K W$. Therefore, K and $W^T K W$ should be viewed as describing the same CS theory, where $W \in \text{GL}_N(\mathbb{Z})$.

2.2 Polynomial description

As explained previously, the purpose of reviewing CS theories in $d = 2 + 1$ is to generalize them into fracton models in $d = 3 + 1$, by viewing the indices i and j of K_{ij} as coordinates in a third spatial direction and taking the thermodynamic limit $N \rightarrow \infty$. In order to take the thermodynamic limit, a certain translation symmetry must be imposed. A K matrix of size rN is said to have period r if $K_{i+r, j+r} = K_{ij}$, where the indices are mod rN . This is a translation symmetry along the diagonal of K . Such a periodic K matrix has a polynomial description, which I introduce now.

Translation symmetry naturally invites Fourier transform. If K has period r , then its Fourier transform is an $r \times r$ matrix $K(e^{iq})$ which is a function of the crystal momentum q . For example, the K matrix

$$K = \begin{pmatrix} \ddots & & & & & & & & \\ & 0 & 3 & 1 & & & & & \\ & 3 & 0 & & & & & & \\ & 1 & & 0 & 3 & 1 & & & \\ & & & 3 & 0 & & & & \\ & & & 1 & & 0 & & & \\ & & & & & & \ddots & & \end{pmatrix}_{2N \times 2N} \quad (2.6)$$

has period $r = 2$, and its Fourier transform is

$$K(e^{iq}) = \begin{pmatrix} e^{iq} + e^{-iq} & 3 \\ 3 & 0 \end{pmatrix}.$$

Focusing on real q turns out to be too limiting, so I replace e^{iq} by a symbol u , which essentially allows q to be complex. It is helpful to view u as a meaningless symbol, and thus $K(e^{iq})$ becomes $K(u)$, an $r \times r$ matrix over Laurent polynomials with integer coefficients. Here, a *Laurent polynomial* is a polynomial with possibly negative degree terms. In the example (2.6),

$$K(u) = \begin{pmatrix} u + u^{-1} & 3 \\ 3 & 0 \end{pmatrix}.$$

Laurent polynomials have an *involution* given by $p^\dagger(u) = p(u^{-1})$, which is similar to complex conjugation on \mathbb{C} . The involution is used to define Hermitian conjugation $K^\dagger(u) = K^T(u^{-1})$, and K is symmetric if and only if $K(u)$ is Hermitian.

In Sections 2.3 – 2.6, I will use this polynomial description to compute various observables of periodic CS theories.

2.3 GSD: Non-degenerate case

The first observable of a periodic CS theory that I compute is its GSD, assuming non-degeneracy. As explained in Section 2.1, this is equivalent to finding $\det(K)$.

It turns out that the key object in this calculation is the *determinant polynomial* $D(u) = \det(K(u))$. Since K is symmetric, $D(u)$ satisfies $D(u^{-1}) = D(u)$. Let

$$D(u) = \sum_{k=-\xi}^{\xi} c_k u^k,$$

where $c_{-k} = c_k$ and $c_\xi \neq 0$. The main result is

$$\det(K) = (-1)^{\xi(N+1)} c_\xi^N \prod_{l=1}^{2\xi} (1 - u_l^N), \quad (2.7)$$

where u_l are the roots of $D(u)$, $l = 1, \dots, 2\xi$.

To prove (2.7), note that $\det(K)$ can be written in Fourier space as

$$\det(K) = \prod_{j=0}^{N-1} \det(K(\omega^j)) = \prod_{j=0}^{N-1} D(\omega^j), \quad (2.8)$$

where $\omega = e^{2\pi i/N}$. Also, $D(u)$ can be factorized in terms of its roots as

$$D(u) = c_\xi u^{-\xi} \prod_{l=1}^{2\xi} (u - u_l).$$

Thus (2.8) simplifies to

$$\begin{aligned} \det(K) &= \prod_{j=0}^{N-1} \left[c_\xi \omega^{-j\xi} \prod_{l=1}^{2\xi} (\omega^j - u_l) \right] \\ &= c_\xi^N \left[\prod_{j=0}^{N-1} \omega^{-j\xi} \right] \cdot \prod_{l=1}^{2\xi} \left[\prod_{j=0}^{N-1} (\omega^j - u_l) \right]. \end{aligned}$$

A straightforward calculation shows that $\prod_j \omega^{-j\xi} = 1$. Furthermore, by viewing u_l as a variable in its own right, it can be shown that

$$\prod_{j=0}^{N-1} (\omega^j - u_l) = (-1)^{N+1} (1 - u_l^N).$$

This is because both sides of the equation have the same leading coefficient as polynomials in u_l and the same roots at $u_l = \omega^j$. Thus (2.7) follows.

I now demonstrate the possible behavior of (2.7) through three examples with period $r = 1$. Due to the c_ξ^N term in (2.7), $\det(K)$ always has an exponential growth if $|c_\xi| > 1$. Therefore, all three examples are chosen to have $c_\xi = 1$.

1. Let

$$D(u) = u + 3 + u^{-1}, \quad (2.9)$$

whose roots are $(-3 \pm \sqrt{5})/2$. The GSD of the theory is

$$\text{GSD} = \left(\frac{3 + \sqrt{5}}{2}\right)^N + \left(\frac{3 - \sqrt{5}}{2}\right)^N - 2(-1)^N. \quad (2.10)$$

For large N , the GSD is dominated by the first term and grows exponentially with an irrational base $(3 + \sqrt{5})/2$, while the second term makes sure that the GSD is an integer.

2. Let

$$D(u) = u + 2 + u^{-1}, \quad (2.11)$$

whose root is -1 with multiplicity 2. The theory has

$$|\det(K)| = \begin{cases} 4, & \text{if } N \text{ is odd,} \\ 0, & \text{if } N \text{ is even.} \end{cases}$$

Thus $\text{GSD} = 4$ when N is odd. However, the GSD cannot be inferred from $\det(K)$ when N is even since $\det(K) = 0$ in this case. As will be explained in Section 2.5, actually $\text{GSD} = N$ when N is even.

3. Let

$$D(u) = u^2 - 2u - 2u^{-1} + u^{-2}. \quad (2.12)$$

Two of the four roots of $D(u)$ are real, namely $u_1 \approx 2.3$ and $u_2 = u_1^{-1}$; the other two are on the unit circle, namely $u_3 = e^{2\pi i s}$ and $u_4 = u_3^{-1}$, where $s \approx 0.31$. Importantly, s is irrational [33], so u_3 and u_4 are not roots of unity. By (2.7), $\det(K) \neq 0$ for all integer N . For large N , the theory has

$$\text{GSD} \approx 2u_1^N (1 - \cos(2\pi N s)),$$

which oscillates inside an exponential envelope.

Incidentally, if $|c_\xi| = 1$ and all roots u_l are on the unit circle, then all u_l are roots of unity [34]. Therefore, if the GSD is bounded, then it must cycle over a finite list of integers periodically.

2.4 Braiding statistics: Non-degenerate case

Next, I calculate the braiding statistics of anyons. Besides non-degeneracy, I also assume that the determinant polynomial $D(u)$ has no root on the unit circle. This additional assumption is a sufficient but not necessary condition for non-degeneracy, as can be seen from the example (2.11) with N even and from the example (2.12). The case where $D(u)$ has roots on the unit circle will be discussed in Section 4.3. Again as explained in Section 2.1, the braiding statistics are encoded in K^{-1} . As a

motivating example, consider the K matrix (2.9). In the limit $1 \ll |i - j| \ll N$, this theory has

$$(K^{-1})_{ij} \approx \frac{(-1)^{i-j}}{\sqrt{5}} \left(\frac{3 - \sqrt{5}}{2} \right)^{|i-j|}. \quad (2.13)$$

Therefore, the braiding statistic decays exponentially as the anyon labels i and j get farther apart. In Chapter 3, these labels will be interpreted as a third spatial coordinate, so the braiding statistic in this example decays exponentially in space but is not strictly local. Due to the novelty of this exponential decay, the calculations in this section are focused on understanding the decay for $1 \ll |i - j| \ll N$ rather than figuring out the exact expression for K^{-1} .

The polynomial description again comes in handy in this calculation, since K^{-1} is the inverse Fourier transform of $K(u)^{-1}$. Note that

$$K(u)^{-1} = \frac{\text{Adj}(K(u))}{\det(K(u))} = \frac{\text{Adj}(K(u))}{D(u)}, \quad (2.14)$$

where $\text{Adj}(K(u))$ is the adjugate matrix of $K(u)$. The entries of $\text{Adj}(K(u))$ are polynomials in the entries of $K(u)$ and thus are Laurent polynomials with finitely many terms. This means that any exponential decay in K^{-1} must be attributed to $1/D(u)$. Indeed, if one ignores $\text{Adj}(K(u))$, for example by assuming that the period $r = 1$, then the entries of K^{-1} are the coefficients of $1/D(u)$ expanded as a Laurent series. Therefore, the key part of this calculation is the Laurent series expansion of $1/D(u)$, which is a standard exercise in complex functions.

I now calculate the Laurent series of $1/D(u)$. To start with, the **distinct** roots of $D(u)$ can be put into two classes: $u_\alpha^<$ inside the unit circle with multiplicity Γ_α , and $u_\alpha^> = (u_\alpha^<)^{-1}$ outside the unit circle with the same multiplicity Γ_α . Now $1/D(u)$ is a meromorphic function with poles at $u_\alpha^<$ and $u_\alpha^>$, so there exist constants $b_{\alpha m}$, $m = 1, \dots, \Gamma_\alpha$, such that the function

$$\frac{1}{D(u)} - \sum_\alpha \sum_{m=1}^{\Gamma_\alpha} \frac{b_{\alpha m} (u_\alpha^>)^m}{(u_\alpha^> - u)^m} = \frac{1}{D(u)} - \sum_\alpha \sum_{m=1}^{\Gamma_\alpha} \frac{b_{\alpha m}}{(1 - u_\alpha^< u)^m}$$

has no pole outside the unit circle. Since $D(u^{-1}) = D(u)$, the function

$$g(u) = \frac{1}{D(u)} - \sum_\alpha \sum_{m=1}^{\Gamma_\alpha} \frac{b_{\alpha m}}{(1 - u_\alpha^< u)^m} - \sum_\alpha \sum_{m=1}^{\Gamma_\alpha} \frac{b_{\alpha m}}{(1 - u_\alpha^< u^{-1})^m} \quad (2.15)$$

has no pole at all. Therefore, $g(u)$ is a constant function

$$g(u) = g(\infty) = - \sum_\alpha \sum_{m=1}^{\Gamma_\alpha} b_{\alpha m}. \quad (2.16)$$

Rearranging (2.15) and (2.16) gives

$$\frac{1}{D(u)} = \sum_{\alpha} \sum_{m=1}^{\Gamma_{\alpha}} \frac{b_{\alpha m}}{(1 - u_{\alpha}^{\leq} u)^m} + \sum_{\alpha} \sum_{m=1}^{\Gamma_{\alpha}} \frac{b_{\alpha m}}{(1 - u_{\alpha}^{\leq} u^{-1})^m} - \sum_{\alpha} \sum_{m=1}^{\Gamma_{\alpha}} b_{\alpha m}. \quad (2.17)$$

The next step is to expand (2.17) as a Laurent series. However, this is not the usual Laurent series in complex analysis where one cares about its region of convergence. Instead, the Laurent series here is simply a formal sum from which K^{-1} can be inferred. Such a formal sum need not be unique. For example, the function $1/(1-u)$ has two Laurent series

$$\frac{1}{1-u} = 1 + u + u^2 + \dots = -u^{-1} - u^{-2} - u^{-3} - \dots.$$

This ambiguity arises because K is treated in the $N \rightarrow \infty$ limit, and is similar to the sensitivity of the Green's function of a differential operator to the boundary condition. Here, the correct choice of Laurent series is determined by demanding that K^{-1} be well-defined when N is finite. For this purpose, I choose

$$\begin{aligned} \frac{1}{1 - u_{\alpha}^{\leq} u} &= \sum_{k=0}^{\infty} (u_{\alpha}^{\leq})^k u^k, \\ \frac{1}{1 - u_{\alpha}^{\leq} u^{-1}} &= \sum_{k=0}^{\infty} (u_{\alpha}^{\leq})^k u^{-k}. \end{aligned} \quad (2.18)$$

These choices will be explained soon. A straightforward calculation then gives

$$\begin{aligned} \frac{1}{(1 - u_{\alpha}^{\leq} u)^m} &= \sum_{k=0}^{\infty} \frac{(k+m-1)!}{k!} (u_{\alpha}^{\leq})^k u^k, \\ \frac{1}{(1 - u_{\alpha}^{\leq} u^{-1})^m} &= \sum_{k=0}^{\infty} \frac{(k+m-1)!}{k!} (u_{\alpha}^{\leq})^k u^{-k}. \end{aligned}$$

This yields the Laurent series

$$\begin{aligned} \frac{1}{D(u)} &= \sum_{\alpha} \sum_{m=1}^{\Gamma_{\alpha}} \left[b_{\alpha m} \sum_{k=0}^{\infty} \frac{(k+m-1)!}{k!} (u_{\alpha}^{\leq})^k (u^k + u^{-k}) \right] - \sum_{\alpha} \sum_{m=1}^{\Gamma_{\alpha}} b_{\alpha m} \\ &= \sum_{k=-\infty}^{\infty} \left[\sum_{\alpha} \sum_{m=1}^{\Gamma_{\alpha}} \frac{(|k|+m-1)!}{|k|!} b_{\alpha m} (u_{\alpha}^{\leq})^{|k|} \right] u^k. \end{aligned} \quad (2.19)$$

The coefficients of (2.19) decay (a bit more slowly than) exponentially unless $D(u)$ is a constant. If, say, u_1^{\leq} has the largest magnitude among all u_{α}^{\leq} , then the coefficients decay like

$$\frac{(|k| + \Gamma_1 - 1)!}{|k|!} |u_1^{\leq}|^{|k|} \sim |k|^{\Gamma_1 - 1} |u_1^{\leq}|^{|k|}. \quad (2.20)$$

Of course, K^{-1} is a matrix of finite size rN , so the correspondence of K^{-1} and $K(u)^{-1}$ via Fourier transform is only correct in the $N \rightarrow \infty$ limit. For finite N , the

u^k and u^{k+N} terms in (2.19) should be identified and their coefficients should be summed up. By choosing the Laurent series (2.18), the sum of these coefficients is finite, and the decay pattern of K^{-1} does not change qualitatively as long as N is large. Since the decay of K^{-1} is already understood qualitatively, I will not try to determine the constants $b_{\alpha m}$ explicitly.

Finally, I take $\text{Adj}(K(u))$ back into consideration. Since $\text{Adj}(K(u))$ appears in the numerator of (2.14), it might have some cancellation with $D(u)$ in the denominator, which makes certain rows of K^{-1} decay faster than (2.20). However, I claim that the slowest possible decay pattern, or at least its exponential part $|u_1^<|^{|k|}$, must be attained in some row of K^{-1} . The proof uses the following theorem [35]:

Theorem 1. If complex coefficients are allowed in all Laurent polynomials, then $K(u)$ can be put into *Smith normal form*

$$S(u) = V(u)K(u)W(u) = \text{diag}(s_1(u), \dots, s_r(u)),$$

where $S(u)$, $V(u)$ and $W(u)$ are $r \times r$ matrices over Laurent polynomials with complex coefficients, the Laurent polynomials $\det(V(u))$ and $\det(W(u))$ are non-zero constants, and $s_1(u) \mid \dots \mid s_r(u)$ (consecutive divisibility). Furthermore,

$$\text{gcd}\{\text{Adj}(K(u))_{ij} : i, j = 1, \dots, r\} = \prod_{k=1}^{r-1} s_k(u), \quad (2.21)$$

where “gcd” means greatest common divisor.

An obvious consequence of this theorem is that $D(u) = \prod_{k=1}^r s_k(u)$. Now if any factor $u - u_\alpha^<$ divides all entries of $\text{Adj}(K(u))$ and hence their gcd, then it must divide $s_k(u)$ for some $1 \leq k \leq r - 1$. Since $s_k(u)$ always divides $s_r(u)$, the factor $u - u_\alpha^<$ also divides $s_r(u)$. Suppose, say, that $\text{Adj}(K(u))_{11}$ has the lowest power of $u - u_\alpha^<$ among all entries of $\text{Adj}(K(u))$, and that the power of $u - u_\alpha^<$ in $\text{Adj}(K(u))_{11}$ is p . By (2.21), the power of $u - u_\alpha^<$ in $\prod_{k=1}^{r-1} s_k(u)$ is also precisely p . Therefore, the power of $u - u_\alpha^<$ in $D(u)$ is $\Gamma_\alpha > p$, since $s_r(u)$ must contain some extra factors of $u - u_\alpha^<$. These extra factors of $u - u_\alpha^<$ make sure that the coefficients of $\text{Adj}(K(u))_{11}$ decay at least as slowly as $|u_\alpha^<|^{|k|}$.

2.5 GSD: Degenerate case

In this section, I consider degenerate CS theories. The nature of such theories is well-understood, and it is not my intention to bring a fundamentally new understanding. Instead, I focus on computing the GSD of a degenerate periodic CS theory using the polynomial description.

The Polyakov mechanism

Naively, $\det(K) = 0$ implies that the spectrum (2.2) is gapless. However, the theory is actually gapped due to the renowned Polyakov mechanism [36], which I explain now in the example $K = (0)$, i.e., $d = 2 + 1$ Maxwell theory. The essence of the Polyakov mechanism is the proliferation of instantons in $d = 2 + 1$ Lorentzian space-time. For convenience of calculation, I choose instead to work in $d = 3$ Euclidean space, where instantons become monopoles. The field strength of a monopole decays like r^{-2} , so a UV regularized monopole has finite energy and thus can proliferate. In contrast, a monopole in a non-degenerate CS theory also carries electric charge, so its field strength decays like r^{-1} . Therefore, the energy of a monopole has an IR divergence and hence monopoles are irrelevant in a non-degenerate CS theory.

The quantitative treatment of monopoles is easier if the theory is dualized. In the dual theory, $F_{\mu\nu}$ is viewed as an independent two-form field instead of the field strength of A_μ . To enforce the Bianchi identity on $F_{\mu\nu}$, a Lagrange multiplier involving a real scalar field ϕ is added to the Lagrangian (in Euclidean space):

$$\mathcal{L} = \frac{1}{4g^2} F_{\mu\nu} F^{\mu\nu} + \frac{i}{4\pi} \epsilon^{\mu\nu\rho} \phi \partial_\mu F_{\nu\rho}.$$

Dirac quantization implies that the magnetic charge

$$\frac{1}{4\pi} \int d^3x \epsilon^{\mu\nu\rho} \partial_\mu F_{\nu\rho}$$

is always an integer, so ϕ is a compact boson with period 2π . Integrating out $F_{\mu\nu}$ yields the dual Lagrangian of a free compact boson

$$\mathcal{L} = \frac{g^2}{8\pi^2} \partial_\mu \phi \partial^\mu \phi.$$

The magnetic U(1) symmetry acts as $\phi \mapsto \phi + c$, and the basic monopole operator is $e^{i\phi}$. The two-point function of the monopole operator is

$$\langle e^{-i\phi(x^\mu)} e^{i\phi(0)} \rangle \sim \exp\left(\frac{4\pi^2}{g^2} \int \frac{d^3k}{(2\pi)^3} \frac{e^{ik_\mu x^\mu}}{k^2}\right) \sim e^{\pi/g^2 r},$$

where $r = |x^\mu|$. As $r \rightarrow \infty$, the two-point function approaches a non-zero constant. Therefore, the magnetic U(1) symmetry is broken spontaneously and the theory is gapless. A gap is opened up by the relevant perturbation $\cos(\phi)$, which breaks the magnetic U(1) symmetry explicitly.

The analysis above can be generalized to the case where K has size N . As explained earlier in this section, the only relevant monopoles are those without electric charge. Therefore, the flux vector Φ of a relevant monopole satisfies $K\Phi = -Q = 0$. Note that the flux of a monopole is integral, whereas the flux vector of an anyon is not integral unless the anyon is trivial. Due to various requirements of integrality, the

treatment of such theories is more complicated than naive linear algebra, and I demonstrate the general procedure with the example [37]

$$K = \begin{pmatrix} 1 & 1 \\ 1 & 1 \end{pmatrix}.$$

The basic relevant monopole has magnetic charge vector $\Phi = (-1, 1)^T$. Define new fields \tilde{A}_μ^i via (2.5) where

$$W = \begin{pmatrix} 1 & -1 \\ 0 & 1 \end{pmatrix},$$

which is chosen such that Φ is the second column of W . The K matrix for \tilde{A}_μ^i is

$$\tilde{K} = W^T K W = \begin{pmatrix} 1 & 0 \\ 0 & 0 \end{pmatrix}.$$

Since \tilde{K} is diagonal, it may seem that \tilde{A}_μ^1 and \tilde{A}_μ^2 are decoupled. However, this is not true once the Maxwell term in the Lagrangian (2.1) is taken into account. If (2.1) is generalized to

$$\mathcal{L} = -\frac{1}{4g^2} \sum_{ij} Z_{ij} F_{\mu\nu}^i F^{j,\mu\nu} + \frac{1}{4\pi} \sum_{ij} K_{ij} \epsilon^{\mu\nu\rho} A_\mu^i \partial_\nu A_\rho^j,$$

where Z starts as the identity matrix, then the new fields \tilde{A}_μ^i have

$$\tilde{Z} = W^T Z W = \begin{pmatrix} 1 & -1 \\ -1 & 2 \end{pmatrix}.$$

Consequently, \tilde{A}_μ^1 and \tilde{A}_μ^2 are coupled together by the off-diagonal entries of \tilde{Z} . The next step is to dualize \tilde{A}_μ^2 into a compact scalar field ϕ , which gives the dual Lagrangian (in Euclidean space)

$$\mathcal{L} = \frac{g^2}{16\pi^2} \partial_\mu \phi \partial^\mu \phi - \frac{i}{8\pi} \epsilon^{\mu\nu\rho} \tilde{F}_{\mu\nu}^1 \partial_\rho \phi + \frac{1}{8g^2} \tilde{F}^{1,\mu\nu} \tilde{F}_{\mu\nu}^1 + \frac{i}{4\pi} \epsilon^{\mu\nu\rho} \tilde{A}_\mu^1 \partial_\nu \tilde{A}_\rho^1.$$

The second term is a topological term. It is a total derivative but is still non-trivial, because \tilde{A}_μ^1 and ϕ are both compact fields. The topological term affects correlation functions involving the vortex line of ϕ , which corresponds to the Wilson line of \tilde{A}^2 before dualization. However, it does not affect the spectrum of the theory or correlation functions involving only \tilde{A}_μ^1 and ϕ , since they are perturbative properties of the theory. Therefore, for these purposes \tilde{A}_μ^1 and ϕ are essentially decoupled, and the theory effectively has $K = (1)$.

I conclude the example above with a point of caution: The flux vector $\Phi = (-1, 1)^T$ must be integral, so it cannot be rescaled into a unit vector in this example. Consequently, W cannot be chosen to be orthogonal or unitary. In fact, W cannot even

have orthogonal columns when Φ is its second column. Therefore, basic number theory is indispensable when studying CS theories, and one must be very careful with any intuition originating from linear algebra of complex matrices.

To generalize this example to arbitrary K , the following theorem is useful [35]:

Theorem 2. An $N \times N$ integer matrix K can be put into *Smith normal form*

$$S = VKW = \text{diag}(s_1, \dots, s_N), \quad (2.22)$$

where S , V and W are $N \times N$ integer matrices, $V, W \in \text{GL}_N(\mathbb{Z})$, and $s_1 | \dots | s_N$ (consecutive divisibility). Furthermore,

$$\text{gcd}\{\text{minor of } K \text{ of order } m\} = \prod_{k=1}^m s_k, \quad (2.23)$$

where ‘‘gcd’’ means greatest common divisor, and a *minor* of K of order m is the determinant of an $m \times m$ submatrix of K .

Theorem 2 is a sister theorem of Theorem 1, and both are elementary results in algebra [35]. If K is degenerate, then the last few s_k 's are 0. Let N_0 be the nullity of K and $N_1 = N - N_0$, so $s_{N_1+1} = \dots = s_N = 0$. Note that N_0 generally depends on N but is always bounded as N increases. Consider the change of variables (2.5) where W is taken from (2.22). The new K matrix is

$$\tilde{K} = W^T K W = W^T V^{-1} V K W = W^T V^{-1} S.$$

This shows that \tilde{K} can be obtained by multiplying a diagonal matrix S on the left, so \tilde{K} takes the form

$$\tilde{K} = \begin{pmatrix} \hat{K}_{N_1 \times N_1} & 0_{N_1 \times N_0} \\ K'_{N_0 \times N_1} & 0_{N_0 \times N_0} \end{pmatrix},$$

where \hat{K} is non-degenerate. Meanwhile, \tilde{K} is symmetric, so actually

$$\tilde{K} = \begin{pmatrix} \hat{K}_{N_1 \times N_1} & \\ & 0_{N_0 \times N_0} \end{pmatrix}. \quad (2.24)$$

As explained earlier in this section, when studying correlation functions involving only $\tilde{A}_\mu^1, \dots, \tilde{A}_\mu^{N_1}$, the system can be treated as a non-degenerate CS theory parameterized by \hat{K} . Now the ground space is protected by the algebra of the Wilson loops of $\tilde{A}_\mu^1, \dots, \tilde{A}_\mu^{N_1}$, so this simplified treatment applies, and the theory has

$$\text{GSD} = \left| \det(\hat{K}) \right| = \prod_{k=1}^{N_1} |s_k|. \quad (2.25)$$

To reiterate, the GSD (up to a minus sign) is given by the product of the non-zero entries of the Smith normal form of K . In the rest of this section, I aim to express (2.25) using explicit data in the polynomial description. In particular, I will focus on understanding the dependence of the GSD on N .

Perturbative calculation of GSD

At first glance, it is not obvious how the polynomial description is related to the Smith normal form. For a generic K matrix with period r and size rN , none of the matrices S , V and W in (2.22) is periodic. Moreover, the process of throwing away the 0's on the diagonal of S as required by (2.25) also seems to have nothing to do with periodicity. In order to reveal the connection between the polynomial description and the Smith normal form, I add a perturbation ϵ (times the identity) to K and turn it into $K + \epsilon$. Since $K + \epsilon$ is not integral, it does not physically correspond to a gauge invariant CS theory. Instead, this perturbation is merely a mathematical technique. Now W in (2.22) acts on $K + \epsilon$ as

$$\begin{aligned} W^T(K + \epsilon)W &= \begin{pmatrix} F(\epsilon)_{N_1 \times N_1} & G(\epsilon)_{N_1 \times N_0} \\ G^T(\epsilon)_{N_0 \times N_1} & H(\epsilon)_{N_0 \times N_0} \end{pmatrix} \\ &= \begin{pmatrix} \hat{K} + \mathcal{O}(\epsilon) & \mathcal{O}(\epsilon) \\ \mathcal{O}(\epsilon) & \mathcal{O}(\epsilon) \end{pmatrix}, \end{aligned} \quad (2.26)$$

where $N_0 + N_1 = rN$. Thus to leading order in ϵ ,

$$\begin{aligned} \det(K + \epsilon) &= \det(W^T(K + \epsilon)W) \\ &= \det(H(\epsilon)) \det(\hat{K}) \\ &= \pm \det(H(\epsilon)) \cdot \text{GSD}, \end{aligned}$$

and hence

$$\text{GSD} = \pm \frac{\det(K + \epsilon)}{\det(H(\epsilon))}. \quad (2.27)$$

This is the key equation for calculating the GSD, because the numerator is the determinant of a **non-degenerate** periodic matrix and is therefore tractable. In the rest of this section, I first state the main result and then prove it by studying the numerator and denominator of (2.27) separately.

The main result is as follows: Let u_α be the **distinct** roots of $D(u)$, and Γ_α the multiplicity of u_α . Note that these notations are not the same as those in Section 2.3 or 2.4. Define also an index set

$$I = \{\alpha : u_\alpha^N = 1\},$$

which labels roots corresponding to gapless modes when the system size is N . The set I generally depends on N , and when discussing the dependence of the GSD on N , I only consider those values of N that yield the same I . For example, in the context of the K matrix (2.11), I only consider even N . For $\alpha \in I$, let Δ_α be the nullity of $K(u_\alpha)$, an $r \times r$ Hermitian matrix. Then

$$\text{GSD} = \pm \mathcal{C} N^{\sum_{\alpha \in I} (\Gamma_\alpha - \Delta_\alpha)} c_\xi^N \prod_{\alpha \notin I} (1 - u_\alpha^N)^{\Gamma_\alpha}, \quad (2.28)$$

where \mathcal{C} is a constant independent of N . The precise value of \mathcal{C} is a complicated expression involving basic algebraic number theory, and I will not try to determine it in this thesis. Practically, \mathcal{C} is most conveniently fixed by fitting (2.28) for some small N . The dependence of the GSD on N has a polynomial part besides the usual exponential part. To explain the polynomial part intuitively, I temporarily define Γ_α as the *algebraic multiplicity* of u_α , and Δ_α as the *geometric multiplicity* of u_α . These nomenclatures are designed to draw analogy with standard linear algebra. In linear algebra, the polynomial of interest is the characteristic polynomial of a matrix, and the quantity $\Gamma_\alpha - \Delta_\alpha$ intuitively measures the obstacle to diagonalize the matrix. In a degenerate CS theory, $\Gamma_\alpha - \Delta_\alpha$ measures the contribution of u_α , where $\alpha \in I$, to the polynomial growth of the GSD. In the K matrix (2.11) with even N , the root -1 has $\Gamma = 2$ and $\Delta = 1$, so $\text{GSD} \propto N$.

To prove (2.28), I begin by calculating the numerator of (2.27). According to (2.7), $\det(K + \epsilon)$ is determined by the roots of $\det(K(u) + \epsilon)$, which are obtained by perturbing the roots u_α of $\det(K(u)) = D(u)$. In the new notations, (2.7) becomes

$$\det(K) = \pm c_\xi^N \prod_\alpha (1 - u_\alpha^N)^{\Gamma_\alpha}. \quad (2.29)$$

If $\alpha \notin I$, then to leading order in ϵ , there is no correction to the $(1 - u_\alpha^N)^{\Gamma_\alpha}$ factor in (2.29). On the other hand, if $\alpha \in I$, then $\det(K(u) + \epsilon)$ can be expanded in the vicinity of u_α as

$$\det(K(u) + \epsilon) = \eta_\alpha (u - u_\alpha)^{\Gamma_\alpha} + \sum_{k=1}^r b_k \epsilon^k + \dots, \quad (2.30)$$

where $\eta_\alpha \neq 0$, b_k are some coefficients, and “ \dots ” stands for higher order terms in $u - u_\alpha$. I claim that the smallest k such that $b_k \neq 0$ is $k = \Delta_\alpha$. To prove this claim, take (2.30) with $u = u_\alpha$, which gives

$$\det(K(u_\alpha) + \epsilon) = \sum_{k=1}^r b_k \epsilon^k.$$

Let λ_i be the eigenvalues of the Hermitian matrix $K(u_\alpha)$ such that $\lambda_i = 0$ for $i = 1, \dots, \Delta_\alpha$ and $\lambda_i \neq 0$ for $i = \Delta_\alpha + 1, \dots, r$. Then

$$\det(K(u_\alpha) + \epsilon) = \prod_{i=1}^r (\lambda_i + \epsilon).$$

Therefore, the coefficient b_k is the sum of all possible products of $r - k$ eigenvalues. If $k < \Delta_\alpha$, then such a product must involve λ_i for some $i = 1, \dots, \Delta_\alpha$ and hence vanish. On the other hand,

$$b_{\Delta_\alpha} = \prod_{i=\Delta_\alpha+1}^r \lambda_i \neq 0,$$

and the claim follows. Thus (2.30) becomes

$$\det(K(u) + \epsilon) = \eta_\alpha (u - u_\alpha)^{\Gamma_\alpha} + b_{\Delta_\alpha} \epsilon^{\Delta_\alpha} + \dots .$$

The roots of $\det(K(u) + \epsilon)$ are

$$u_{\alpha,m}(\epsilon) = u_\alpha + (B_\alpha \epsilon^{\Delta_\alpha})^{1/\Gamma_\alpha} e^{2\pi i m / \Gamma_\alpha},$$

where $m = 0, \dots, \Gamma_\alpha - 1$ labels the new roots, $B_\alpha = -b_{\Delta_\alpha} / \eta_\alpha$, and $(B_\alpha \epsilon^{\Delta_\alpha})^{1/\Gamma_\alpha}$ is a fixed choice of Γ_α th root of $B_\alpha \epsilon^{\Delta_\alpha}$. The fact that there are Γ_α roots is expected, because the Γ_α degenerate roots of $D(u)$ at u_α are split by the perturbation. Each new root has a contribution of

$$\begin{aligned} 1 - u_{\alpha,m}(\epsilon)^N &= 1 - u_\alpha^N - N u_\alpha^{N-1} (B_\alpha \epsilon^{\Delta_\alpha})^{1/\Gamma_\alpha} e^{2\pi i m / \Gamma_\alpha} + \dots \\ &= -N u_\alpha^{-1} (B_\alpha \epsilon^{\Delta_\alpha})^{1/\Gamma_\alpha} e^{2\pi i m / \Gamma_\alpha} + \dots \end{aligned}$$

to the numerator of (2.27), where I used the fact that $u_\alpha^N = 1$. Multiplied together, the Γ_α roots near u_α have a contribution of

$$\begin{aligned} \prod_{m=0}^{\Gamma_\alpha-1} (1 - u_{\alpha,m}(\epsilon)^N) &= \prod_{m=0}^{\Gamma_\alpha-1} \left[-N u_\alpha^{-1} (B_\alpha \epsilon^{\Delta_\alpha})^{1/\Gamma_\alpha} e^{2\pi i m / \Gamma_\alpha} \right] + \dots \\ &= (-N u_\alpha^{-1})^{\Gamma_\alpha} (B_\alpha \epsilon^{\Delta_\alpha}) \exp\left(\frac{2\pi i}{\Gamma_\alpha} \sum_{m=0}^{\Gamma_\alpha-1} m\right) + \dots \\ &= -N^{\Gamma_\alpha} u_\alpha^{-\Gamma_\alpha} B_\alpha \epsilon^{\Delta_\alpha} + \dots . \end{aligned} \tag{2.31}$$

Using (2.29) and accounting for the roots u_α where $\alpha \notin I$, the numerator of (2.27) is found to be

$$\det(K + \epsilon) = \pm c_\xi^N \prod_{\alpha \in I} (N^{\Gamma_\alpha} B_\alpha \epsilon^{\Delta_\alpha}) \prod_{\alpha \notin I} (1 - u_\alpha^N)^{\Gamma_\alpha} + \dots, \tag{2.32}$$

where the $u_\alpha^{-\Gamma_\alpha}$ factor in (2.31) does not appear because u_α^{-1} is also a root.

Next, I discuss the denominator of (2.27). By (2.26), if U is the $rN \times N_0$ matrix consisting of the last N_0 columns of W , then

$$H(\epsilon) = U^T (K + \epsilon) U = \epsilon U^T U.$$

In fact, the columns of U form a basis of the integral kernel of K . On the other hand, let U_0 be the $rN \times N_0$ matrix whose columns are orthogonal complex vectors spanning the complex kernel of K . These vectors have fixed crystal momenta and polarizations. They are not chosen to be unit vectors, but instead are chosen to have length (i.e., Euclidean norm) N each. Thus as N increases in such a way that the index set I is fixed, the columns of U_0 are just the same patterns repeated $\mathcal{O}(N)$

times. Since the columns of either U or U_0 form a basis for the complex kernel of K , they are related by column operations. In other words, for each N there exists an $N_0 \times N_0$ invertible complex matrix C such that $U = U_0 C$. Due to the periodic structure of the columns of U_0 , the same C actually works for all N . Therefore,

$$\det(H(\epsilon)) = \det(\epsilon C^T U_0^T U_0 C) = \epsilon^{N_0} \det(C)^2 \det(U_0^T U_0).$$

By construction of U_0 , every entry of $U_0^T U_0$ is proportional to N , so

$$\det(H(\epsilon)) \propto \epsilon^{N_0} N^{N_0}. \quad (2.33)$$

Finally, using $N_0 = \sum_{\alpha \in I} \Delta_\alpha$ to cancel all the ϵ 's and absorbing various constant factors into an overall constant \mathcal{C} , (2.32) and (2.33) are combined into (2.28).

2.6 Fusion group

Finally, I study the fusion group of a periodic CS theory. According to Section 2.1 and Theorem 2, the fusion group of a non-degenerate CS theory is

$$G = \mathbb{Z}^N / K\mathbb{Z}^N = \prod_{k=1}^N \mathbb{Z}_{s_k}, \quad (2.34)$$

where s_k are the diagonal entries of the Smith normal form of K . By the discussions in Section 2.5, (2.34) also works for degenerate CS theories with the convention that \mathbb{Z}_0 is the trivial group. As a motivating example, consider the K matrix (2.9). Numerics suggest that the fusion group is

$$G = \mathbb{Z}_{F_N} \times \mathbb{Z}_{5F_N}, \quad (2.35)$$

where F_N is the N th Fibonacci number. Even though (2.35) has not been and will not be proved rigorously in this thesis, it hints at a peculiar feature which will be important when discussing foliation in Chapter 3: that G has only two cyclic components for arbitrarily large N . Here, cyclic components are defined such that, for example, $\mathbb{Z}_6 = \mathbb{Z}_2 \times \mathbb{Z}_3$ is viewed as one cyclic component.

This is indeed a general feature of periodic CS theories with period $r = 1$, as summarized in the following proposition:

Proposition 3. Suppose that K has period $r = 1$, with $K(u) = (D(u))$ and

$$D(u) = \sum_{k=-\xi}^{\xi} c_k u^k.$$

If $D(u)$ is *primitive*, i.e., $\gcd\{c_k\} = 1$, then the fusion group G of K has at most 2ξ cyclic components.

If $D(u)$ is not primitive and $\gcd\{c_k\} = b$, then Proposition 3 can be applied to the integer matrix K/b . After multiplying b back, it is clear that the fusion group G of K has at least $N - 2\xi$ cyclic components that are \mathbb{Z}_b . Therefore mathematically, primitivity of $D(u)$ can be assumed without loss of generality. However, the assumption that $r = 1$ is crucial for the proof of the proposition, and I do not know whether any analogous statement holds for higher periods.

I now prove Proposition 3. Using the notations of Theorem 2, the goal is to show that $s_1 = \dots = s_{N-2\xi} = 1$. Since s_k are integers, it suffices to show that $\prod_{k=1}^{N-2\xi} s_k = 1$, or equivalently by (2.23), that

$$\gcd\{\text{minor of } K \text{ of order } N - 2\xi\} = 1. \quad (2.36)$$

Therefore, I will pick some submatrices of K obtained by deleting 2ξ rows and 2ξ columns, and show that their determinants are coprime as a whole. First, consider the submatrix

$$M_\xi = \begin{pmatrix} c_\xi & & & & \\ c_{\xi-1} & c_\xi & & & \\ \vdots & \ddots & \ddots & & \\ 0 & \cdots & c_{\xi-1} & c_\xi & \end{pmatrix}.$$

Clearly $\det(M_\xi) = c_\xi^{N-2\xi}$ since M_ξ is lower-triangular. Next, consider the submatrix

$$M_{\xi-1} = \begin{pmatrix} c_{\xi-1} & c_\xi & & & & \\ c_{\xi-2} & c_{\xi-1} & c_\xi & & & \\ \vdots & \ddots & \ddots & \ddots & & \\ 0 & \cdots & c_{\xi-2} & c_{\xi-1} & c_\xi & \\ 0 & 0 & \cdots & c_{\xi-2} & c_{\xi-1} & \end{pmatrix}.$$

When expanding $\det(M_{\xi-1})$ into a sum of terms using the definition of determinant, a term either is $c_{\xi-1}^{N-2\xi}$, or contains a factor of c_ξ . Thus $\det(M_{\xi-1}) = c_{\xi-1}^{N-2\xi} + Bc_\xi$ for some integer B . If some prime p divides both $\det(M_\xi)$ and $\det(M_{\xi-1})$, then

$$p|c_\xi^{N-2\xi} \implies p|c_\xi \implies p|c_{\xi-1}^{N-2\xi} \implies p|c_{\xi-1}.$$

Likewise, I define submatrices $M_{\xi-2}, \dots, M_0$, and show inductively that if p divides all $\det(M_k)$ then it also divides all c_k . This contradicts the assumption that $D(u)$ is primitive, so it must be the case that $\gcd\{\det(M_k)\} = 1$. Since a subset of minors is already coprime, the set (2.36) of all minors of order $N - 2\xi$ is also coprime, and hence Proposition 3 is proved.

2.7 Appendix: Determining K matrix from statistics

In this appendix, I answer the following question: Given the anyon fusion group and braiding statistics of a $d = 2 + 1$ abelian topological order, how does one construct a corresponding CS theory? More precisely, the setup of the problem consists of:

1. A finite abelian fusion group G , where the fusion product of x and y is $x + y$.
2. A symmetric bilinear form $b : G \times G \rightarrow \mathbb{Q}/\mathbb{Z}$ which determines the braiding phase $e^{-2\pi i b(x,y)}$ between anyons x and y . Bilinearity means that

$$b(x + y, z) = b(x, z) + b(y, z)$$

and similarly for the second argument.

3. A function $q : G \rightarrow \mathbb{Q}/2\mathbb{Z}$ which determines the topological spin $\theta_x = e^{-\pi i q(x)}$ of an anyon x . The functions q and b are related by

$$b(x, y) = \frac{1}{2} (q(x + y) - q(x) - q(y)).$$

With respect to a minimal generating set $\{e_1, \dots, e_n\}$ of G , q can be written as a matrix (q_{ij}) , where $q_{ii} = q(e_i) \in \mathbb{Q}/2\mathbb{Z}$ and $q_{ij} = b(e_i, e_j) \in \mathbb{Q}/\mathbb{Z}$ if $i \neq j$.

Note that b does not determine q even though the converse is true. Indeed, $q(x) = b(x, x) \bmod 1$, but $q(x)$ itself is defined mod 2. This is the minus sign ambiguity in determining exchange statistic from braiding statistic. I focus mainly on bosonic topological orders and assume modularity of the topological S -matrix. Here, modularity means that q is *non-degenerate*, i.e., if $b(x, y) = 0$ for all y , then $x = 0$. I will comment on fermionic topological orders at the end of this appendix.

The goal is to find a K matrix that produces the (G, q) specified above. Naively, this is achieved by inverting the matrix q . For example, the toric code has

$$q = \begin{pmatrix} 0 & \frac{1}{2} \\ \frac{1}{2} & 0 \end{pmatrix},$$

so a choice of K is

$$K = q^{-1} = \begin{pmatrix} 0 & 2 \\ 2 & 0 \end{pmatrix}.$$

However, q^{-1} is generally not an integer matrix. For example, the three-fermion theory [38] has $G = \mathbb{Z}_2 \times \mathbb{Z}_2$ and

$$q = \begin{pmatrix} 1 & \frac{1}{2} \\ \frac{1}{2} & 1 \end{pmatrix},$$

but q^{-1} is not an integer matrix in this case. Instead, q should be “enlarged” to \tilde{q} by adding transparent bosons (i.e., bosons that braid trivially with every anyon) to the bottom right corner:

$$\tilde{q} = \begin{pmatrix} 1 & \frac{1}{2} & 0 & 0 \\ \frac{1}{2} & 1 & 1 & 0 \\ 0 & 1 & 2 & 1 \\ 0 & 0 & 1 & 2 \end{pmatrix} \Rightarrow K = \tilde{q}^{-1} = \begin{pmatrix} 4 & -6 & 4 & -2 \\ -6 & 12 & -8 & 4 \\ 4 & -8 & 6 & -3 \\ -2 & 4 & -3 & 2 \end{pmatrix}.$$

To obtain an enlargement algorithm that works for arbitrary (G, q) , I follow the strategy by Wall [27, 39]: First I state a structure theorem for (G, q) , which classifies all irreducible building blocks of q and gives an algorithm for decomposing q into these blocks. Then I write down an enlargement for each irreducible block.

Structure theorem

The structure theorem is as follows:

Theorem 4. If (G, q) is non-degenerate, then G can be written as an *orthogonal direct product* $G = \prod_i G_i$, $b(x_i, x_j) = 0$ for all $i \neq j$, such that $(G_i, q|_{G_i})$ is in one of the following irreducible classes labelled by letters A through F :

1. $A_{2^k} \cong \mathbb{Z}_{2^k}$, and $q = (2^{-k})$.
2. $A_{p^k} \cong \mathbb{Z}_{p^k}$, $p > 2$ prime, and $q = (2\alpha p^{-k})$ where α is coprime with p and is a *quadratic residue* mod p (i.e., $\alpha = x^2 \pmod{p}$ for some x). Different choices of α lead to the same q up to a change of generator.
3. $B_{2^k} \cong \mathbb{Z}_{2^k}$, and $q = (-2^{-k})$.
4. $B_{p^k} \cong \mathbb{Z}_{p^k}$, $p > 2$ prime, and $q = (2\beta p^{-k})$ where β is coprime with p and is not a quadratic residue mod p . Different choices of β lead to the same q up to a change of generator.
5. $C_{2^k} \cong \mathbb{Z}_{2^k}$, $k \geq 2$, and $q = (5 \times 2^{-k})$.
6. $D_{2^k} \cong \mathbb{Z}_{2^k}$, $k \geq 2$, and $q = (-5 \times 2^{-k})$.
7. $E_{2^k} \cong \mathbb{Z}_{2^k} \times \mathbb{Z}_{2^k}$, and $q = \begin{pmatrix} 0 & 2^{-k} \\ 2^{-k} & 0 \end{pmatrix}$.
8. $F_{2^k} \cong \mathbb{Z}_{2^k} \times \mathbb{Z}_{2^k}$, and $q = \begin{pmatrix} 2^{1-k} & 2^{-k} \\ 2^{-k} & 2^{1-k} \end{pmatrix}$.

The decomposition into orthogonal direct product is not always unique. For example, $A_{p^k} \times A_{p^k} = B_{p^k} \times B_{p^k}$, and $A_2 \times A_2 \times A_2 = A_2 \times E_2$. The toric code is in class E_2 and the three-fermion theory is in F_2 .

Before explaining how the decomposition in Theorem 4 is performed, I state the following useful lemma:

Lemma 5. Let (G, q) be non-degenerate, H a subgroup of G such that $(H, q|_H)$ is non-degenerate. Then G is the orthogonal direct product of H and H° , where

$$H^\circ = \{g \in G : b(g, h) = 0 \text{ for all } h \in H\}$$

is the orthogonal complement of H . Furthermore, $(H^\circ, q|_{H^\circ})$ is also non-degenerate.

The decomposition in Theorem 4 can be performed with the following three steps:

- **Step 1.** G can be uniquely written as an orthogonal direct product

$$G = \prod_{p \text{ prime}} G_p, \quad (2.37)$$

where G_p is the unique Sylow p -subgroup of G .

- **Step 2.** Without loss of generality, replace G by G_p for fixed p . Let p^r be the *exponent* of G , i.e., the least common multiple of the orders of all elements in G . Write G as a (not necessarily orthogonal) direct product of a *homogeneous* subgroup H of exponent p^r , i.e., $H \cong \mathbb{Z}_{p^r}^m$ for some m , and another subgroup of smaller exponent. It can be shown that $(H, q|_H)$ is non-degenerate. By Lemma 5, $G = H \times H^\circ$ which is an orthogonal direct product, and H° has exponent smaller than p^r . Proceeding in this way, G can be decomposed into an orthogonal direct product of homogeneous subgroups.
- **Step 3.** Again without loss of generality, replace G by a homogeneous group of exponent p^r , $r \geq 1$. Look for $x \in G$ such that $p^r b(x, x) \in \mathbb{Z}_{p^r}$ is coprime with p . Such x need not exist when $p = 2$, but when it exists it is often easy to spot by inspection. However, for generality I present a more organized method; readers may skip this part and jump to Cases 3.1 and 3.2 below. Consider the subgroup $G_0 = \{g \in G : \text{ord}(g) \leq p^{r-1}\}$ of G , where $\text{ord}(g)$ is the order of g , and write $[x]$ for the coset containing x in G/G_0 . Define a new bilinear form $b' : (G/G_0) \times (G/G_0) \rightarrow \mathbb{Q}/\mathbb{Z}$ by

$$b'([x], [y]) = p^{r-1} b(x, y) \in \mathbb{Q}/\mathbb{Z}.$$

Now look for some $[x]$ such that $p b'([x], [x]) \in \mathbb{Z}_p$ is coprime with p . If $p \neq 2$, such $[x]$ always exists, and although this may still require an exhaustive search, the search is easier since G/G_0 has a smaller size than G . If $p = 2$, such $[x]$ exists if and only if the i th diagonal element of $p^{r-1} q$ is non-zero for some i , in which case the generating element $[e_i]$ satisfies the requirement. The next step depends on whether or not such $[x]$ is found:

Case 3.1. Some $[x] \in G/G_0$ is found with $p b'([x], [x])$ coprime with p . Then $(\langle x \rangle, q|_{\langle x \rangle})$ is non-degenerate, where $x \in [x]$ is an arbitrary coset representative and $\langle x \rangle$ is the subgroup of G generated by x . Now apply Lemma 5 which gives $G = \langle x \rangle \times \langle x \rangle^\circ$, and then go back to Step 3.

Case 3.2 (occurs only if $p = 2$). $b'([x], [x]) = 0$ for all $[x] \in G/G_0$. Pick some $x \in G$ of order 2^r , for example a generator $x = e_i$. It can be shown that there exists $y \in G$ (not necessarily unique) such that $b'([x], [y]) = 1/2$. Let $x \in [x]$ and

$y \in [y]$ be arbitrary coset representatives. Then $(\langle x, y \rangle, q|_{\langle x, y \rangle})$ is non-degenerate, and $\langle x, y \rangle \cong E_{2^r}$ or F_{2^r} . Now apply Lemma 5, and then go back to Step 3.

Recursive application of these steps leads to full decomposition of (G, q) .

Enlargement algorithm

Next, I describe how to enlarge the matrix q to \tilde{q} such that $K = \tilde{q}^{-1}$ is an integer matrix with even diagonal, so that K describes a bosonic CS theory. I assume without loss of generality that (G, q) is in one of the classes A through F .

1. $(G, q) \cong A_{2^r}, B_{2^r}$ or E_{2^r} . No enlargement is needed.
2. $(G, q) \cong A_{p^r}$ or B_{p^r} with $p > 2$. Write $q = (np^{-r})$ for some $-p^r < n < p^r$. Then there exist d_1 even and d_2 odd such that $1 = nd_1 - p^r d_2$ and $0 < d_2 < |d_1|$. Next, choose a_1 even such that $a_1 d_2$ is the closest even multiple of d_2 to d_1 , and write $d_1 = a_1 d_2 - d_3$. Applied repeatedly, this algorithm gives

$$\begin{aligned} 1 &= nd_1 - p^r d_2, \\ d_1 &= a_1 d_2 - d_3, \\ d_2 &= a_2 d_3 - d_4, \\ &\dots \\ d_{k-1} &= a_{k-1} d_k - 1, \\ d_k &= a_k, \end{aligned}$$

where $a_j d_{j+1}$ is always the closest even multiple of d_{j+1} to d_j . Then take

$$\tilde{q} = \begin{pmatrix} np^{-r} & 1 & & & & & & \\ & 1 & a_1 & 1 & & & & \\ & & 1 & a_2 & & & & \\ & & & & \ddots & & & \\ & & & & & a_{k-1} & 1 & \\ & & & & & 1 & a_k & \end{pmatrix}.$$

The algorithm employed here is a version of the *Euclidean algorithm*.

3. $(G, q) \cong C_{2^r}$ or D_{2^r} . The Euclidean algorithm still works, although in this case d_1 is odd and d_2 is even.
4. $(G, q) \cong F_{2^r}$. Take

$$\tilde{q} = \begin{pmatrix} 2^{1-r} & 2^{-r} & & & & & & \\ 2^{-r} & 2^{1-r} & & 1 & & & & \\ & & 1 & \frac{2}{3}(2^r + (-1)^{r-1}) & & & 1 & \\ & & & 1 & & & 2(-1)^{r-1} & \end{pmatrix}. \quad (2.38)$$

Example

I demonstrate the aforementioned theorems and algorithms with a coined example

$$G = \mathbb{Z}_8^5 = \langle e_1, \dots, e_5 \rangle,$$

$$q = \begin{pmatrix} \frac{5}{8} & \frac{1}{4} & \frac{1}{8} & 0 & \frac{3}{8} \\ \frac{1}{4} & \frac{5}{4} & 0 & \frac{7}{8} & \frac{1}{4} \\ \frac{1}{8} & 0 & \frac{5}{8} & \frac{7}{8} & \frac{3}{4} \\ 0 & \frac{7}{8} & \frac{7}{8} & \frac{3}{2} & \frac{1}{2} \\ \frac{3}{8} & \frac{1}{4} & \frac{3}{4} & \frac{1}{2} & \frac{7}{8} \end{pmatrix}. \quad (2.39)$$

Since G is already homogeneous, the decomposition algorithm starts at Step 3. First, $e_1^T q e_1 = 5/8$ has additive order 8 mod 1, so $(\langle e_1 \rangle, q|_{\langle e_1 \rangle})$ is non-degenerate. The orthogonal complement $\langle e_1 \rangle^\circ = \langle f_1, f_2, f_3, f_4 \rangle$, where $f_1 = -2e_1 + e_2$, $f_2 = e_1 + 3e_3$, $f_3 = e_4$, and $f_4 = e_1 + e_5$. With respect to these generators, define

$$q_1 = q|_{\langle e_1 \rangle^\circ} = \begin{pmatrix} \frac{3}{4} & \frac{1}{4} & \frac{7}{8} & \frac{1}{2} \\ \frac{1}{4} & 1 & \frac{5}{8} & \frac{5}{8} \\ \frac{7}{8} & \frac{5}{8} & \frac{3}{2} & \frac{1}{2} \\ \frac{1}{2} & \frac{5}{8} & \frac{1}{2} & \frac{1}{4} \end{pmatrix}.$$

Since all diagonal entries of q_1 have denominators at most 4, the algorithm enters Case 3.2. Choose any generator of $\langle e_1 \rangle^\circ$, say f_1 . The equation $f_1^T q_1 y = 1/8$ has a solution $y = -f_3$. The orthogonal complement of $\langle f_1, -f_3 \rangle$ is

$$\langle f_1, -f_3 \rangle^\circ = \langle -3f_1 + f_2, 4f_1 + 4f_3 + f_4 \rangle.$$

With respect to the generators $\{f_1, -f_3, -3f_1 + f_2, 4f_1 + 4f_3 + f_4\}$,

$$q_1 = q_2 \oplus q_3 = \begin{pmatrix} \frac{3}{4} & \frac{1}{8} \\ \frac{1}{8} & \frac{3}{2} \end{pmatrix} \oplus \begin{pmatrix} \frac{1}{4} & \frac{1}{8} \\ \frac{1}{8} & \frac{1}{4} \end{pmatrix},$$

where \oplus is the direct sum of matrices on the direct product group. Picking appropriate generators $\{f_1 + f_3, 2f_1 - 3f_3\}$, the matrix q_2 is put into a standard form

$$q_2 = \begin{pmatrix} 0 & \frac{1}{8} \\ \frac{1}{8} & 0 \end{pmatrix}.$$

To summarize, the decomposition is

$$q \cong \begin{pmatrix} \frac{5}{8} \\ \frac{1}{8} \end{pmatrix} \oplus \begin{pmatrix} 0 & \frac{1}{8} \\ \frac{1}{8} & 0 \end{pmatrix} \oplus \begin{pmatrix} \frac{1}{4} & \frac{1}{8} \\ \frac{1}{8} & \frac{1}{4} \end{pmatrix} \cong C_8 \times E_8 \times F_8 \quad (2.40)$$

with respect to the generators $\{e_1, f_1 + f_3, 2f_1 - 3f_3, -3f_1 + f_2, 4f_1 + 4f_3 + f_4\}$. This decomposition is not unique. It can be shown that

$$q \cong \begin{pmatrix} \frac{5}{8} \\ -\frac{1}{8} \end{pmatrix} \oplus \begin{pmatrix} -\frac{1}{8} \\ -\frac{1}{8} \end{pmatrix} \oplus \begin{pmatrix} -\frac{1}{8} \\ -\frac{1}{8} \end{pmatrix} \oplus \begin{pmatrix} -\frac{1}{8} \\ -\frac{5}{8} \end{pmatrix} \quad (2.41)$$

with respect to some other generators. Next, each summand in (2.40) needs to be enlarged. To enlarge the C_8 , apply the Euclidean algorithm:

$$\begin{aligned} 1 &= 5 \times 13 - 8 \times 8, \\ 13 &= 2 \times 8 - 3, \\ 8 &= 2 \times 3 - (-2), \\ 3 &= (-2) \times (-2) - 1, \\ -2 &= (-2) \times 1. \end{aligned}$$

This gives the enlargement

$$\left(\frac{5}{8}\right) \mapsto \begin{pmatrix} \frac{5}{8} & 1 & & & \\ 1 & 2 & 1 & & \\ & 1 & 2 & 1 & \\ & & 1 & -2 & 1 \\ & & & 1 & -2 \end{pmatrix}.$$

The E_8 does not need enlargement, and the F_8 can be enlarged to (2.38).

Summarizing the above, the total K^{-1} matrix is

$$K^{-1} = \begin{pmatrix} \frac{5}{8} & 1 & & & \\ 1 & 2 & 1 & & \\ & 1 & 2 & 1 & \\ & & 1 & -2 & 1 \\ & & & 1 & -2 \end{pmatrix} \oplus \begin{pmatrix} 0 & \frac{1}{8} \\ \frac{1}{8} & 0 \end{pmatrix} \oplus \begin{pmatrix} \frac{1}{4} & \frac{1}{8} & & \\ \frac{1}{8} & \frac{1}{4} & 1 & \\ & 1 & 6 & 1 \\ & & 1 & 2 \end{pmatrix},$$

and the total K matrix is

$$K = \begin{pmatrix} 104 & -64 & 24 & 16 & 8 \\ -64 & 40 & -15 & -10 & 5 \\ 24 & -15 & 6 & 4 & 2 \\ 16 & -10 & 4 & 2 & 1 \\ 8 & -5 & 2 & 1 & 0 \end{pmatrix} \oplus \begin{pmatrix} 0 & 8 \\ 8 & 0 \end{pmatrix} \oplus \begin{pmatrix} 48 & -88 & 16 & -8 \\ -88 & 176 & -32 & 16 \\ 16 & -32 & 6 & -3 \\ -8 & 16 & -3 & 2 \end{pmatrix}.$$

This is one of many choices of K that give rise to (2.39). Another choice of K can be derived, for example, from (2.41).

Fermionic case

Finally, I consider fermionic topological orders. In this case, a local fermion is both a non-trivial superselection sector and transparent in terms of braiding. Therefore, the non-degeneracy assumption should be modified. I assume that (G, q) is *weakly non-degenerate*, meaning that if $b(x, y) = 0$ for all y and $q(x) = 0$, then $x = 0$.

Suppose that ψ is a transparent fermion. Since ψ has order 2 in G , it falls in G_2 in the decomposition (2.37). Suppose that $\psi = mx$ for some $m \in \mathbb{Z}$ and $x \in G_2$. Then

$$\begin{aligned} 0 &= b(x, 2\psi) = 2mb(x, x) \pmod{2}, \\ 1 &= q(\psi) = m^2b(x, x) \pmod{2}, \end{aligned}$$

so m is odd. However, $2\psi = 2mx = 0 \in G_2$, so $2x = 0$ and hence $\psi = x$. This shows that ψ is not a non-trivial multiple of any x , so G_2 can be decomposed into an orthogonal direct product of $\langle \psi \rangle = \{0, \psi\}$ and $\langle \psi \rangle^\circ$. The end result of this process is the decomposition $G = \mathbb{Z}_2^r \times G'$, where each copy of \mathbb{Z}_2 is generated by a transparent fermion and $(G', q|_{G'})$ is non-degenerate. The bosonic theorems and algorithms can then be applied to $(G', q|_{G'})$.

As an example, consider the $\nu = 1/3$ fractional quantum Hall state. Treated as a bosonic theory, the fusion group is $G = \mathbb{Z}_6 = \langle x \rangle$, and $q = (1/3)$. This theory is weakly non-degenerate, and $3x$ is a transparent fermion. Thus by the discussion above, $G = \mathbb{Z}_2 \times \mathbb{Z}_3 = \langle 3x \rangle \times \langle 2x \rangle$. Now $(\langle 2x \rangle, q|_{\langle 2x \rangle})$ is non-degenerate, where

$$q|_{\langle 2x \rangle} = \begin{pmatrix} 4 \\ 3 \end{pmatrix} = \begin{pmatrix} -2 \\ -3 \end{pmatrix}.$$

The Euclidean algorithm can then be applied to enlarge it to

$$\tilde{q} = \begin{pmatrix} -\frac{2}{3} & 1 \\ 1 & -2 \end{pmatrix} \implies K = \tilde{q}^{-1} = \begin{pmatrix} -6 & -3 \\ -3 & -2 \end{pmatrix}.$$

Finally, the transparent fermion can be restored to give the 3×3 matrix $K \oplus (1)$, which can then be transformed as follows:

$$W \begin{pmatrix} -6 & -3 & \\ -3 & -2 & \\ & & 1 \end{pmatrix} W^T = \begin{pmatrix} 3 & & \\ & -1 & \\ & & -1 \end{pmatrix},$$

where

$$W = \begin{pmatrix} 1 & 0 & 3 \\ 0 & 1 & 1 \\ -1 & 1 & -1 \end{pmatrix}.$$

This shows the equivalence of $K \oplus (1)$, up to decoupled integer quantum Hall states, with the standard K matrix (3) for the $\nu = 1/3$ fractional quantum Hall state.

GAPPED INFINITE-COMPONENT CHERN-SIMONS THEORY

Having prepared the necessary physics and mathematics of periodic CS theories in $d = 2 + 1$ in Chapter 2, I now generalize the theories to fracton models in $d = 3 + 1$. The resulting models not only expand the already large reservoir of fracton models, but more importantly bring up questions concerning the notion of fractonic orders. Indeed, as will be shown in Section 3.2, by far the most fracton models obtained from CS theories do not fit into the foliation paradigm.

The generalization works as follows: Take a CS theory (2.1) whose K matrix has period r and size rN . The indices i and j of K can be viewed as living in a new spatial direction, the z direction. In the thermodynamic limit $N \rightarrow \infty$, the theory becomes a model in $d = 3 + 1$. Such a theory is called an infinite-component Chern-Simons (CS_∞) theory since it has infinitely many gauge field components. Some CS_∞ theories have been studied in the context of $d = 3 + 1$ quantum Hall systems [40–43] where certain unusual properties of braiding statistics, edge states, etc. of such theories were first pointed out. By the spectrum (2.2), a CS_∞ theory is gapped if and only if its determinant polynomial $D(u)$ has no root on the unit circle. In this chapter, I focus on gapped CS_∞ theories, leaving gapless theories to Chapter 4.

Intuitively, the anyons of a CS theory become planons of the corresponding CS_∞ theory restricted to various xy planes, and the latter theory is therefore a fracton model. Since there is no true fracton excitation in a CS_∞ theory that is completely localized on its own, CS_∞ theories are relatively simple fracton models in terms of excitation mobility. However, it is well-known that a CS theory cannot be put on a lattice by naive discretization, and that locality in the CS theory does not always correspond to locality in the lattice model (if one exists). To confirm the legitimacy of the field theories, I present lattice models of CS_∞ theories with quasi-diagonal K matrices in Section 3.3. Here, K is *quasi-diagonal* if all non-zero entries of K are within some finite distance (mod rN) from the diagonal, which was always assumed in Chapter 2. I also show that planons in gapped CS_∞ theories are point excitations with exponentially decaying profiles. Until Section 3.3, I will assume the validity of CS_∞ theories and use the intuitive picture of planons without justification. In Section 3.1, I study the foliation RG applied to CS_∞ theories, and discuss an example of a foliated theory. In Section 3.2, I derive a necessary condition for a CS_∞ theory to be foliated, and discuss an example of a non-foliated theory.

The results in this chapter are based on Refs. [26, 28].

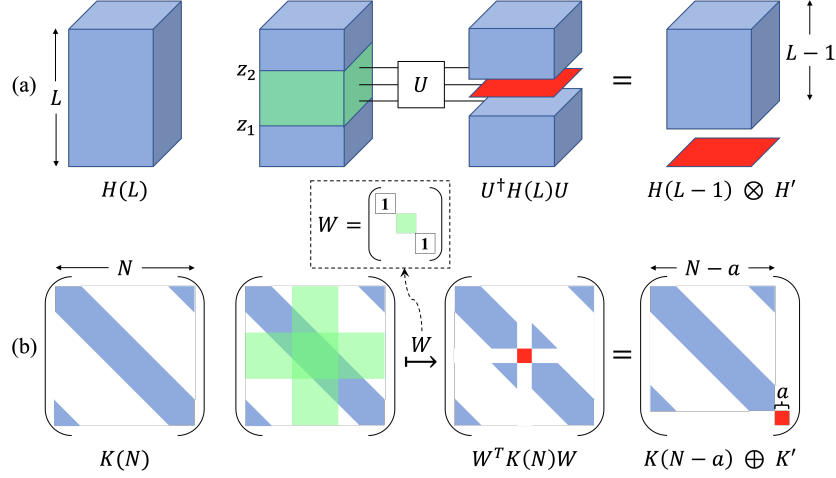


Figure 3.1: The foliation RG on a CS_∞ theory. In subfigure (a), the RG is implemented as a finite-depth local unitary circuit which extracts a $d = 2 + 1$ resource layer. Correspondingly in subfigure (b), the RG acts on the K matrix and decouples a block K' .

3.1 Foliation RG and foliated theories

In this section, I first explain the foliation RG in the context of CS_∞ theories, and then discuss an example of a foliated CS_∞ theory.

Foliation from K matrix

As mentioned in Chapter 1, the foliation RG may perform local unitaries as well as add or remove decoupled $d = 2 + 1$ topological resource states. This is illustrated in Fig. 3.1 (a) (first line), where a system with Hamiltonian $H(L)$ starts with size L in the z direction. A finite-depth local unitary circuit U is applied to the green region defined by $z_1 \leq z \leq z_2$. The result is the same system with Hamiltonian $H(L-1)$ of size $L-1$ in the z direction, together with a decoupled $d = 2 + 1$ gapped system H' (red layer). In a generic fracton model, the foliation RG may be able to change the system size in more than one direction. In a CS_∞ theory, however, non-trivial topological states can only be added or removed in the z direction, if this is possible at all. Furthermore, the foliation RG on a CS_∞ theory has a simple interpretation in terms of the K matrix. As shown in Fig. 3.1 (b) (second line), a quasi-diagonal $K(N)$ starts with size $N \propto L$. Only entries in the blue region can be non-zero. The RG first applies the transformation $K(N) \mapsto W^T K(N) W$, where $W \in \text{GL}_N(\mathbb{Z})$ shown in the dashed box is equal to the identity except in the green block. The action of W on $K(N)$ is within the green cross in the second figure. The result is the direct sum of the same system $K(N-a)$ of size $N-a$ and a decoupled block K' of size $a = O(1)$ (red block).

Example

As a concrete example, consider

$$K = \begin{pmatrix} & m_0 & e_1 & m_1 & e_2 & m_2 & e_3 & m_3 \\ \dots & & & & & & & \\ & 0 & 2 & -1 & & & & \\ & 2 & 0 & & & & & \\ -1 & & 0 & 2 & -1 & & & \\ & & 2 & 0 & & & & \\ & & -1 & & 0 & 2 & -1 & \\ & & & & 2 & 0 & & \\ & & & & -1 & & 0 & \\ & & & & & & & \dots \end{pmatrix}, \quad (3.1)$$

where the column labels are displayed on the top and their meaning will be explained soon. This K matrix describes a twisted one-foliated fracton model [24]. The theory is represented in the polynomial description as

$$K(u) = \begin{pmatrix} -u - u^{-1} & 2 \\ 2 & 0 \end{pmatrix},$$

and $D(u) = -4$. By (2.7), if K has size $2N$, then $\text{GSD} = 4^N$. The anyon statistics of the theory can be read off from

$$K^{-1} = \frac{1}{4} \begin{pmatrix} & m_0 & e_1 & m_1 & e_2 & m_2 & e_3 & m_3 \\ \dots & & & & & & & \\ & 0 & & 1 & & & & \\ & & 0 & 2 & & & & \\ 1 & 2 & 0 & & 1 & & & \\ & & & 0 & 2 & & & \\ & & 1 & 2 & 0 & & 1 & \\ & & & & & 0 & 2 & \\ & & & & 1 & 2 & 0 & \\ & & & & & & & \dots \end{pmatrix}.$$

This explains the naming of the column labels, because the braiding statistics of e_i and m_i are similar to those in a \mathbb{Z}_2 gauge theory where the e and m excitations are bosons and have braiding statistic -1 . However, this K matrix does not represent a simple decoupled stack of \mathbb{Z}_2 gauge theories, because neighboring m excitations have braiding statistic i . This suggests that if the theory is foliated as was claimed, then the $d = 2 + 1$ resource states should be some twisted gauge theory. Indeed, the

foliation RG can be implemented by

$$W = \begin{matrix} & \tilde{e}_0 & \tilde{m}_0 & \tilde{e}^A & \tilde{m}^A & \tilde{e}^B & \tilde{m}^B & \tilde{e}_1 & \tilde{m}_1 \\ \begin{matrix} e_0 \\ m_0 \\ e_1 \\ m_1 \\ e_2 \\ m_2 \\ e_3 \\ m_3 \end{matrix} & \begin{pmatrix} \ddots & & & & & & & & \\ & 1 & & & & & & & \\ & & 1 & & & & 1 & & \\ & & & 1 & & & & -1 & \\ & -1 & & & 1 & & & & \\ & & & & & 1 & & & \\ & & & & & & & 1 & \\ & -1 & & 1 & & & & & 1 \\ & & & & & & & & \ddots \end{pmatrix} \end{matrix}.$$

Outside the region displayed above, W is the identity matrix. The action of W is

$$W^T K W = \begin{matrix} & \tilde{e}_0 & \tilde{m}_0 & \tilde{e}^A & \tilde{m}^A & \tilde{e}^B & \tilde{m}^B & \tilde{e}_1 & \tilde{m}_1 \\ \begin{matrix} \\ \\ \\ \\ \\ \\ \\ \\ \end{matrix} & \begin{pmatrix} \ddots & & & & & & & & \\ & 0 & 2 & & & & & -1 & \\ & 2 & 0 & & & & & & \\ & & & 0 & 2 & -1 & 0 & & \\ & & & 2 & 0 & 0 & 0 & & \\ & & & -1 & 0 & 0 & 2 & & \\ & & & 0 & 0 & 2 & 0 & & \\ -1 & & & & & & & 0 & 2 \\ & & & & & & & 2 & 0 \\ & & & & & & & & \ddots \end{pmatrix} \end{matrix}. \quad (3.2)$$

The middle 4×4 block is decoupled from the rest of the system, and describes a twisted $\mathbb{Z}_2 \times \mathbb{Z}_2$ gauge theory with anyons \tilde{e}^A , \tilde{m}^A , \tilde{e}^B , \tilde{m}^B and their composites. If the middle 4×4 block is removed, then $W^T K W$ becomes a smaller version of (3.1). Therefore, the theory (3.1) is indeed foliated.

3.2 Criterion for foliation and non-foliated theories

While some CS_∞ theories are foliated fracton models, a more surprising finding is that most CS_∞ theories are actually not foliated. In this section, I prove a necessary condition for a CS_∞ theory to be foliated, and formulate the converse (sufficiency of the necessary condition) as an unresolved mathematical problem. I also discuss an example of a non-foliated CS_∞ theory.

Necessary condition

The necessary condition for foliation is as follows:

Proposition 6. A CS_∞ theory is foliated only if its determinant polynomial $D(u)$ is a constant.

As a sanity check, the foliated theory (3.1) has $D(u) = -4$. Also, by far the most CS_∞ theories do not have constant $D(u)$ and are thus not foliated. In particular, a CS_∞ theory with period $r = 1$ is foliated if and only if its K matrix is diagonal, in which case the theory is a simple stack of $d = 2 + 1$ topological orders.

To prove Proposition 6, I start with the observation that the GSD of a foliated theory must be of the **strictly** exponential form ab^N for some constants a and b . This is because the foliation RG always uses the same $d = 2 + 1$ resource state, and the constant b is thus the GSD of this resource state. To be a bit more careful, note that the K matrix (3.1) has period $r = 2$ while the resource state has a K matrix of size 4, as shown in (3.2). In general, the foliation RG may require enlarging r and hence shrinking N . Nevertheless, with an appropriate choice of r and N , the GSD must be of the form ab^N . Therefore, it suffices to prove the following lemma:

Lemma 7. If $D(u)$ is not a constant, then the GSD sequence $\{\text{GSD}_N\}$ has no subsequence $\{\text{GSD}_{mN}\}$, where m is a positive integer, that depends on N strictly exponentially.

For simplicity, I prove Lemma 7 for $m = 1$, i.e., the entire sequence $\{\text{GSD}_N\}$. This may seem obvious by looking at (2.7), but it is safer to have a proof. The proof can be generalized easily to arbitrary m . Since (2.7) can be written as a finite sum of exponentials in N , the sequence $\{\text{GSD}_N\}$ is the solution to a finite order linear recurrence relation

$$\lambda_t \text{GSD}_{N+t} + \lambda_{t-1} \text{GSD}_{N+t-1} + \cdots + \lambda_0 \text{GSD}_N = 0, \quad (3.3)$$

where λ_i are constants and $\lambda_t, \lambda_0 \neq 0$. Thus t is the order of the recurrence relation. If $\text{GSD}_N = ab^N$, then $\text{GSD}_N/ab^N = 1$ is also a sum of exponentials. Therefore without loss of generality, I assume that $\text{GSD}_N = 1$ for all positive integer N . Given initial conditions, a recurrence relation works both forwards and backwards. For (3.3), initial conditions can be specified by the values of t consecutive terms of the sequence. For example,

$$\text{GSD}_2 = \cdots = \text{GSD}_{N+1} = 1 \implies \text{GSD}_1 = 1.$$

Therefore, if t consecutive terms are 1, then the previous term must also be 1. This conclusion holds for all integer N , not necessarily positive, so

$$\text{GSD}_1 = \cdots = \text{GSD}_N = 1 \implies \text{GSD}_0 = 1.$$

Of course, $N \leq 0$ does not make sense physically, but the point here is that the mathematical formula (2.7) must yield 1 for all integer N . However, if $D(u)$ has any

root u_l , then (2.7) implies that $\text{GSD}_0 = 0$, which is a contradiction. The conclusion is that $D(u)$ cannot have a root and is hence a constant. The same proof also works for any subsequence $\{\text{GSD}_{mN}\}$, since it is still a sum of exponentials in N and can still be extended to GSD_0 . This completes the proof of Proposition 6.

Example

As a concrete example, consider the CS_∞ theory with period $r = 1$ and

$$K(u) = (D(u)) = (u + 3 + u^{-1}). \quad (3.4)$$

This is essentially (2.9) with large N . By Proposition 6, this theory is not foliated. Its GSD is given by (2.10), which is not strictly exponential in N . For large N , the GSD is asymptotically exponential in N with an irrational base $(3 + \sqrt{5})/2$. By (2.13), for $1 \ll |i - j| \ll N$, the charges of A_μ^i and A_μ^j have a braiding statistic that decays with an irrational base $(3 - \sqrt{5})/2$. Therefore, the braiding statistics are not strictly local, which is impossible in a foliated theory. In a foliated model, when each resource layer is inserted, the foliation RG may apply a local unitary to incorporate the layer into the bulk. The anyons that come from the layers may therefore acquire a different (but still local) profile in the z direction when becoming a planon. In particular, if the unitaries have exponentially decaying tails, then so can the planon profiles, which is not surprising. However, it is impossible for the planons to have exponentially decaying tails in their statistics since unitary transformations cannot change statistics. The only residual freedom when mapping the anyons in the resource layers into planons is to relabel them, i.e., to choose new generators of the fusion group, but this $\text{GL}_N(\mathbb{Z})$ transformation cannot produce exponentially decaying tails in the statistics.

Furthermore, as mentioned in Section 2.6, numerics suggest that the fusion group G of the theory (3.4) is given by (2.35). Although (2.35) is not proved, Proposition 3 shows that G has at most two cyclic components. Therefore, planons become more and more fractionalized as N increases. In contrast, the fusion group of a foliated CS_∞ theory must be of the form $G = H \times G_0^N$, where H is an overhead, G_0 is the fusion group of the resource layer, and N is defined appropriately for the foliation RG. All of these peculiar features are shared by gapped CS_∞ theories with non-constant $D(u)$, and new notions of phases beyond foliation need to be invented for such theories to be understood in a unified picture.

Conjecture on sufficiency

Finally, I comment on the converse of Proposition 6. Since the period $r = 1$ case is a clear dichotomy, I assume that $r > 1$. If $D(u)$ is a constant, then the GSD is strictly exponential in N , the statistics are strictly local in the z direction, and the

fusion group is not well-understood. Therefore, there is no obvious evidence against foliation, but neither have I managed to prove foliation. Nevertheless, I will propose a conjecture, in the hope that it will be proved or disproved in the future.

The conjecture uses the polynomial description, where the foliation RG is applied to a CS_∞ theory periodically to add or remove multiple resource layers simultaneously. Consider quasi-diagonal $W \in \text{GL}_N(\mathbb{Z})$ with the same period r as K . By (2.7), $W(u)$ satisfies $\det(W(u)) = \pm 1$. Then all entries of $W(u)^{-1} = \pm \text{Adj}(W(u))$ have finitely many terms, so W^{-1} is also quasi-diagonal. This means that both W and W^{-1} preserve locality in the z direction (see more discussions of locality in Section 3.3), so at least in the sense of a quantum cellular automaton [44], W is a valid transformation of K . Let $L = \mathbb{Z}[u, u^{-1}]$ be the ring of Laurent polynomials with integer coefficients. Mathematically, $K(u)$ is a Hermitian bilinear form on the L -module $M = L^r$, with involution $p^\dagger(u) = p(u^{-1})$. The discussion of locality above shows that every mathematically legitimate basis of L^r is also physically legitimate. Therefore, the module M can be viewed abstractly without specifying a basis.

Now I describe the mathematical procedure for enlarging the period of K from r to nr . I start with a simple example where $r = 1$,

$$K(u) = (c_3u^3 + c_2u^2 + c_1u + c_0 + c_1u^{-1} + c_2u^{-2} + c_3u^{-3}),$$

and $n = 2$. After the period is doubled, $K(u)$ is transformed to

$$K_2(u) = \begin{pmatrix} c_2u + c_0 + c_2u^{-1} & c_3u + c_1 + c_1u^{-1} + c_3u^{-2} \\ c_3u^2 + c_1u + c_1 + c_3u^{-1} & c_2u + c_0 + c_2u^{-1} \end{pmatrix}.$$

Heuristically, $K_2(u)$ is obtained from $K(u)$ by grouping together the c_k terms according to $k \bmod 2$, and then changing the powers of u from k to $k/2$ (rounded up or down if needed). To generalize this example, let $L_n = \mathbb{Z}[u^n, u^{-n}]$, a subring of L . There is a ring isomorphism $\phi : L \rightarrow L_n$ given by $\phi(u) = u^n$, as well as a projection of L_n -modules $\pi : L \rightarrow L_n$ given by

$$\pi(u^k) = \begin{cases} u^k, & \text{if } n|k, \\ 0, & \text{otherwise.} \end{cases}$$

Since L_n is a subring of L , the L -module M is naturally also an L_n -module of dimension nr . I denote the latter by M_n , which is the same set as M but with a different underlying ring. For example, if $r = 3$, $n = 2$ and $\{e_1, e_2, e_3\}$ is a basis for M , then $\{e_1, e_2, e_3, u^{-1}e_1, u^{-1}e_2, u^{-1}e_3\}$ is a basis for M_n . Through ϕ , the L_n -module M_n can also be viewed as an L -module. To reiterate, M and M_n are both L -modules, but with different actions of L . The original bilinear form $K(u)$ should be replaced by a new bilinear form $K_n(u)$ on the L -module M_n , given by

$$K_n(u) : M_n \times M_n \xrightarrow{K(u)} L \xrightarrow{\pi} L_n \xrightarrow{\phi^{-1}} L.$$

Written as a matrix, $K_n(u)$ has size nr and its entries take values in L , as expected. The conjecture is as follows:

Conjecture 8. If $D(u) = \det(K(u))$ is a constant, then there exist integers $0 < m < n$ and $W(u) \in \text{GL}_{nr}(L)$ such that

$$W^T(u)K_n(u)W(u) = K_m(u) \oplus R(u),$$

where $R(u)$ is a matrix of size $n - m$ whose entries are all constants.

If Conjecture 8 is true, then $R(u)$ describes a stack of decoupled resource layers, and the theory is therefore foliated. In an alternative, weaker version of the conjecture, the requirement that $R(u)$ be a constant matrix may be loosened or dropped, giving a generalized definition of foliation. Even more generally, $K(u)$ may not be an RG fixed point, and $K_m(u)$ in Conjecture 8 may be replaced by some other matrix $K'(u)$ which itself is an RG fixed point.

3.3 Lattice construction

So far in this chapter, I have studied properties of CS_∞ theories without addressing a crucial question: Are CS_∞ theories legitimate $d = 3 + 1$ models? In particular, can the indices i and j of K really be interpreted as spatial coordinates? After all, the CS gauge fields A^i are not local degrees of freedom and can have complicated commutation relations. For example, when the Maxwell coupling $g \rightarrow \infty$,

$$[A_x^i, A_y^j] \propto (K^{-1})_{ij}.$$

In the non-foliated theory (3.4), for example, K^{-1} is given by (2.13) and all of its entries are non-zero. This means that if i and j are interpreted naively as spatial coordinates in the z direction, then the gauge field A^i in the i th layer has a non-trivial commutation relation with the gauge field A^j in the j th layer even though they are very far apart.

The problem of interpreting the indices i and j is also related to the question of what the fractional excitations look like and, in particular, whether an excitation whose charge vector is a standard basis vector e_i has a local profile in the z direction. In the CS formulation, the answer to the latter seems to be positive, because such an excitation is a unit gauge charge of the gauge field A^i and can be created (in the $g \rightarrow \infty$ limit) simply by the Wilson line of A^i . However, this appears to be at odds with the fact that the i th excitation has a non-trivial braiding statistic with the j th excitation no matter how far apart they are.

In this section, I clarify these issues by presenting a lattice construction whose low-energy effective theory is given by (2.1). This construction works for any CS_∞ theory with a quasi-diagonal K matrix, i.e., an integer symmetric matrix whose entries are

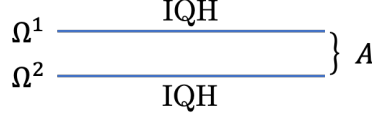


Figure 3.2: Lattice model realizing $K = (2)$. The matter content of the system is two IQH layers Ω^1 and Ω^2 (blue lines) with Chern number $C^l = 1$. The layers are coupled each with unit charge to a dynamical U(1) gauge fields A .

bounded by some finite number and are zero beyond a certain distance from the main diagonal (with periodic boundary condition). Therefore, all such CS_∞ theories are legitimate $d = 3 + 1$ local models. I also write down the explicit forms of the string operators of fractional excitations and show that in gapped CS_∞ theories, the elementary excitations are local in the z direction and are hence point excitations.

Lattice model

For clarity, I start with a toy example $K = (2)$, which contains much of the relevant physics despite its simplicity. I then proceed to the less trivial example of the non-foliated theory (3.4). Finally, I generalize the lattice construction to an arbitrary quasi-diagonal K with bounded entries.

The $K = (2)$ CS theory is known to be realizable as a chiral spin liquid [45]. Here, I instead present a more complicated construction so that it can be generalized to CS_∞ theories. First, take two integer quantum Hall (IQH) layers Ω^l , $l = 1, 2$, with Chern number $C^l = 1$ (Fig. 3.2). Each layer is a free fermion hopping model in the xy plane. The fermions in each layer carry unit charge under a charge conservation symmetry, which can be gauged by coupling to a dynamical U(1) gauge field A_μ . The gauging procedure starts by adding gauge degrees of freedom $A_{\mathbf{r}\mathbf{r}'}$ on the horizontal links $\langle \mathbf{r}\mathbf{r}' \rangle$ of the lattice, where \mathbf{r} and \mathbf{r}' are vectors with two components labelling the sites in each layer. As usual, I define the electric field $E_{\mathbf{r}\mathbf{r}'}$ as the conjugate momentum of $A_{\mathbf{r}\mathbf{r}'}$, with $[A_{\mathbf{r}\mathbf{r}'}, E_{\mathbf{r}\mathbf{r}'}] = i$. The Hamiltonian after gauging is

$$\begin{aligned}
 H = & \sum_{l=1,2} \sum_{\langle \mathbf{r}\mathbf{r}' \rangle} u_{\mathbf{r}\mathbf{r}'} e^{iA_{\mathbf{r}\mathbf{r}'}} c_{l,\mathbf{r}'}^\dagger c_{l,\mathbf{r}} \\
 & + \sum_{\langle \mathbf{r}\mathbf{r}' \rangle} g_E (E_{\mathbf{r}\mathbf{r}'})^2 - g_B \sum_p \cos B_p + g_Q \sum_{\mathbf{r}} (Q_{\mathbf{r}})^2,
 \end{aligned} \tag{3.5}$$

where $u_{\mathbf{r}\mathbf{r}'}$ is the IQH hopping coefficient with Chern number $C^l = 1$, B_p is the flux of A through plaquette p , and

$$Q_{\mathbf{r}} = (\nabla \cdot \mathbf{E})_{\mathbf{r}} - \sum_{l=1,2} c_{l,\mathbf{r}}^\dagger c_{l,\mathbf{r}} \tag{3.6}$$

is the Gauss's law term (Fig. 3.3). Note that the Gauss's law is imposed here as an energetic constraint rather than a Hilbert space constraint.

$$B_p^i = A_{12}^i + A_{23}^i + A_{34}^i + A_{41}^i$$

$$Q_r^i = E_{r1}^i + E_{r2}^i + E_{r3}^i + E_{r4}^i - \sum_l q^{il} c_{l,r}^\dagger c_{l,r}$$

Figure 3.3: The flux and Gauss's law terms in the lattice Hamiltonian of a CS or CS_∞ theory. In the example $K = (2)$, the index i is dropped, and $q^{il} = 1$ for $l = 1, 2$.

At low energy, the model is described by an effective CS theory

$$\mathcal{L} = -\frac{1}{4\pi} \sum_{l=1,2} C^l \epsilon^{\mu\nu\lambda} a_\mu^l \partial_\nu a_\lambda^l + \frac{1}{2\pi} \sum_{l=1,2} \epsilon^{\mu\nu\lambda} A_\mu \partial_\nu a_\lambda^l,$$

where a_μ^l is the emergent U(1) gauge field of the IQH layer Ω^l , and the Maxwell term is omitted. The K matrix of this theory with respect to the basis (a^1, a^2, A) is

$$K_0 = \begin{pmatrix} -1 & 0 & 1 \\ 0 & -1 & 1 \\ 1 & 1 & 0 \end{pmatrix}. \quad (3.7)$$

Note that an IQH layer with Chern number 1 corresponds to a -1 in the K matrix. Now apply the transformation $K_0 \mapsto \tilde{K}_0 = W^T K_0 W$ with

$$W = \begin{pmatrix} 1 & 0 & 1 \\ 0 & 1 & 1 \\ 0 & 0 & 1 \end{pmatrix}.$$

This gives

$$\tilde{K}_0 = \begin{pmatrix} -1 & 0 & 0 \\ 0 & -1 & 0 \\ 0 & 0 & 2 \end{pmatrix}$$

in terms of the new fields

$$\begin{pmatrix} \tilde{a}^1 \\ \tilde{a}^2 \\ \tilde{A} \end{pmatrix} = W^{-1} \begin{pmatrix} a^1 \\ a^2 \\ A \end{pmatrix} = \begin{pmatrix} a^1 - A \\ a^2 - A \\ A \end{pmatrix}.$$

As desired, \tilde{K}_0 contains the decoupled block $K = (2)$ in its lower right corner. It also contains two decoupled IQH layers, but these have no anyon content. Therefore, the lattice construction described here realizes not exactly the $K = (2)$ theory, but a very close fermionic cousin of it represented by \tilde{K}_0 .

Next, I discuss the non-foliated CS_∞ theory (3.4). To realize this theory as a lattice model, take infinitely many IQH layers Ω^l , $l \in \mathbb{Z}$, each with Chern number $C^l = 1$. Then couple the layers to infinitely many dynamical $U(1)$ gauge fields A^i , $i \in \mathbb{Z}$, as follows (Fig. 3.4): Fermions in layers $\Omega^1, \Omega^2, \Omega^3$ have unit charge under A^1 , those in layers $\Omega^3, \Omega^4, \Omega^5$ have unit charge under A^2 , those in layers $\Omega^5, \Omega^6, \Omega^7$ have unit charge under A^3 , etc. This model has an effective CS_∞ theory with K matrix

$$K_0 = \begin{pmatrix} \ddots & & & & & & & & \\ & -1 & 1 & & & & & & \\ & & -1 & 1 & & & & & \\ & 1 & 1 & 0 & 1 & & & & \\ & & & 1 & -1 & & 1 & & \\ & & & & & -1 & 1 & & \\ & & & & 1 & 1 & 0 & 1 & \\ & & & & & & 1 & -1 & \\ & & & & & & & & \ddots \end{pmatrix}$$

with respect to the basis $(\dots, a^1, a^2, A^1, a^3, a^4, A^2, a^5, \dots)$. Now let

$$W = \begin{pmatrix} \ddots & & & & & & & & \\ & 1 & 1 & & & & & & \\ & & 1 & 1 & & & & & \\ & & & 1 & & & & & \\ & & & 1 & 1 & & 1 & & \\ & & & & & 1 & 1 & & \\ & & & & & & 1 & & \\ & & & & & & 1 & 1 & \\ & & & & & & & & \ddots \end{pmatrix}.$$

This W is a local transformation because it can be written as

$$W = W_1 W_2 = \begin{pmatrix} \ddots & & & & & & & & \\ & 1 & 1 & & & & & & \\ & & 1 & & & & & & \\ & & & 1 & & & & & \\ & & & & 1 & 1 & & & \\ & & & & & 1 & & & \\ & & & & & & 1 & 1 & \\ & & & & & & & 1 & \\ & & & & & & & & \ddots \end{pmatrix} \begin{pmatrix} \ddots & & & & & & & & \\ & 1 & & & & & & & \\ & & 1 & 1 & & & & & \\ & & & 1 & & & & & \\ & & & & 1 & 1 & & & \\ & & & & & 1 & & & \\ & & & & & & 1 & 1 & \\ & & & & & & & 1 & \\ & & & & & & & & \ddots \end{pmatrix}.$$

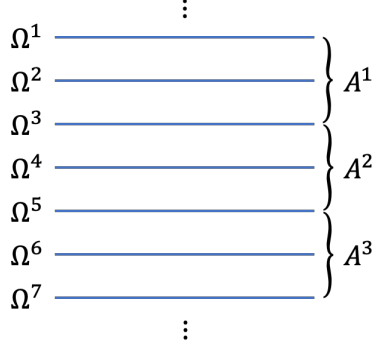


Figure 3.4: Lattice model realizing the CS_∞ theory with $K(u) = (u + 3 + u^{-1})$. The matter content of the system is infinitely many IQH layers Ω^l (blue lines) with Chern number $C^l = 1$. The layers are coupled with unit charge to infinitely many dynamical U(1) gauge fields A^i in the way indicated by the curly brackets.

Each W_k is a product of non-overlapping general linear transformations acting on three nearest neighbor dimensions. This shows that locality is preserved when the lattice model is mapped to the effective CS_∞ theory. The transformation yields

$$\tilde{K}_0 = W^T K_0 W = \begin{pmatrix} \ddots & & & & & & & & & & \\ & & -1 & & & & & & & & \\ & & & -1 & & & & & & & \\ & & & & 3 & & & 1 & & & \\ & & & & & -1 & & & & & \\ & & & & & & -1 & & & & \\ & & & & & & & 1 & & 3 & \\ & & & & & & & & & & -1 \\ & & & & & & & & & & \ddots \end{pmatrix}.$$

The desired matrix K can be extracted from the rows and columns of \tilde{K}_0 with indices $\{\dots, 3, 6, 9, \dots\}$, and the rest of \tilde{K}_0 is decoupled IQH layers.

These two examples can be summarized into a lattice construction that works for any quasi-diagonal K with bounded entries. First, take a stack of IQH layers Ω^l . The Chern number of the layer Ω^l is $C^l = \pm 1$, to be fixed later. Now add gauge degrees of freedom $A_{\mathbf{r}\mathbf{r}'}^i$ and their conjugate momenta $E_{\mathbf{r}\mathbf{r}'}^i$ to the horizontal links $\langle \mathbf{r}\mathbf{r}' \rangle$ and impose the commutation relation $[A_{\mathbf{r}\mathbf{r}'}^j, E_{\mathbf{r}\mathbf{r}'}^k] = i\delta_{jk}$ as usual. Then couple Ω^l to A^i with charge q^{il} , also to be fixed later. The resulting Hamiltonian is

$$H = \sum_l \sum_{\langle \mathbf{r}\mathbf{r}' \rangle} u_{l,\mathbf{r}\mathbf{r}'} \exp \left(i \sum_i q^{il} A_{\mathbf{r}\mathbf{r}'}^i \right) c_{l,\mathbf{r}'}^\dagger c_{l,\mathbf{r}} + \sum_i \left[\sum_{\langle \mathbf{r}\mathbf{r}' \rangle} g_E (E_{\mathbf{r}\mathbf{r}'}^i)^2 - g_B \sum_p \cos B_p^i + g_Q \sum_{\mathbf{r}} (Q_{\mathbf{r}}^i)^2 \right], \quad (3.8)$$

where $u_{l,\mathbf{r}\mathbf{r}'}$ is the IQH hopping coefficient determined by C^l , B_p^i is the flux of A^i through plaquette p , and

$$Q_{\mathbf{r}}^i = (\nabla \cdot \mathbf{E})_{\mathbf{r}}^i - \sum_l q^{il} c_{l,\mathbf{r}}^\dagger c_{l,\mathbf{r}} \quad (3.9)$$

is the Gauss's law term (Fig. 3.3). The fermion and gauge field layers are considered as interlaced in the z direction. The interactions are local as long as only a finite number of neighboring layers are charged under each A^i , or equivalently, as long as each row and column of q^{il} has bounded support. The latter condition is indeed satisfied when q^{il} are fixed later. The low-energy field theory of (3.8) is given by

$$\mathcal{L} = -\frac{1}{4\pi} \sum_l C^l \epsilon^{\mu\nu\lambda} a_\mu^l \partial_\nu a_\lambda^l + \frac{1}{2\pi} \sum_{il} q^{il} \epsilon^{\mu\nu\lambda} A_\mu^i \partial_\nu a_\lambda^l, \quad (3.10)$$

where the Maxwell term is omitted.

A particular K matrix is realized by appropriate choices of Ω^l , C^l and q^{il} as follows:

1. For each index i of K such that

$$\sigma_i = K_{ii} - \sum_{j \neq i} K_{ij} \neq 0,$$

add to the lattice model IQH layers $\Omega_{\text{d}}^{i,s}$, where $s = 1, 2, \dots, |\sigma_i|$ and the subscript “d” stands for “diagonal”. The layer $\Omega_{\text{d}}^{i,s}$ has Chern number $C_{\text{d}}^i = \text{sgn}(\Delta_i)$ and carries +1 charge under A^i only. The emergent gauge field of $\Omega_{\text{d}}^{i,s}$ is denoted by $a_{\text{d}}^{i,s}$. If $\sigma_i = 0$, no diagonal layer is needed.

2. For each pair $i < j$ such that $K_{ij} \neq 0$, add to the lattice model IQH layers $\Omega_{\text{o}}^{ij,t}$, where $t = 1, 2, \dots, |K_{ij}|$ and the subscript “o” stands for “off-diagonal”. The layer $\Omega_{\text{o}}^{ij,t}$ has Chern number $C_{\text{o}}^{ij} = \text{sgn}(K_{ij})$ and carries +1 charge under A^i and A^j only. The emergent gauge field of $\Omega_{\text{o}}^{ij,t}$ is denoted by $a_{\text{o}}^{ij,t}$.

These notations are different from those in the two examples discussed earlier, and I now describe how the different notations are identified. Let \mathcal{A} be the collection of emergent and physical gauge fields. For $K = (2)$,

$$\begin{aligned} \mathcal{A} &= (a^1, a^2, A) \\ &= (a_{\text{d}}^{1,1}, a_{\text{d}}^{1,1}, A^1), \end{aligned}$$

with no “off-diagonal” gauge field. For $K(u) = (u + 3 + u^{-1})$,

$$\begin{aligned} \mathcal{A} &= (\dots, a^1, a^2, A^1, a^3, a^4, A^2, a^5, \dots) \\ &= (\dots, a_{\text{o}}^{01,1}, a_{\text{d}}^{1,1}, A^1, a_{\text{o}}^{12,1}, a_{\text{d}}^{2,1}, A^2, a_{\text{o}}^{23,1}, \dots). \end{aligned}$$

In general, since K is quasi-diagonal with bounded entries, by choosing a suitable ordering of \mathcal{A} , the gauge fields can always be interlaced in the z direction in such a way that the interaction is local. Let K_0 be the K matrix of the CS theory (3.10) with respect to the basis \mathcal{A} . Next, apply the transformation $\tilde{\mathcal{A}}^i = \sum_j (W^{-1})^{ij} \mathcal{A}^j$, $\tilde{K}_0 = W^T K_0 W$ defined by

$$\begin{aligned}\tilde{a}_d^{i,s} &= a_d^{i,s} - \text{sgn}(\sigma_i) A^i, \\ \tilde{a}_o^{ij,t} &= a_o^{ij,t} - \text{sgn}(K_{ij}) (A^i + A^j), \\ \tilde{A}^i &= A^i.\end{aligned}$$

This transformation is local in the sense that W can be decomposed into a finite-depth circuit (i.e., a finite product) of local, block-diagonal integer matrices. In fact, the circuit has depth 2. The first step of the circuit is to map

$$\begin{aligned}a_d^{i,s} &\mapsto a_d^{i,s} - \text{sgn}(\sigma_i) A^i, \\ a_o^{ij,t} &\mapsto a_o^{ij,t} - \text{sgn}(K_{ij}) A^i,\end{aligned}$$

and the second step is to map

$$a_o^{ij,t} \mapsto a_o^{ij,t} - \text{sgn}(K_{ij}) A^j.$$

Each step is block diagonal because each a is modified by at most one A , and each block is local because the fields are arranged in the z direction such that each A^i is some finite distance away from each $a_d^{i,s}$ and $a_o^{ij,t}$. The \tilde{a}_d and \tilde{a}_o fields are in decoupled IQH states, and the \tilde{A} fields have the desired K matrix.

String operators

I now study the string operators of the fractional excitations in the lattice model (3.8). I work in the $g_E = 0$ limit, and will discuss later the case where g_E is non-zero but small. For simplicity, I first consider the example $K = (2)$ studied earlier in this section. The lattice model (3.5) of this example has effective CS theory (3.7). The only non-trivial fractional excitation of the theory is a semion, whose charge vector is $Q = (0, 0, 1)^T$. The flux vector attached to Q is

$$2\pi\Phi = -2\pi K_0^{-1} Q = \begin{pmatrix} -\pi \\ -\pi \\ -\pi \end{pmatrix}. \quad (3.11)$$

The $-\pi$ fluxes of the fields a^1 and a^2 are interpreted as $-1/2$ fermion charges in each fermion layer. Therefore, the semion consists of a $+1$ **external** charge, a $-\pi$ dynamical flux, a $-1/2$ charge in Ω^1 and a $-1/2$ charge in Ω^2 .

The string operator \mathcal{W} of the semion consists of three parts, $\mathcal{W} = \mathcal{W}_1 \mathcal{W}_2 \mathcal{W}_3$, as follows (Fig. 3.5):

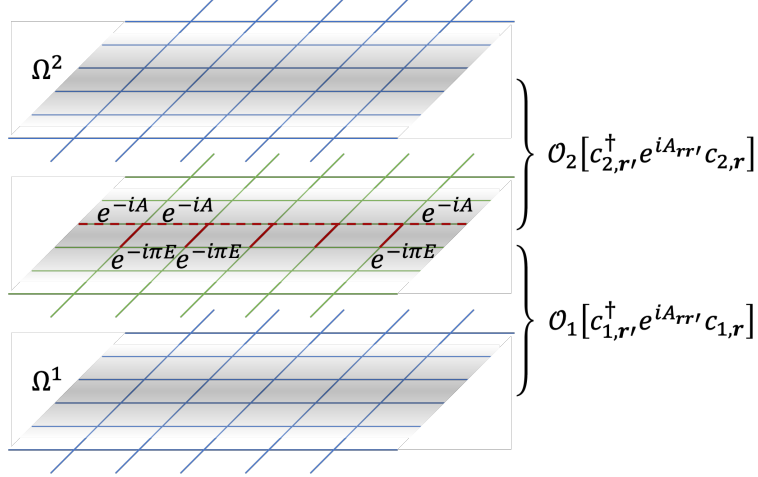


Figure 3.5: The string operator for the lattice model of the CS theory with $K = (2)$. Fermions live in the blue layers Ω^1 and Ω^2 , and the gauge field in the middle, green layer. The operators \mathcal{O}_l are generated by hopping operators $c_{l,r}^\dagger e^{iA_{rr'}} c_{l,r}$. The action of \mathcal{O}_l is non-trivial only near the path (grey region), and is exponentially close to the identity away from the path. The string operator \mathcal{W} consists of e^{-iA} acting on the dashed red line, $e^{-i\pi E}$ acting on the solid red segments and \mathcal{O}_1 , \mathcal{O}_2 acting near the path.

1. $\mathcal{W}_1 = \prod_{\text{path}} e^{-iA}$ acts on the dynamical gauge field A along the path and creates a $+1$ external charge at the end of the path (and a -1 charge at the start).
2. $\mathcal{W}_2 = \prod_{\perp \text{path}} e^{-i\pi E}$ acts on the dynamical gauge field A along adjacent links to the right of and perpendicular to the path, and creates a $-\pi$ flux at the end of the path.
3. \mathcal{W}_3 is the quasi-adiabatic response [46] of the fermions to the $-\pi$ flux insertion. More precisely, in each gauge field sector $\{A_{rr'}\}$ of the Hilbert space, an external $-\pi$ flux is inserted adiabatically. This adiabatic insertion is implemented by an evolution operator $\mathcal{W}_3[A]$, which depends on A , on the fermion Hilbert space. As the fermion hopping model is not exactly solvable, the exact expression for $\mathcal{W}_3[A]$ is not known except for the fact that it is of the form

$$\mathcal{W}_3[A] = \mathcal{O}_1 \left[c_{1,r}^\dagger e^{iA_{rr'}} c_{1,r} \right] \mathcal{O}_2 \left[c_{2,r}^\dagger e^{iA_{rr'}} c_{2,r} \right],$$

where \mathcal{O}_l are some gauge invariant operators generated by the hopping operators $c_{l,r}^\dagger e^{iA_{rr'}} c_{l,r}$. Nevertheless, properties of quasi-adiabatic evolution make sure that $\mathcal{W}_3[A]$ is local and acts only near the path (grey region in Fig. 3.5). A $-1/2$ charge in Ω^1 and a $-1/2$ charge in Ω^2 are accumulated in the process near the end of the string operator, which correspond to the $-\pi$ fluxes of a^1 and a^2 .

The correctness of the string operator can be confirmed by computing the semion braiding phase, which is expected to be $-2\pi Q^T K_0^{-1} Q = -\pi$. To see this from the string operator, I break the overall commutation relation into the commutations of:

1. \mathcal{W}_1 with \mathcal{W}_2 . This takes a $+1$ charge counterclockwise around a $-\pi$ flux, giving a phase of $-\pi$.
2. \mathcal{W}_2 with \mathcal{W}_1 . This gives a phase of $-\pi$ for the same reason.
3. $\mathcal{W}_2\mathcal{W}_3$ with itself. This contributes a phase π which can be understood as the Berry phase obtained due to the following actions on the fermions: increase the (background) flux in the x direction by π , increase the flux in the y direction by π , decrease the flux in the x direction by π , and finally decrease the flux in the y direction by π . In each IQH layer, the Berry phase over the entire flux parameter space $[0, 2\pi)^2$ is 2π . The Berry phase over a quarter of the parameter space is therefore $\pi/2$. Since there are two IQH layers, the total phase is π .
4. \mathcal{W}_1 with itself, \mathcal{W}_1 with \mathcal{W}_3 and \mathcal{W}_3 with \mathcal{W}_1 . All of these are trivial.

Summing these up, the total braiding phase is $-\pi - \pi + \pi = -\pi$ as expected. Of course, phases are defined mod 2π , but the calculation above keeps track of, for example, $-\pi$ versus π . Therefore, this calculation extends naturally to general K .

So far I have worked within the $g_E = 0$ limit, where \mathcal{W} is shown to be a string operator for the charge vector $Q = (0, 0, 1)^T$. In fact, in this limit there are many other string operators for Q that commute with the Hamiltonian except near the end points. For example, one could take $\mathcal{W}' = \mathcal{W}'_1 \mathcal{W}'_2 \mathcal{W}'_3$ where $\mathcal{W}'_1 = \prod_{\text{path}} e^{-iA}$ as before, $\mathcal{W}'_2 = \prod_{\perp \text{path}} e^{i\theta E}$ for arbitrary θ and \mathcal{W}'_3 is the quasi-adiabatic response of the fermions to a θ flux insertion. To see why the correct \mathcal{W} must satisfy the flux-charge attachment condition (3.11), consider turning on a small $g_E > 0$, much smaller than the other couplings in the Hamiltonian and the Landau level spacing. Now if the string operator creates a θ flux and hence a $\theta/2\pi$ charge in each IQH layer, then Gauss's law (3.6) implies that

$$\nabla \cdot \mathbf{E} = 1 + \frac{\theta}{\pi}.$$

If $\nabla \cdot \mathbf{E} \neq 0$, then the electric energy diverges at least logarithmically. Therefore, the only choice of θ is $\theta = -\pi$, so that $\nabla \cdot \mathbf{E} = 0$. As such, when $g_E > 0$, it is possible to modify \mathcal{W} in a region near the path such that the electric energy is finite. Furthermore, since g_E is small, the gauge field sectors $\{A_{\mathbf{r}\mathbf{r}'}\}$ that are present in the ground state can differ from the flat configuration $B \equiv 0$ at most by a small perturbation. Therefore, even with the new hopping coefficients $u_{l,\mathbf{r}\mathbf{r}'} e^{iA_{\mathbf{r}\mathbf{r}'}}$, the fermions are still in a $C^l = 1$ IQH state, so the $-\pi$ flux is indeed bound with a

$-1/2$ charge in each layer. The exact expression of the new \mathcal{W} is not important, and the braiding statistic remains unchanged as long as the correct amount of external charge, fermion charge and flux are created.

A similar construction of string operators works for CS_∞ theories. When $g_E = 0$, the string operator \mathcal{W}^i corresponding to standard basis vector e_i takes the form $\mathcal{W}^i = \mathcal{W}_1^i \mathcal{W}_2^i \mathcal{W}_3^i$. First, $\mathcal{W}_1^i = \prod_{\text{path}} e^{-iA^i}$ creates a $+1$ external A^i charge. Next,

$$\mathcal{W}_2^i = \prod_{\perp\text{path}} \exp \left[-2\pi i \sum_j (K^{-1})^{ij} E^j \right]$$

creates fluxes according to the i th row of K^{-1} , which is required by Gauss's law (3.9) when a small $g_E > 0$ is present. The IQH layers then respond quasi-adiabatically, giving an evolution operator \mathcal{W}_3^i . The braiding statistic of \mathcal{W}^i and \mathcal{W}^j results from the commutations of \mathcal{W}_1^i with \mathcal{W}_2^j , \mathcal{W}_2^i with \mathcal{W}_1^j , and $\mathcal{W}_2^i \mathcal{W}_3^i$ with $\mathcal{W}_2^j \mathcal{W}_3^j$. In particular, the commutation of $\mathcal{W}_2^i \mathcal{W}_3^i$ with $\mathcal{W}_2^j \mathcal{W}_3^j$ correspond to the following actions on the fermions: increase the (background) A^k flux in the x direction by $2\pi (K^{-1})^{ik}$ for all k , increase the A^l flux in the y direction by $2\pi (K^{-1})^{jl}$ for all l , decrease the A^k flux in the x direction by $2\pi (K^{-1})^{ik}$ for all k , and finally decrease the A^l flux in the y direction by $2\pi (K^{-1})^{jl}$ for all l . A diagonal layer $\Omega_d^{k,s}$ is coupled to A^k only, and contributes a Berry phase of

$$\theta_{d,\text{ij}}^k = 2\pi \text{sgn}(\Delta_k) (K^{-1})^{ik} (K^{-1})^{jk},$$

On the other hand, an off-diagonal layer $\Omega_o^{kl,t}$, $k < l$, is coupled to A^k and A^l , and contributes

$$\theta_{o,\text{ij}}^{kl} = 2\pi \text{sgn}(K_{kl}) \left[(K^{-1})^{ik} + (K^{-1})^{il} \right] \left[(K^{-1})^{jk} + (K^{-1})^{jl} \right].$$

The braiding phase of $\mathcal{W}_2^i \mathcal{W}_3^i$ with $\mathcal{W}_2^j \mathcal{W}_3^j$ is then

$$\sum_k |\Delta_k| \theta_{d,\text{ij}}^k + \sum_{k < l} |K_{kl}| \theta_{o,\text{ij}}^{kl} = 2\pi (K^{-1})^{ij},$$

as can be confirmed by a straightforward calculation. Summarizing the above, the total braiding phase is

$$-2\pi (K^{-1})^{ij} - 2\pi (K^{-1})^{ij} + 2\pi (K^{-1})^{ij} = -2\pi (K^{-1})^{ij},$$

as expected.

The string operators also reveal the profiles of fractional excitations in the z direction, which is determined by the fractional part of K^{-1} ; the integral part of K^{-1} corresponds to local fermion and integer flux excitations. As explained in Section 2.4, if a CS_∞ theory is gapped, then either K^{-1} is quasi-diagonal, or each row of K^{-1}

decays (a bit more slowly than) exponentially. Consequently, both \mathcal{W}_2^i and \mathcal{W}_3^i are at least exponentially close to the identity away from the center of the planon in the z direction (\mathcal{W}_1^i is always local in the z direction). Therefore, \mathcal{W}^i is local in the z direction with an exponentially decaying tail, and the fractional excitations are localized particles.

In contrast, as will be shown in Section 4.3, fractional excitations in a gapless CS_∞ theory are not localized particles but have localized energy profiles. The flux of such an excitation does not decay in the z direction, and is more and more spread out in the xy plane as $|z|$ increases.

GAPLESS INFINITE-COMPONENT CHERN-SIMONS THEORY

In the study of phases of matter at zero temperature, gapless models are treated with much more caution than gapped models. This thesis is no different – so far, I have avoided discussing gapless CS_∞ theories. The reason is that gapless theories do not have the protection of the adiabatic theorem like gapped theories, and are therefore often unstable under perturbation by relevant operators. Consequently, the stability of a gapless theory must be carefully justified before any further physical properties can be calculated.

The spectrum of a CS theory is given by (2.2). If any eigenvalue of K is 0, then the theory is classically gapless; the Polyakov mechanism then gaps out the theory as explained in Section 2.5. To simplify the discussion of CS_∞ theories, I assume that K has period $r = 1$ so that $K(u) = (D(u))$. Depending on the context, I use the notation $K(u)$ for either the 1×1 matrix $K(u)$ or its determinant polynomial $D(u)$. Let $\lambda(q) = K(e^{iq})$ be the eigenvalues of K , where $-\pi < q \leq \pi$. If N is finite, then q is quantized to unit $2\pi/N$; in the $N \rightarrow \infty$ limit, there is no quantization condition on q . In these new notations, the spectrum of a CS_∞ theory is

$$\omega^2 = k_x^2 + k_y^2 + \left(\frac{g^2}{2\pi} \lambda(q) \right)^2.$$

The CS_∞ theory is classically gapless if and only if $K(u)$ has roots $u_\alpha = e^{iq_\alpha}$ on the unit circle, and the gapless modes are photons. The momentum q_α is called a *gapless momentum*. Let Γ_α be the multiplicity of u_α in $K(u)$, also known as the *algebraic multiplicity* of u_α in Section 2.5, and define $\Gamma_{\max} = \max\{\Gamma_\alpha\}$. Note that here u_α denotes only the roots of $K(u)$ on the unit circle, not all roots. Similarly, Γ_{\max} is the maximum of the multiplicities of the roots on the unit circle. As will be shown in Sections 4.3 and 4.4, theories with $\Gamma_{\max} = 1$ have very different properties from those with $\Gamma_{\max} > 1$. These differences can be traced back to a simple scaling law of the spectrum that depends on Γ_α . Specifically, in the vicinity of a gapless momentum q_α , the eigenvalue $\lambda(q)$ can be expanded as

$$\lambda(q) \approx \lambda_\alpha (q - q_\alpha)^{\Gamma_\alpha}.$$

Note that λ_α is a coefficient, not an eigenvalue. The spectrum is then

$$\omega^2 \approx k_x^2 + k_y^2 + m_\alpha^2 (q - q_\alpha)^{\Gamma_\alpha}, \quad (4.1)$$

where $m_\alpha = g^2 \lambda_\alpha / 2\pi$ is a mass scale. This spectrum has a Lifshitz scale symmetry

$$\omega \mapsto \Lambda \omega, \quad k_x \mapsto \Lambda k_x, \quad k_y \mapsto \Lambda k_y, \quad (q - q_\alpha) \mapsto \Lambda^{1/\Gamma_\alpha} (q - q_\alpha). \quad (4.2)$$

If $\Gamma_\alpha = 1$, then (4.1) gives a linear dispersion relation, and (4.2) becomes the usual isotropic scale symmetry. If $\Gamma_\alpha = 1$ for all α and hence $\Gamma_{\max} = 1$, then the theory has no intrinsic length scale at low energy. This brings the hope of having topological observables in CS_∞ theories with $\Gamma_{\max} = 1$, and such observables are indeed found in Section 4.3 which are invariant under diffeomorphisms in the txy space.

All of these properties of gapless CS_∞ theories that I have demonstrated or promised are only trustworthy if the theories are stable. Therefore, this chapter starts with Section 4.1 where I show that gapless CS_∞ theories are always stable and remain gapless under any local perturbations. In Section 4.2, I discuss an exotic one-form symmetry of gapless CS_∞ theory and show that part of the symmetry is broken spontaneously. In Section 4.3, I calculate various observables of a CS_∞ theory including electric potential, braiding statistics and correlation functions of Wilson lines. In particular, I show that if the theory has $\Gamma_{\max} = 1$, then the planon braiding phase is invariant under diffeomorphisms in the txy space. This calculation also implies that the planons are not localized particles but have localized energy profiles. Specifically, the flux of a planon does not decay in the z direction, and is more and more spread out in the xy plane as $|z|$ increases. Nevertheless, I will continue to use the word “planon” for simplicity. In Section 4.4, I write down fully continuous low-energy effective theories for gapless CS_∞ theories with $\Gamma_{\max} = 1$. A class of gapless CS_∞ theories is also studied in Refs. [47, 48].

The results in this chapter are based on Ref. [29].

4.1 Stability

The primary reason why a CS_∞ theory might be unstable is monopole proliferation due to the Polyakov mechanism. As explained in Section 2.5, the magnetic charge vector Φ of a relevant monopole must be an integer null vector of K . Intuitively, such a vector Φ is a linear combination of Fourier modes and thus cannot be local. Therefore, monopole operators of relevant monopoles are extended objects in the z direction, and cannot be included as a perturbation in $d = 3 + 1$. This intuition is substantiated by the following lemma:

Lemma 9. In the $N \rightarrow \infty$ limit, every integer null vector Φ of K with bounded entries is periodic.

This lemma is obvious when N is finite. What makes the lemma non-trivial in the $N \rightarrow \infty$ limit is the possibility of having *incommensurate* gapless momenta q_α such that $q_\alpha/2\pi$ is irrational. In this case, the periods of the complex Fourier modes cannot be chosen to all be integers. The requirement of bounded entries is physically motivated, since otherwise the monopole would have infinite energy per layer. I will prove the lemma at the end of this section. For the purpose of proving stability, it

suffices to know that Φ cannot be local.

In fact, more compromises can be made in the argument for stability. Even if the extended monopole operators of relevant monopoles are added as perturbations to the Lagrangian, only finitely many gapless modes are gapped out as a result. These do not include the gapless modes with incommensurate gapless momenta q_α , or the whole continuum of nearly gapless modes with small eigenvalues $\lambda(q)$. Therefore, the theory remains gapless.

There is one more concern for stability. When the theory has a gapless momentum $q_\alpha \neq 0$, a phenomenon called “staging” may occur where translation symmetry in the z direction is broken spontaneously [40, 41, 49]. To understand the effect of staging on the stability of the theory, consider perturbing the CS_∞ Lagrangian by

$$\frac{1}{4g^2} \sum_{ij} (\delta Z)_{ij} F_{\mu\nu}^i F^{j,\mu\nu},$$

where δZ is an invertible matrix with small entries which does not have translation symmetry (or has translation symmetry but with a higher period). This breaks the translation symmetry in the z direction explicitly and changes the spectrum. The new spectrum is determined by the eigenvalues of $(1 + \delta Z)^{-1}K$, but this matrix has the same nullity as K , so the spectrum remains gapless. Therefore, spontaneous or explicit breaking of translation symmetry in the z direction does not lead to instability of a gapless CS_∞ theory.

To conclude this section, I prove Lemma 9 in a manner similar to the proof of Lemma 7. By assumption, Φ satisfies a linear recurrence relation of order 2ξ ,

$$\sum_{k=-\xi}^{\xi} c_k \Phi_{n+k} = 0. \quad (4.3)$$

Let $S_i = (\Phi_i, \dots, \Phi_{i+2\xi-1})$ be a segment of Φ of length 2ξ . Since the entries of Φ are bounded by some integer R , the segments S_i have at most $(2R + 1)^{2\xi}$ distinct possibilities. Therefore, there exist $p < q$ such that $S_p = S_q$. Since S_i is designed to have length 2ξ , it can serve as an initial condition for the recurrence relation (4.3). Starting from the initial condition S_p and moving along the vector Φ by $q - p$ steps, the result is the same $S_q = S_p$. Now using S_q as the initial condition, the recurrence relation (4.3) must yield $S_{2q-p} = S_q$. Repeated application of this argument shows that Φ has period at most $q - p$.

4.2 Exotic one-form symmetry

Having established its stability, I now discuss the properties of a CS_∞ theory. I start with an exotic one-form symmetry of the theory, which has an antisymmetric

two-form conserved current J_{ab} , given in Euclidean signature by

$$J = \begin{pmatrix} 0 & \frac{i}{g^2} F_{\tau x}^z & \frac{i}{g^2} F_{\tau y}^z & \frac{1}{2\pi} F_{xy}^z \\ \frac{i}{g^2} F_{x\tau}^z & 0 & \frac{i}{g^2} F_{xy}^z & \frac{1}{2\pi} F_{y\tau}^z \\ \frac{i}{g^2} F_{y\tau}^z & \frac{i}{g^2} F_{yx}^z & 0 & \frac{1}{2\pi} F_{\tau x}^z \\ \frac{1}{2\pi} F_{yx}^z & \frac{1}{2\pi} F_{\tau y}^z & \frac{1}{2\pi} F_{x\tau}^z & 0 \end{pmatrix}.$$

Here, the index z is dimensionless and plays the role of the indices i and j of K . I use Latin letters such as a, b for $\{\tau, x, y, z\}$, and Greek letters such as μ, ν for $\{\tau, x, y\}$. Define the action of K on J as the natural matrix multiplication

$$(KJ)(z) = \sum_k c_k J(z+k),$$

where c_k are the coefficients of $K(u)$, and the τ, x and y coordinates are not shown. The current J satisfies the conservation equations

$$\begin{aligned} \partial_\tau J_{\tau z} + \partial_x J_{xz} + \partial_y J_{yz} &= 0, \\ \partial_\tau J_{\tau x} + \partial_y J_{yx} - K J_{zx} &= 0, \\ \partial_\tau J_{\tau y} + \partial_x J_{xy} - K J_{zy} &= 0, \\ \partial_x J_{x\tau} + \partial_y J_{y\tau} - K J_{z\tau} &= 0. \end{aligned} \tag{4.4}$$

The first of these equations is a Bianchi identity, while the other three follow from the equation of motion of (2.1)

$$\frac{1}{g^2} \partial_\nu F^{i,\mu\nu} + \frac{i}{2\pi} K_{ij} \epsilon^{\mu\nu\rho} \partial_\nu A_\rho^j = 0.$$

If K is replaced formally by $-\partial_z$, then (4.4) becomes the conservation equations for a one-form symmetry in, for example, $d = 4$ Maxwell theory [50]. This is why the symmetry here is considered a one-form symmetry.

Conserved charges

A one-form symmetry should have three types of charges that are conserved as a function of τ . They are obtained, respectively, by integrating or summing J in the xy , yz and zx planes in appropriate ways. These conserved charges are not usually distinguished in a Lorentz invariant theory, but since z is a discrete coordinate here and the theory does not have full Lorentz invariance, I treat them as three different types of charges. The first type of charge is an integer magnetic charge

$$Q_z = \int dx dy J_{\tau z} = \Phi.$$

Here, the subscript “ z ” in Q_z is part of the name, not the value of a coordinate. By the fourth equation in (4.4), Q_z is subject to a constraint

$$KQ_z = \int dx dy (\partial_x J_{x\tau} + \partial_y J_{y\tau}) = 0. \quad (4.5)$$

In this sense, Q_z is also “conserved” as a function of z , which is expected since a conserved charge of a one-form symmetry should satisfy two conservation laws. The other two types of charges are not as straightforward to write down. Since the operator K in (4.4) is not $-\partial_z$, the appropriate summation in the z direction is not \sum_z , but a modified version of it. To understand this modification, note that the integration measure in $\int dz$ (which is the continuous version of \sum_z) is the constant function 1, which precisely spans the kernel of the operator $-\partial_z$. Likewise, if $\{v_l(z)\}$ is a basis for the kernel of K , where l labels the basis vectors, then the second and third types of conserved charges are generated by

$$\begin{aligned} Q_{x,l} &= \int dy \sum_z v_l(z) J_{\tau x}(z), \\ Q_{y,l} &= \int dx \sum_z v_l(z) J_{\tau y}(z). \end{aligned} \quad (4.6)$$

Clearly, $Q_{x,l}$ and $Q_{y,l}$ are related by rotation, so I focus on $Q_{x,l}$ without loss of generality. The conservation of $Q_{x,l}$ as a function of τ can be derived from the second equation in (4.4),

$$\partial_\tau Q_{x,l} = - \int dy \sum_z v_l(z) [\partial_y J_{yx}(z) - (K J_{zx})(z)] = 0,$$

where I used

$$\sum_z v_l(z) (K J_{zx})(z) = v_l^T K J_{zx} = (K v_l)^T J_{zx} = 0.$$

Similarly, $Q_{x,l}$ is also conserved as a function of x ,

$$\partial_x Q_{x,l} = \int dy \sum_z v_l(z) [\partial_y J_{y\tau}(z) - (K J_{z\tau})(z)] = 0.$$

The symmetry transformation generated by the charge $Q_{x,l}$ shifts the gauge fields $A(z)$ (previously written as A^z) by a flat gauge field κ_l ,

$$A(z) \mapsto A(z) + v_l(z) \kappa_l, \quad (4.7)$$

which is similar to the action of the electric one-form symmetry in $d = 4$ Maxwell theory. For this reason, $Q_{x,l}$ and $Q_{y,l}$ are considered as **electric** charges. Therefore, the one-form symmetry of a gapless CS_∞ theory has both a magnetic charge and generally many electric charges, where the former is defined by its action which shifts the **magnetic** photon by a flat gauge field after dualization. This is unlike $d = 4$ Maxwell theory where the electric and magnetic one-form symmetries are separate, with a mixed ’t Hooft anomaly.

't Hooft anomaly

A natural question is then whether the one-form symmetry of a gapless CS_∞ theory has any 't Hooft anomaly. To answer this question, consider coupling the one-form symmetry to a background gauge field C_{ab} . To linear order in C_{ab} , this adds a term $iC_{ab}J^{ab}$ to the Lagrangian

$$\mathcal{L} = -\frac{1}{4g^2}F_{\mu\nu}F^{\mu\nu} + \frac{i}{4\pi}\epsilon^{\mu\nu\rho}KA_\mu\partial_\nu A_\rho. \quad (4.8)$$

In (4.8), I removed the overall sum over z in (2.1) to obtain a Lagrangian density in $d = 4$. I also switched to Euclidean signature and made the matrix multiplication in the CS term implicit. The conservation equations (4.4) imply that C_{ab} has a background gauge symmetry

$$\begin{aligned} C_{\mu\nu} &\mapsto C_{\mu\nu} + \partial_\mu\sigma_\nu - \partial_\nu\sigma_\mu, \\ C_{\mu z} &\mapsto C_{\mu z} + \partial_\mu\sigma_z + K\sigma_\mu. \end{aligned} \quad (4.9)$$

The dynamical fields A_μ transform under the background gauge symmetry as

$$A_\mu \mapsto A_\mu + \sigma_\mu. \quad (4.10)$$

After including quadratic terms in C_{ab} , the Lagrangian becomes

$$\mathcal{L} = \frac{1}{4g^2}(F_{\mu\nu} - C_{\mu\nu})(F^{\mu\nu} - C^{\mu\nu}) + \frac{i}{4\pi}\epsilon^{\mu\nu\rho}KA_\mu\partial_\nu A_\rho + \frac{i}{2\pi}\epsilon^{\mu\nu\rho}C_{\mu z}\partial_\nu A_\rho. \quad (4.11)$$

Combining (4.9) and (4.10), the Lagrangian (4.11) transforms under the background gauge symmetry anomalously as

$$\mathcal{L} \mapsto \mathcal{L} - \frac{i}{4\pi}\epsilon^{\mu\nu\rho}K\sigma_\mu\partial_\nu\sigma_\rho + \frac{i}{2\pi}\epsilon^{\mu\nu\rho}C_{\mu z}\partial_\nu\sigma_\rho, \quad (4.12)$$

where total derivative terms are omitted.

The anomaly can be cancelled by coupling the system to a symmetry protected topological (SPT) phase in one higher dimension [51]. The SPT phase is described by the Lagrangian

$$\mathcal{L}_{\text{SPT}} = -\frac{i}{4\pi}\epsilon^{\mu\nu\rho\lambda}C_{\mu\nu}\partial_\rho C_{\lambda z} - \frac{i}{16\pi}\epsilon^{\mu\nu\rho\lambda}C_{\mu\nu}KC_{\rho\lambda}. \quad (4.13)$$

The gauge field C_{ab} is extended from the boundary to the bulk by allowing the Greek indices such as μ, ν to take values in $\{\tau, x, y, w\}$. The gauge symmetry acts in the same way as (4.9) but now with Greek indices valued in $\{\tau, x, y, w\}$. The SPT Lagrangian (4.13) transforms under the gauge symmetry as

$$\begin{aligned} \mathcal{L}_{\text{SPT}} &\mapsto \mathcal{L}_{\text{SPT}} + \frac{i}{8\pi}\epsilon^{\mu\nu\rho\lambda}(C_{\mu\nu}K\partial_\rho\sigma_\lambda - KC_{\mu\nu}\partial_\rho\sigma_\lambda) \\ &\quad + \frac{i}{4\pi}\epsilon^{\mu\nu\rho\lambda}\partial_\mu(K\sigma_\nu\partial_\rho\sigma_\lambda) - \frac{i}{2\pi}\epsilon^{\mu\nu\rho\lambda}\partial_\mu(C_{\nu z}\partial_\rho\sigma_\lambda). \end{aligned} \quad (4.14)$$

Note that since there is no overall sum over z , the term in (4.14) with coefficient $i/8\pi$ is non-zero. However, on a closed manifold, the SPT action is gauge invariant. On an open manifold with periodic boundary condition in the z direction, the gauge transformation (4.14) of the bulk SPT Lagrangian (4.13) generates a boundary term which exactly cancels the anomalous term in the gauge transformation (4.12) of the boundary Lagrangian (4.11). Since the SPT action is non-trivial on closed manifold, the one-form symmetry has a genuine 't Hooft anomaly.

Compactness

Next, I discuss the compactness of the one-form symmetry of a gapless CS_∞ theory. As can be seen from the constraint (4.5) on the magnetic charge as well as the construction (4.6) of electric charges, it is important to understand the complex kernel V of K and the integer vectors therein. These, together with the action (4.7) of the electric charges on the compact gauge fields, will lead to a decomposition of the one-form symmetry into a compact part and a non-compact part.

Given the roots $u_\alpha = e^{iq_\alpha}$ of $K(u)$ on the unit circle, define an index set

$$I = \{\alpha : q_\alpha/2\pi \in \mathbb{Q}\},$$

which labels the gapless momenta q_α that are *commensurate*; those q_α such that $\alpha \notin I$ are called *incommensurate*. This set I is similar to the index set in Section 2.5 with the same name. Write

$$V = V_c \oplus V_{\bar{c}},$$

where V_c (resp. $V_{\bar{c}}$) is the complex vector space spanned by commensurate (resp. incommensurate) Fourier modes. To understand V_c , first take an integer $N > 0$ such that $u_\alpha^N = 1$ for all $\alpha \in I$. By considering the CS theory where K has size N , it can be shown that V_c is spanned by integer null vectors of K . The argument here is similar to the one used when discussing the denominator of (2.27) in Section 2.5. Meanwhile, Lemma 9 implies that in the $N \rightarrow \infty$ limit, bounded integer null vectors of K are all in V_c . Therefore, V_c can be obtained by complexifying the abelian group of bounded integer null vectors of K , and hence has an integral basis $\{v_l : l = 1, \dots, d_c\}$ where $d_c = |I|$. On the other hand, not much can be said about $V_{\bar{c}}$ other than the fact that it can have a real basis $\{v_l : l = d_c + 1, \dots, d_c + d_{\bar{c}}\}$ for some $d_{\bar{c}}$. A basis for V is then $\{v_l : l = 1, \dots, d_c + d_{\bar{c}}\}$. Since the magnetic charge Q_z of the one-form symmetry is an integer, (4.5) implies that Q_z is generated by v_l , $l = 1, \dots, d_c$, with integer coefficients. On the other hand, the electric charges Q_x and Q_y in (4.6) are generated by all v_l , $l = 1, \dots, d_c + d_{\bar{c}}$.

The compactness of the one-form symmetry can be understood from the symmetry transformation (4.7). If $l = 1, \dots, d_c$ and the holonomies of the gauge parameter

κ_l are in $2\pi\mathbb{Z}$, then the transformation (4.7) is trivial. Therefore, the first d_c basis vectors v_l correspond to compact $U(1)$ symmetries and integer charges, while the last $d_{\bar{c}}$ basis vectors v_l correspond to non-compact \mathbb{R} symmetries and real charges. The full symmetry group is $U(1)^{d_c} \times \mathbb{R}^{d_{\bar{c}}}$.

Spontaneous symmetry breaking

Finally, I study the spontaneous breaking of the one-form symmetry of a gapless CS_∞ theory. Here, I focus on the magnetic part of the symmetry, which turns out to be unbroken. In Section 4.3, I will show that Wilson lines of the theory obey Coulomb law and hence that the electric part of the one-form symmetry is broken spontaneously [50]. The resulting Goldstone modes are massless photons.

Consider a degenerate CS theory (2.1) whose K matrix has finite size N . For simplicity, I assume that the nullity of K is 1. Two simple examples of such theories can be found in Section 2.5, and here I study the general theory using the same dualization procedure. Let W be as in Theorem 2, and $Z = W^T W$. In Euclidean signature, the dual Lagrangian is

$$\begin{aligned} \mathcal{L} = & \frac{g^2}{8\pi^2 Z_{NN}} \partial_\mu \phi \partial^\mu \phi + \frac{i}{4\pi} \sum_{i=1}^{N-1} \frac{Z_{Ni}}{Z_{NN}} \epsilon^{\mu\nu\rho} F_{\mu\nu}^i \partial_\rho \phi \\ & + \frac{1}{4g^2} \sum_{i,j=1}^{N-1} \hat{Z}_{ij} F_{\mu\nu}^i F^{j,\mu\nu} + \frac{i}{4\pi} \sum_{i,j=1}^{N-1} \hat{K}_{ij} \epsilon^{\mu\nu\rho} A_\mu^i \partial_\nu A_\rho^j, \end{aligned}$$

where ϕ is the dual compact boson, \hat{K} is defined in (2.24), and

$$\hat{Z}_{ij} = Z_{ij} - \frac{Z_{Ni} Z_{Nj}}{Z_{NN}}.$$

The two-point function of the monopole operator is

$$\left\langle e^{-i\phi(x^\mu)} e^{i\phi(0)} \right\rangle \sim \exp \left[\frac{\pi Z_{NN}}{g^2} \left(\frac{1}{r} - \frac{1}{r_0} \right) \right], \quad (4.15)$$

where $r = |x^\mu|$, and r_0 is a length scale that regulates (4.15). Now $Z_{NN} = \sum_i W_{Ni}^2$ and W_{Ni} is periodic in i , so $Z_{NN} \propto N$. When studying correlation functions in CS_∞ theories at long distance, the $N \rightarrow \infty$ limit is always taken before the $r \rightarrow \infty$ limit. Therefore, for $r > r_0$, the two-point function (4.15) decays to 0 as $N \rightarrow \infty$. This means that the magnetic part of the one-form symmetry is unbroken.

4.3 Observables

I now calculate various observables of a gapless CS_∞ theory, namely the electric potential and braiding statistics of planons, as well as the general correlation function of Wilson lines. All calculation are performed in Euclidean signature. Mathematically, the calculations are essentially Fourier transforms of the corresponding quantities in a CS theory with only one gauge field, so I start by reviewing the latter.

Preparation: Observables of CS theory

Consider a CS theory in Euclidean signature

$$\mathcal{L} = \frac{1}{4g^2} F^{\mu\nu} F_{\mu\nu} + \frac{i}{4\pi} K \epsilon^{\mu\nu\rho} A_\mu \partial_\nu A_\rho. \quad (4.16)$$

Unlike previously, the gauge field A here is not required to be compact, so $K \in \mathbb{R}$ without any quantization condition. This choice is made because K will be replaced later by $K(e^{iq})$ in a CS_∞ theory, and the latter generally takes value in \mathbb{R} . Since all of the observables computed in this section only require perturbative calculations in A , the compactness of A does not matter. Furthermore, the relevant monopoles in a CS_∞ theory are extended objects, and the magnetic part of the one-form symmetry is shown in Section 4.2 to be unbroken. Since monopole operators do not appear explicitly in perturbative calculations and they correspond to an unbroken symmetry, they can be safely overlooked in this section. Therefore, I treat (4.16) as a classical theory even if $K = 0$, and simply ignore the Polyakov mechanism. In what follows, I list some basic properties of the theory. Since the theory is quadratic in A , the calculations are straightforward and many details are omitted.

The propagator of the theory (4.16) in Euclidean space is

$$G_{\mu\nu}(k) = \frac{1}{g^2} \langle A_\mu(k) A_\nu(-k) \rangle = \frac{k^2 \delta_{\mu\nu} - k_\mu k_\nu - m \epsilon_{\mu\nu\rho} k^\rho}{k^2 (k^2 + m^2)}, \quad (4.17)$$

where $m = g^2 K / 2\pi$ and $|m|$ is the mass of the photon. The Fourier transform of (4.17) to real space is the Green's function

$$G_{\mu\nu}(x) = \frac{1}{g^2} \langle A_\mu(x) A_\nu(0) \rangle = \int \frac{d^3 k}{(2\pi)^3} G_{\mu\nu}(k) e^{ikx}. \quad (4.18)$$

If C_1 and C_2 are two closed loops, then the correlation function of Wilson loops is

$$\langle W(C_1) W(C_2) \rangle = \exp \left[-g^2 \oint_{C_1} dx_1^\mu \oint_{C_2} dx_2^\nu G_{\mu\nu}(x_1 - x_2) \right]. \quad (4.19)$$

The real part of the Green's function is

$$\text{Re}[G_{\mu\nu}(x)] = \int \frac{d^3 k}{(2\pi)^3} \frac{k^2 \delta_{\mu\nu} - k_\mu k_\nu}{k^2 (k^2 + m^2)} e^{ikx}. \quad (4.20)$$

Spacetime symmetry constrains it to be of the form

$$\text{Re}[G_{\mu\nu}(x)] = h_0(m, r) \delta_{\mu\nu} + h_2(m, r) \frac{x_\mu x_\nu}{r^2},$$

where $r = |x^\mu|$. The functions $h_0(m, r)$ and $h_2(m, r)$ can be determined by specializing to $(\tau, x, y) = (r, 0, 0)$. First, the trace of (4.18) gives

$$\begin{aligned} 3h_0(m, r) + h_2(m, r) &= \int \frac{d^3 k}{(2\pi)^3} \frac{2}{k^2 + m^2} e^{ikx} \\ &= \int_0^\infty \frac{k^2 dk}{2\pi} \int_0^\pi \frac{\sin(\theta) d\theta}{2\pi} \frac{2}{k^2 + m^2} e^{ikr \cos(\theta)} \\ &= \frac{e^{-|m|r}}{2\pi r}. \end{aligned} \quad (4.21)$$

Second, (4.18) with $\mu = \nu = \tau$ gives

$$\begin{aligned} h_0(m, r) + h_2(m, r) &= \int \frac{d^3k}{(2\pi)^3} \frac{k^2 - k_\tau^2}{k^2(k^2 + m^2)} e^{ikx} \\ &= \int_0^\infty \frac{k^2 dk}{2\pi} \int_0^\pi \frac{\sin(\theta) d\theta}{2\pi} \frac{\sin^2(\theta)}{k^2 + m^2} e^{ikr \cos(\theta)} \\ &= \frac{1 - (1 + |m|r)e^{-|m|r}}{2\pi m^2 r^3}. \end{aligned} \quad (4.22)$$

Thus $h_0(m, r)$ and $h_2(m, r)$ can be solved from (4.21) and (4.22), and

$$\text{Re}[G_{\mu\nu}(x)] = \frac{e^{-|m|r}}{6\pi r} \delta_{\mu\nu} + \frac{1}{4\pi r} \left[\frac{1}{m^2 r^2} - \left(\frac{1}{3} + \frac{1}{|m|r} + \frac{1}{m^2 r^2} \right) e^{-|m|r} \right] Q_{\mu\nu},$$

where $Q_{\mu\nu}$ is the (traceless) quadrupole tensor

$$Q_{\mu\nu} = \frac{3x_\mu x_\nu - r^2 \delta_{\mu\nu}}{r^2}. \quad (4.23)$$

The imaginary part of the Green's function is

$$\text{Im}[G_{\mu\nu}(x)] = \int \frac{d^3k}{(2\pi)^3} \frac{im\epsilon_{\mu\nu\rho} k^\rho}{k^2(k^2 + m^2)} e^{ikx}. \quad (4.24)$$

Spacetime symmetry constrains it to be of the form

$$\text{Im}[G_{\mu\nu}(x)] = h_1(m, r) \frac{\epsilon_{\mu\nu\rho} x^\rho}{r}.$$

The function $h_1(m, r)$ can also be determined by specializing to $(\tau, x, y) = (r, 0, 0)$.

Taking (4.24) with $\mu = x, \nu = y$,

$$\begin{aligned} h_1(m, r) &= \int \frac{d^3k}{(2\pi)^3} \frac{imk_\tau}{k^2(k^2 + m^2)} e^{ikx} \\ &= \int_0^\infty \frac{k^2 dk}{2\pi} \int_0^\pi \frac{\sin(\theta) d\theta}{2\pi} \frac{imk \cos(\theta)}{k^2(k^2 + m^2)} e^{ikr \cos(\theta)} \\ &= -\frac{1 - (1 + |m|r)e^{-|m|r}}{4\pi m r^2}. \end{aligned} \quad (4.25)$$

This gives

$$\text{Im}[G_{\mu\nu}(x)] = -\frac{1 - (1 + |m|r)e^{-|m|r}}{m} \frac{\epsilon_{\mu\nu\rho} x^\rho}{4\pi r^3}.$$

I consider two limits of the Green's function. In the limit $|m|r \gg 1$, the Green's function reduces to that of a non-degenerate CS theory

$$G_{\mu\nu}(x) = -\frac{i}{m} \frac{\epsilon_{\mu\nu\rho} x^\rho}{4\pi r^3}. \quad (4.26)$$

The real part of $G_{\mu\nu}(x)$ is suppressed by a factor of $1/|m|r$. The correlation function (4.19) of Wilson lines reduces to the familiar form

$$\langle W(C_1)W(C_2) \rangle = \exp \left[-\frac{2\pi i}{K} \text{link}(C_1, C_2) \right],$$

where $\text{link}(C_1, C_2)$ is the linking number of the loops C_1 and C_2 . In the opposite limit $|m|r \ll 1$, the Green's function reduces to that of a Maxwell theory

$$G_{\mu\nu}(x) = \frac{x_\mu x_\nu + r^2 \delta_{\mu\nu}}{8\pi r^3}. \quad (4.27)$$

The imaginary part of $G_{\mu\nu}(x)$ is suppressed by a factor of $|m|r$, an important fact for the discussion of planon braiding statistics in a CS_∞ theory.

The theory (4.16) can be coupled to electric charges by adding a term $iA_\mu j^\mu$ to the Lagrangian, where j^μ is the current. The equation of motion becomes

$$\frac{i}{g^2} \partial_\nu F^{\mu\nu} - \frac{1}{2\pi} K \epsilon^{\mu\nu\rho} \partial_\nu A_\rho = j_\mu.$$

For a static charge at $(x, y) = (0, 0)$, the solution is

$$\begin{aligned} A_\tau &= -\frac{ig^2}{2\pi} K_0(|m|r), \\ A_i &= \frac{g^2}{2\pi} \frac{\epsilon_{ij} x^j}{mr^2} [1 - |m|r K_1(|m|r)], \end{aligned} \quad (4.28)$$

where K_0 and K_1 are modified Bessel functions of the second kind. The electric potential of the static charge is then

$$V(r) = iA_\tau(r) = \frac{g^2}{2\pi} K_0(|m|r). \quad (4.29)$$

Asymptotically [52],

$$K_0(x) \approx \begin{cases} -\log\left(\frac{x}{2}\right) - \gamma, & \text{if } 0 < x \ll 1, \\ \sqrt{\frac{\pi}{2x}} e^{-x}, & \text{if } x \gg 1, \end{cases} \quad (4.30)$$

where γ is the Euler-Mascheroni constant. Therefore, the potential (4.29) reduces to the $\log(r)$ classical Coulomb potential when $|m|r \ll 1$, and decays exponentially when $|m|r \gg 1$. Suppose that another electric charge traverses a circle of radius r centered at the static charge. This process generates a braiding phase [53]

$$\phi(r) = \oint A = -\frac{2\pi}{K} (1 - |m|r K_1(|m|r)), \quad (4.31)$$

where A is given by (4.28). If $K \neq 0$, then the $r \rightarrow \infty$ limit of (4.31) is the expected $\phi(\infty) = -2\pi/K$. However, if $K = 0$, then $\phi(\infty) = 0$, as can be seen from the $K \rightarrow 0$ limit of (4.31).

Electric potential

The first observable of a gapless CS_∞ theory that I compute is the potential of an electric charge. The electric potential $V(r, z)$ in a gapless CS_∞ theory is the Fourier of the potential (4.29) in the CS theory (4.16),

$$V(r, z) = \frac{g^2}{2\pi} \int_{-\pi}^{\pi} \frac{dq}{2\pi} K_0(|m(q)|r) e^{iqz}, \quad (4.32)$$

where $r = |x^\mu|$, $m(q) = g^2 K(q)/2\pi$, and K_0 is a modified Bessel function of the second kind. By the asymptotic form (4.30) of K_0 , the electric potential (4.32) in a gapless CS_∞ theory in the limit $g^2 r \gg 1$ is dominated by light photon modes with small $|m(q)|$. For simplicity, assume that the theory has only one pair of gapless momenta $\pm q_1$, and that $m(q) \approx m_1(q - q_1)^{\Gamma_1}$ near q_1 . Although it does not cover, for example, $K(u) = (u + 2 + u^{-1})$ which has only one gapless momentum, this assumption is general enough for understanding the phenomenology. Using (4.30),

$$V(r, z) \approx \frac{g^2}{\pi} \int_{-\infty}^{\infty} \frac{dq}{2\pi} K_0(|m_1||q|^{\Gamma_1} r) \cos(q_1 z) e^{iqz} \quad (4.33)$$

$$\sim \begin{cases} \frac{\cos(q_1 z)}{|z|}, & \text{if } |z|^{\Gamma_1} \gg g^2 r, \\ \frac{\cos(q_1 z)}{r^{1/\Gamma_1}}, & \text{if } g^2 r \gg |z|^{\Gamma_1}. \end{cases} \quad (4.34)$$

In (4.33), I extended the integration range from the vicinity of q_1 to $(-\infty, \infty)$ and used the new integration variable $q - q_1$; similarly for $-q_1$, where I used the variable $q + q_1$. Both cases of (4.34) are in the limit $g^2 r \gg 1$, and overall constant factors are omitted. The potential $V(r, z)$ at $g^2 r \gg |z|^{\Gamma_1}$ therefore has a power law decay in r , and the decay is slower for larger Γ_1 . This is different from the potential of a degenerate CS theory, which is confining both classically and quantum mechanically.

The electric potential is closely related to the expectation value of a single Wilson loop. Consider two static charges separated by (x^μ, z) , where $|x^\mu| = r$. They are represented by Wilson lines $W(C_1)$ and $W(C_2)$, where C_i are straight lines in the τ direction. If the τ direction is compactified to have a large period $T \gg r, g^{-2}z$, then $C_1 \cup C_2$ (with appropriate orientations) is approximately a large rectangle. The Wilson loop on this rectangle has expectation value

$$\langle W(C_1)W(C_2) \rangle \sim e^{-V(r,z)T}.$$

By (4.34), the potential $V(r, z)$ decays with a power law envelope, which is a type of Coulomb law in a general sense. Charged operators (Wilson lines in this case) obeying Coulomb law is a signature of the spontaneous breaking of a one-form symmetry [50]. Therefore, the electric part of the one-form symmetry of a gapless CS_∞ theory is broken spontaneously, as claimed in Section 4.2.

Braiding statistics

Next, I compute the braiding statistics of planons. Since the theory is gapless, it is not clear whether the statistics are topological. Therefore, I start with a simple setup where one planon sits statically at the origin, and another planon traverses a circle centered at the origin. The two planons are separated by (r, z) . By taking the

Fourier transform of (4.31), the braiding phase is

$$\phi(r, z) = -g^2 \int_{-\pi}^{\pi} \frac{dq}{2\pi} \frac{1}{m(q)} [1 - |m(q)|rK_1(|m(q)|r)] e^{iqz}, \quad (4.35)$$

where K_1 is a Bessel function of the second kind. Asymptotically [52],

$$K_1(x) \approx \begin{cases} \frac{1}{x} + \frac{x}{2} \log(x), & \text{if } 0 < x \ll 1, \\ \sqrt{\frac{\pi}{2x}} e^{-x}, & \text{if } x \gg 1. \end{cases} \quad (4.36)$$

If the theory is gapped, then the $K_1(\dots)$ term in (4.35) can be dropped, and the braiding phase is

$$\phi(\infty, z) = -2\pi \int_{-\pi}^{\pi} \frac{dq}{2\pi} \frac{e^{iqz}}{\lambda(q)} = -2\pi (K^{-1})_{0z}, \quad (4.37)$$

as expected. However, the theory of interest here is gapless, and (4.35) should be treated more carefully. The physics depends qualitatively on $\Gamma_{\max} = \max\{\Gamma_{\alpha}\}$.

First, suppose that $\Gamma_{\max} = 1$. This means that no root u_{α} of $K(u)$ on the unit circle is repeated. The integrand of (4.35) involves the function

$$f_r(m) = \frac{1}{m} [1 - |m|rK_1(|m|r)]. \quad (4.38)$$

In Fig. 4.1, I plot $f_r(m)$ for a range of r 's. It is finite everywhere and vanishes at $m = 0$. The latter fact can be traced back to the suppression of the imaginary part of the Green's function in the $|m|r \ll 1$ limit, as is seen in (4.27). As r increases, $f_r(m)$ becomes a better and better approximation to $1/m$ except when $|m|$ is small. Therefore, the parameter r can be viewed effectively as a cutoff which prevents the divergence of the integral (4.35). Since $f_r(m)$ is a odd in m and $m(q)$ is linear in $q - q_{\alpha}$ near each q_{α} , the braiding phase converges to the Cauchy principal value of the integral (4.37),

$$\phi(\infty, z) = -2\pi \text{PV} \int_{-\pi}^{\pi} \frac{dq}{2\pi} \frac{e^{iqz}}{\lambda(q)}. \quad (4.39)$$

Here, if the integrand $g(x)$ of an integral diverges at x_0 inside the integration range (x_1, x_2) , then the *Cauchy principal value* of the integral is defined as

$$\text{PV} \int_{x_1}^{x_2} dx g(x) = \lim_{\epsilon \rightarrow 0^+} \left(\int_{x_1}^{x_0 - \epsilon} dx g(x) + \int_{x_0 + \epsilon}^{x_2} dx g(x) \right). \quad (4.40)$$

In (4.35), $1/r$ effectively plays the role of the cutoff ϵ in the definition (4.40) of the Cauchy principal value.

The braiding phase (4.39) can be expressed using the polynomial description. This is achieved, assuming $z \geq 0$ for now, by the change of variable $u = e^{iq}$ which turns (4.39) into a contour integral

$$\phi(\infty, z) = -2\pi \text{PV} \oint \frac{du}{2\pi i} \frac{u^{z-1}}{K(u)}. \quad (4.41)$$

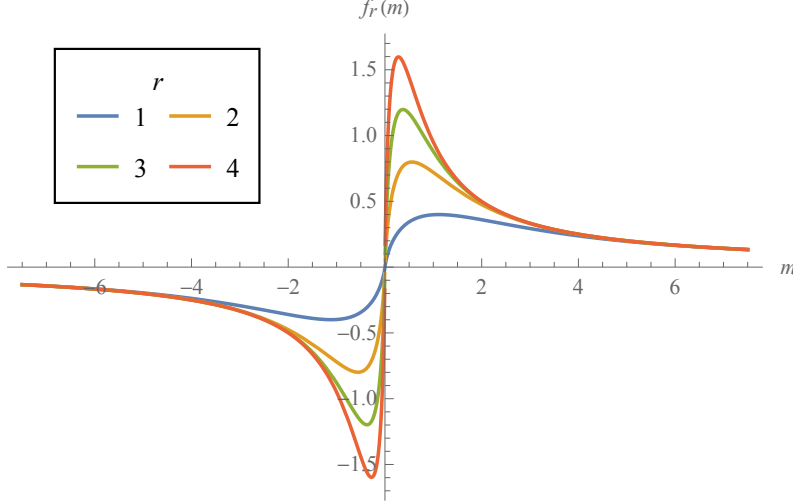


Figure 4.1: The function $f_r(m)$ given by (4.38) for $r = 1, 2, 3, 4$. The larger r is, the more $f_r(m)$ looks like $1/m$.

Let u_α be the roots of $K(u)$ on the unit circle, as has been the convention in this chapter. Also temporarily let \tilde{u}_β be the roots of $K(u)$ inside the unit circle. By the residue theorem, the integral (4.41) simplifies to

$$\phi(\infty, z) = -2\pi \left[\frac{1}{2} \sum_{\alpha} u_{\alpha}^{|z|-1} \text{Res}_{u_{\alpha}} \left(\frac{1}{K(u)} \right) + \sum_{\beta} \tilde{u}_{\beta}^{|z|-1} \text{Res}_{\tilde{u}_{\beta}} \left(\frac{1}{K(u)} \right) \right], \quad (4.42)$$

where $\text{Res}_x(1/K(u))$ is the residue of $1/K(u)$ at x . Unlike the electric potential, the braiding phase when $\Gamma_{\max} = 1$ is not dominated by light photon modes. Mathematically, this is because the $(q - q_\alpha)^{-1}$ decay of $1/\lambda(u)$ **away from** q_α is not fast enough. Writing ϵ for a cutoff, the contribution of $(q - q_\alpha)^{-1}$ to the braiding phase (4.39) away from q_α is

$$-2\pi i \int_{|q|>\epsilon} \frac{dq \sin(qz)}{2\pi \lambda_\alpha q} e^{iq_\alpha z},$$

which is finite but not small. Therefore, (4.39) cannot be approximated by light photon modes. The assumption $z \geq 0$ is used to make sure that the integrand of the contour integral (4.41) has no pole at 0, and the $z < 0$ case in (4.42) is derived from the fact that $\phi(\infty, z)$ is even in z . Importantly, the terms in (4.42) corresponding to the roots u_α on the unit circle have an extra factor of $1/2$. In other words, the roots u_α only contribute **half** of their residues to the braiding phase. To understand this factor of $1/2$, note that according to the definition (4.40) of the Cauchy principal value, the contour in (4.41) is cut open in the vicinity of every root u_α on the unit circle. To evaluate the integral, one may close the contour by including a small semicircle around each u_α and then subtracting them. If the semicircles are inside the unit circle as drawn in Fig. 4.2 (a), then the closed contour does not pick up

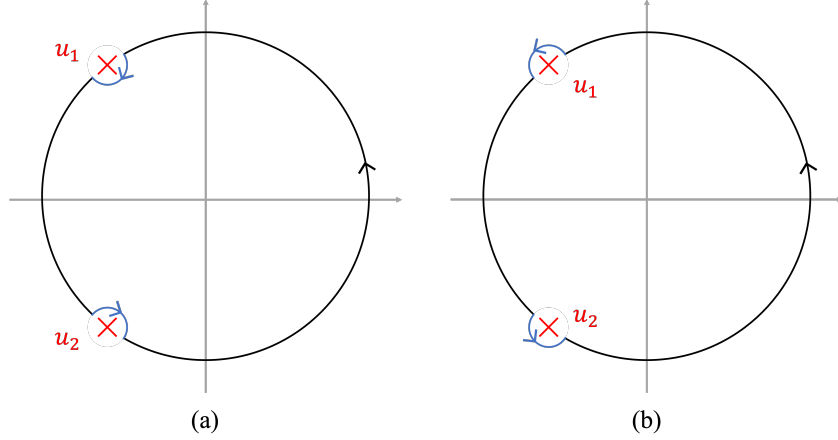


Figure 4.2: Evaluation of the Cauchy principal value integral (4.41) by adding small semicircles (blue). The contour is cut open near the roots u_1 and $u_2 = u_1^{-1}$ which, for simplicity, are assumed to be the only roots of $K(u)$. In subfigure (a), clockwise semicircles are added inside the unit circle, and the closed contour picks up no pole. Alternatively, in subfigure (b), counterclockwise semicircles are added outside the unit circle, and the closed contour picks up both poles. The two methods give the same answer after correctly subtracting the contributions of the semicircles.

the poles at u_α . Meanwhile, the added clockwise semicircle integral is minus half of the residues at u_α because the added pieces are semicircles. Subtracting the latter from the former yields the Cauchy principal value, which includes half of the residues at u_α . Alternatively, if the semicircles are outside the unit circle as shown in Fig. 4.2 (b), then the closed contour picks up all poles at u_α . After subtracting the counterclockwise semicircle integrals, the result is again half of the residues at u_α . As expected, these two ways of closing the contour give the same answer.

For large $|z|$, the braiding phase (4.42) is dominated by roots u_α on the unit circle,

$$\phi(\infty, z) = -\pi \sum_{\alpha} u_{\alpha}^{|z|-1} \text{Res}_{u_{\alpha}} \left(\frac{1}{k(u)} \right) = -i \sum_{\alpha} \frac{g^2}{2m_{\alpha}} e^{iq_{\alpha}|z|}. \quad (4.43)$$

Instead of exponentially decaying statistics in gapped CS_{∞} theories, gapless CS_{∞} theories with $\Gamma_{\max} = 1$ have planon statistics which oscillate in z . Of course, the calculation here is only for particular planon trajectories (one static and the other circular), and it is unclear whether the braiding phase has any topological invariance. As will be derived from the correlation function of Wilson lines at the end of this section, the planon braiding phase $\phi(r, z)$ at large r is indeed invariant under diffeomorphisms in the τxy space, provided that $\Gamma_{\max} = 1$.

Second, suppose that $\Gamma_{\max} > 1$. The braiding phase $\phi(r, z)$ turns out to diverge as

$r \rightarrow \infty$. This divergence can be explained in the simple example

$$K(u) = (-u + 2 - u^{-1}). \quad (4.44)$$

The theory has only one gapless momentum $q_1 = 0$, with multiplicity $\Gamma_1 = 2$. The eigenvalue of K near q_1 is $\lambda(q) \approx q^2$. The braiding phase is still given by the Cauchy principal value integral (4.39). However, $1/\lambda(q) \rightarrow +\infty$ as $q \rightarrow 0$ from both sides of the real axis, so (4.39) diverges despite the Cauchy principal value regularization. In contrast, in a theory with $\Gamma_{\max} = 1$, there is no divergence because $1/\lambda(q)$ switches sign as q goes across each gapless momentum. For a more detailed understanding of the divergence in the example (4.44), consider the braiding phase with finite r . Since (4.39) suggests that the divergence is due to light photon modes, the braiding phase (4.35) can be approximated by

$$\phi(r, z) = -2\pi \int_{-\infty}^{\infty} \frac{dq}{2\pi} \frac{1}{q^2} \left[1 - \frac{g^2 q^2 r}{2\pi} K_1 \left(\frac{g^2 q^2 r}{2\pi} \right) \right] e^{iqz}.$$

Simplifying with the asymptotic form (4.36) of K_1 ,

$$\phi(r, z) = \int \frac{dq}{2\pi} \frac{g^4 q^2 r^2}{4\pi} \log \left(\frac{g^2 q^2 r}{2\pi} \right) e^{iqz}, \quad (4.45)$$

where implicitly, the integral is properly regulated to avoid any divergence. If $z = 0$, or more generally $g^2 r \gg z^2$, then the e^{iqz} factor in (4.45) can be dropped. Thus by dimensional analysis,

$$\phi(r, z) \propto r^{1/2}.$$

Therefore, the braiding phase of two elementary planons depends on the trajectories of the planons and has no topological invariance. However, some composite planons can still have topologically invariant braiding phases. In the example (4.44), such composite planons are generated by dipoles with no net charge, consisting of elementary planons in (exactly two) adjacent layers with opposite charge. Intuitively, this is because the Laurent polynomial

$$\frac{K(u)}{u-1} = -1 + u^{-1}$$

has no repeated root and therefore falls into the $\Gamma_{\max} = 1$ case. Here, the denominator $u - 1$ is chosen to represent the dipole (more on this in Section 6.4). Even though $-1 + u^{-1}$ is not invariant under $u \mapsto u^{-1}$ and hence cannot represent a K matrix, it provides the appropriate mathematical intuition.

More generally, consider a theory with $\Gamma_{\max} > 1$. Near a gapless momentum q_α , the photon mass is (up to a minus sign)

$$m(q) = m_\alpha (q - q_\alpha)^{\Gamma_\alpha} \left[1 + b_1 (q - q_\alpha) + b_2 (q - q_\alpha)^2 + \dots \right],$$

where b_i are some coefficients that are generically non-zero. Thus

$$\frac{1}{m(q)} = \frac{1}{m_\alpha} [(q - q_\alpha)^{-\Gamma_\alpha} - b_1(q - q_\alpha)^{1-\Gamma_\alpha} + (b_1^2 - b_2)(q - q_\alpha)^{2-\Gamma_\alpha} + \dots]. \quad (4.46)$$

Generically, since $\Gamma_{\max} > 1$, either the first or the second term of (4.46) diverges in $q - q_\alpha$ with an even power. Although this argument assumes $b_1 \neq 0$ and does not cover all possibilities, it can be shown that a theory with $\Gamma_{\max} > 1$ always has a gapless momentum q_α and a term in the expansion (4.46) near q_α which diverges in $q - q_\alpha$ with an even power. Then the same argument as in the example (4.44) shows that the braiding phase of two elementary planons diverges as $r \rightarrow \infty$.

Correlation function of Wilson lines

Finally, I compute the correlation function of Wilson lines. As promised several times in this chapter, the calculation reveals the topological property of planon braiding statistics as well as the spatial profiles of planons.

Let C_1 and C_2 be two closed loops in the τxy space. The correlation function of the Wilson loop of A^z on C_1 and the Wilson loop of A^0 on C_2 is

$$\langle W^z(C_1)W^0(C_2) \rangle = \exp \left[-g^2 \oint_{C_1} dx_1^\mu \oint_{C_2} dx_2^\nu G_{\mu\nu}(x_1 - x_2, z) \right]. \quad (4.47)$$

Here, $G_{\mu\nu}(x_1 - x_2, z)$ is the Green's function and can be obtained from (4.18) by Fourier transform,

$$G_{\mu\nu}(x, z) = \int_{-\pi}^{\pi} \frac{dq}{2\pi} G_{\mu\nu}(m(q), x) e^{iqz}.$$

The most interesting physics occurs when $\Gamma_{\max} = 1$, which I assume unless stated otherwise.

By (4.20), the real part of the Green's function is

$$\text{Re}[G_{\mu\nu}(x, z)] = \int_{-\pi}^{\pi} \frac{dq}{2\pi} \int \frac{d^3k}{(2\pi)^3} \frac{k^2 \delta_{\mu\nu} - k_\mu k_\nu}{k^2 (k^2 + m(q)^2)} e^{ikx + iqz}. \quad (4.48)$$

In the limit $g^2 r \gg 1$, $\text{Re}[G_{\mu\nu}(x, z)]$ is dominated by light photon modes and can be approximated by

$$\text{Re}[G_{\mu\nu}(x, z)] = \sum_{\alpha} \int_{-\infty}^{\infty} \frac{dq}{2\pi} \int \frac{d^3k}{(2\pi)^3} \frac{k^2 \delta_{\mu\nu} - k_\mu k_\nu}{k^2 (k^2 + m_\alpha^2 q^2)} e^{ikx + i(q+q_\alpha)z}, \quad (4.49)$$

where m_α is the coefficient in the expansion $m(q) \approx m_\alpha(q - q_\alpha)$ near q_α . I also changed the integration variable to $q - q_\alpha$ near q_α and extended the integration range to $(-\infty, \infty)$. This integral can be evaluated explicitly, and the result is

$$\begin{aligned} & \text{Re}[G_{\mu\nu}(x, z)] \\ &= \sum_{\alpha} \frac{e^{iq_\alpha z}}{4\pi^2 |m_\alpha| r^2} \left[\frac{2}{3(1 + \zeta_\alpha^2)} \delta_{\mu\nu} + \left(1 - \frac{1}{3(1 + \zeta_\alpha^2)} - \zeta_\alpha \cot^{-1}(\zeta_\alpha) \right) Q_{\mu\nu} \right], \end{aligned} \quad (4.50)$$

where $Q_{\mu\nu}$ is the (traceless) quadrupole tensor defined in (4.23), and ζ_α are dimensionless variables defined by

$$\zeta_\alpha = \frac{z}{|m_\alpha|r}. \quad (4.51)$$

The variables ζ_α are of the same order as z/g^2r , but depend individually on the gapless momenta q_α . As a consistency check for the approximation by light photon modes, (4.50) decays like r^{-2} as $r \rightarrow \infty$, which is slower than the r^{-3} decay of the integrand of (4.48) when q is away from the gapless momenta.

The magnitude $|\langle W^z(C_1)W^0(C_2) \rangle|$ of the correlation function can be obtained by substituting the real part of the Green's function (4.50) into (4.47). Note that if the $e^{iq_\alpha z}$ factors are removed from (4.50), then each summand has mass dimension 2 under the scale transformation

$$t \mapsto \Lambda t, \quad x \mapsto \Lambda x, \quad y \mapsto \Lambda y, \quad z \mapsto \Lambda z. \quad (4.52)$$

Therefore, the magnitude of the correlation function is of the form

$$|\langle W^z(C_1)W^0(C_2) \rangle| = \exp \left[\sum_\alpha e^{iq_\alpha z} F_\alpha(C_1, C_2) \right], \quad (4.53)$$

where $F_\alpha(C_1, C_2)$ are scale invariant functions. This is related to the scale invariance of the low-energy spectrum (4.1) when $\Gamma_{\max} = 1$.

By (4.24), the imaginary part of the Green's function is

$$\text{Im}[G_{\mu\nu}(x, z)] = - \int_{-\pi}^{\pi} \frac{dq}{2\pi} \frac{\epsilon_{\mu\nu\rho} x^\rho}{4\pi r^3} h_r(m(q)) e^{iqz}, \quad (4.54)$$

where the function

$$h_r(m) = \frac{1 - e^{-|m|r}(1 + |m|r)}{m}$$

is a modified version of the function $h_1(m, r)$ in (4.25). The behavior of $h_r(m)$ is similar to that of $f_r(m)$ in (4.38). It vanishes at $m = 0$ for all $r > 0$. As r increases, it becomes a better and better approximation to the function $1/m$ except when m is close to zero. Therefore, if $g^2r \gg 1$ and $g^2r \gg |z|$, then (4.54) can be approximated by the Cauchy principal value integral

$$\text{Im}[G_{\mu\nu}(x, z)] = - \text{PV} \int_{-\pi}^{\pi} \frac{dq}{2\pi} \frac{e^{iqz}}{m(q)} \frac{\epsilon_{\mu\nu\rho} x^\rho}{4\pi r^3} + \dots. \quad (4.55)$$

The $g^2r \gg |z|$ assumption is to make sure that the integrand of (4.54) varies slowly as a function of q , and the “ \dots ” in (4.55) is the correction due to finite r . The leading order correction comes from light photon modes for which $h_r(m)$ deviates from $1/m$ significantly, given by

$$\begin{aligned} & \sum_\alpha \int_{-\infty}^{\infty} \frac{dq}{2\pi} \frac{e^{-|m_\alpha q|r}(1 + |m_\alpha q|r)}{m_\alpha q} \frac{\epsilon_{\mu\nu\rho} x^\rho}{4\pi r^3} e^{i(q+q_\alpha)z} \\ &= i \sum_\alpha \frac{e^{iq_\alpha z}}{\pi m_\alpha} \left(\frac{\zeta_\alpha}{1 + \zeta_\alpha^2} + \tan^{-1}(\zeta_\alpha) \right) \frac{\epsilon_{\mu\nu\rho} x^\rho}{4\pi r^3}, \end{aligned} \quad (4.56)$$

where I used the same approximation as in (4.49), and ζ_α are given by (4.51). Putting (4.55) and (4.56) together, the imaginary part of the Green's function is

$$\begin{aligned} & \text{Im}[G_{\mu\nu}(x, z)] \\ &= \left[-\text{PV} \int_{-\pi}^{\pi} \frac{dq}{2\pi} \frac{e^{iqz}}{m(q)} + i \sum_{\alpha} \frac{e^{iq_{\alpha}z}}{\pi m_{\alpha}} \left(\frac{\zeta_{\alpha}}{1 + \zeta_{\alpha}^2} + \tan^{-1}(\zeta_{\alpha}) \right) \right] \frac{\epsilon_{\mu\nu\rho} x^{\rho}}{4\pi r^3}. \end{aligned} \quad (4.57)$$

This equation holds in the limit $g^2 r \sim |z| \gg 1$. In fact, by a more careful analysis, it can be shown that the relative error in (4.57) is at most $\mathcal{O}(|z|^{-1+\delta})$ for any $\delta > 0$. In the limit $g^2 r \sim |z| \gg 1$, the principal value integral in (4.57) can be treated using the same approximation as in (4.43) which discards the contribution from roots of $K(u)$ inside the unit circle. The result is

$$\text{Im}[G_{\mu\nu}(x, z)] = i \sum_{\alpha} \frac{e^{iq_{\alpha}z}}{m_{\alpha}} \left[-\frac{1}{2} \text{sgn}(z) + \frac{1}{\pi} \left(\frac{\zeta_{\alpha}}{1 + \zeta_{\alpha}^2} + \tan^{-1}(\zeta_{\alpha}) \right) \right] \frac{\epsilon_{\mu\nu\rho} x^{\rho}}{4\pi r^3}, \quad (4.58)$$

where ‘‘sgn’’ is the sign function.

The phase $\phi(C_1, C_2, z)$ of the correlation function $\langle W^z(C_1)W^0(C_2) \rangle$ can be obtained by substituting the imaginary part of the Green's function (4.57) into (4.47). First, consider the limit $g^2 r \gg 1$ and $g^2 r \gg |z|$. This is the limit where discussions of the topological invariance of the planon braiding phase usually take place. By (4.55), the phase is

$$\phi(C_1, C_2, z) = -2\pi \text{PV} \int_{-\pi}^{\pi} \frac{dq}{2\pi} \frac{e^{iqz}}{\lambda(q)} \text{link}(C_1, C_2).$$

This agrees with the result (4.43) for the particular configuration where one planon circles around another, static planon. The phase depends on C_1 and C_2 only through their linking number $\text{link}(C_1, C_2)$, which can be traced back to the fact that (4.55) depends on x only through the CS Green's function (4.26). Therefore, the braiding phase of planons at large separation r is topological in the sense that it is invariant under diffeomorphisms in the txy space. Unlike gapped topological or fracton models, the magnitude (4.53) of the correlation function is not 1 even for large r , and the topological invariance only applies to the **phase** of the correlation function.

Second, consider the limit $g^2 r \sim |z| \gg 1$. Due to the presence of ζ_{α} in (4.58), the phase of the correlation function is no longer topological. However, this limit reveals the spatial profiles of planons. To see this, take C_1 to be a straight line extending in the τ direction, and C_2 a circle at a fixed time centered at C_1 . By (4.58), the phase of the correlation function is

$$\phi(r, z) = -i \sum_{\alpha} \frac{g^2 e^{iq_{\alpha}|z|}}{2m_{\alpha}} \left(1 - \frac{|z|}{\sqrt{m_{\alpha}^2 r^2 + z^2}} \right). \quad (4.59)$$

This result can also be derived from (4.35) by focusing on the light photon modes. By (4.43), the total flux of a planon in each xy plane oscillates but does not decay

in the z direction. Then by either the scale symmetry (4.52) (up to factors of $e^{iq_\alpha|z|}$) or the explicit formula (4.59), the flux is more and more spread out in the xy plane as $|z|$ increases. Therefore, the energy profile of a planon in a gapless CS_∞ theory with $\Gamma_{\max} = 1$ is localized, but the planon itself is not a localized particle as far as braiding statistics are concerned.

I end this section with some brief comments on the correlation function of Wilson lines in a theory with $\Gamma_{\max} > 1$. Given the electric potential (4.34), the magnitude of the correlation function is expected to decay as

$$|\langle W^z(C_1)W^0(C_2) \rangle| \sim \exp \left[-(g^2 r)^{1-1/\Gamma_{\max}} \right]$$

in the limit $g^2 r \gg 1$. As for the phase of the correlation function, I consider the example (4.44). In this example, the braiding phase (4.45) is invariant under the Lifshitz scale symmetry

$$r \mapsto \Lambda r, \quad z \mapsto \Lambda^{1/2} z.$$

Therefore, the planons in a gapless CS_∞ theory with $\Gamma_{\max} > 1$ are not localized particles but have localized energy profiles, as is the case when $\Gamma_{\max} = 1$. The flux of a planon spreads out in the xy plane even more quickly as $|z|$ increases than in theories with $\Gamma_{\max} = 1$.

4.4 Effective field theory

In a CS_∞ theory, the t , x and y coordinates are continuous, while the z coordinate is discrete. Naturally, one wonders if there is a fully continuous field theory that captures the low-energy physics of a gapless CS_∞ theory. As shown throughout this chapter, gapless CS_∞ theories with $\Gamma_{\max} = 1$ have particularly nice properties, all of which are related to the isotropic scaling symmetry (4.52) at low energy. In this section, I write down and discuss fully continuous effective theories for gapless CS_∞ theories with $\Gamma_{\max} = 1$.

Let b be the physical lattice spacing in the z direction, and define

$$\hat{z} = zb, \quad \hat{g}^2 = g^2 b.$$

The continuum limit is achieved by taking $b \rightarrow 0$ while holding the dimensionless coupling \hat{g} fixed, which corresponds to the limit $g^2 r \sim |z| \gg 1$ in the CS_∞ theory. Indeed, all observables computed in Section 4.3 in this limit are dominated by light photon modes. Define a **complex** gauge field $\hat{A}_\alpha(\hat{z})$ for each gapless momentum q_α , which varies slowly in z . The fields $\hat{A}_\alpha(\hat{z})$ are related to the original fields A^z by

$$A^z = \sum_{\alpha} e^{iq_\alpha z} \hat{A}_\alpha(zb), \quad (4.60)$$

where heavy fields with momenta away from q_α are omitted. Since A^z are real gauge fields, the continuum fields are constrained by $\hat{A}_{\alpha^*}(\hat{z}) = \hat{A}_\alpha^\dagger(\hat{z})$, where α^* is defined by $q_{\alpha^*} = -q_\alpha$. Therefore, each pair of gauge fields $\hat{A}_\alpha(\hat{z})$ and $\hat{A}_{\alpha^*}(\hat{z})$ share a non-compact gauge group \mathbb{R}^2 .

The action of the CS_∞ theory is of course

$$S = \int d^3x \sum_z \mathcal{L}, \quad (4.61)$$

where \mathcal{L} is given by (2.1). The effective action is obtained by substituting (4.60) into (4.61) and then taking the continuum limit,

$$S_{\text{eff}} = \int d^3x d\hat{z} \sum_\alpha \left(\frac{1}{2\hat{g}^2} \hat{F}_{\alpha,\mu\nu}^\dagger \hat{F}_\alpha^{\mu\nu} + \frac{\lambda_\alpha}{4\pi} \epsilon^{\mu\nu\rho} \partial_z \hat{A}_{\alpha,\mu} \partial_\nu \hat{A}_{\alpha,\rho}^\dagger \right), \quad (4.62)$$

where λ_α is the coefficient in the expansion $\lambda(q) \approx \lambda_\alpha(q - q_\alpha)$ near q_α . To derive (4.62), I replaced $b \sum_z$ by $\int d\hat{z}$, and used the fact that $\hat{A}_\alpha(\hat{z})$ are slowly varying fields and therefore satisfy the constraint

$$\sum_z \left[e^{iq_\alpha z} \hat{A}_\alpha(zb) \right] \left[e^{-iq_\beta z} \hat{A}_\beta^\dagger(zb) \right] = \sum_z \delta_{\alpha\beta} \hat{A}_\alpha(zb) \hat{A}_\beta^\dagger(zb).$$

This constraint basically says that since $\hat{A}_\alpha(zb)$ and $\hat{A}_\beta^\dagger(zb)$ have small momenta in the z direction while the gapless momenta are discrete (i.e., separated), the total momentum of the LHS vanishes only if $\alpha = \beta$. The effective action (4.62) is invariant under the isotropic scale transformation (4.52), and all couplings in the action are dimensionless. As can be shown by straightforward calculations, the effective action reproduces the low-energy spectrum (4.1) of the corresponding CS_∞ theory, as well as its Green's function (4.50) and (4.58) in the limit $g^2 r \sim |z| \gg 1$. A notable exception is the braiding phase of planons, which is defined (and proved to be topological) in the limit $g^2 r \gg |z|$ and $g^2 r \gg 1$. Therefore, the braiding phase cannot be obtained from the effective action unless $|z| \gg 1$. Mathematically, this is because the braiding phase receives contribution from both the roots of $K(u)$ on the unit circle and those inside the unit circle, while the effective action does not account for the latter.

GSD OF FRACTON MODELS: AN OPERATOR ALGEBRA APPROACH

In Chapters 3 and 4, I studied fracton models beyond the foliation paradigm in the form of CS_∞ theories. A natural question is then: What is the appropriate notion of fractonic orders for these models? Unfortunately, I do not know the answer. Nevertheless, in certain non-foliated fracton models that are somewhat less exotic than CS_∞ theories, known as (non-abelian) cage-net models [17], a generalized version of foliation can be applied. This generalized foliation RG is the topic of Chapter 6, where I will demonstrate the RG process on the example of the Ising cage-net model (“Ising cage-net” for short). Meanwhile, this chapter is dedicated to proving the absence of a foliation structure in Ising cage-net by computing its GSD.

Ising cage-net is exactly solvable, and its GSD can be obtained with standard string-net or cage-net methods. However, these methods usually involve complicated combinatorial expressions that rely heavily on details at the lattice level. To avoid this problem, I introduce an approach to calculating the GSD of a fracton model that uses intrinsic features of the model such as anyon fusion, braiding and quantum dimension. When applied to Ising cage-net, this approach gives

$$\text{GSD} = \frac{1}{8} (E_3 + E_2 + 5E_1 + 45), \quad (5.1)$$

where $E_3 = 9^{L_x+L_y+L_z}$, $E_2 = 9^{L_x+L_y} + 9^{L_y+L_z} + 9^{L_z+L_x}$, and $E_1 = 9^{L_x} + 9^{L_y} + 9^{L_z}$. Since the GSD does not depend strictly exponentially on the system size, the model is not foliated.

This new method for calculating the GSD can be motivated by well-known facts concerning topological orders. The GSD of a $d = 2 + 1$ topological order equals the number of anyons [38]. Although it only uses intrinsic properties of the topological order, this statement fails in higher dimensions. For example, the $d = 3 + 1$ toric code has $\text{GSD} = 8$ but only two types of fractional excitations, namely a charge point excitation and a flux loop excitation [8]. This problem is remedied by considering instead the algebra A_0 of logical operators of the model. Here, a *logical operator* is an operator that acts on the ground space \mathcal{H}_0 , typically by creating, tunnelling and eventually annihilating a pair of fractional excitations. The dimension of A_0 as a complex vector space is $\dim(A_0) = \dim(\mathcal{H}_0)^2 = \text{GSD}^2$. As shown in Fig. 5.1, in the $d = 3 + 1$ toric code, the logical operators are a string (blue) for the charge and a membrane (red) for the flux. Each pair of string and membrane operators in Fig. 5.1 is equivalent to a pair of Pauli matrices X and Z , and therefore generates

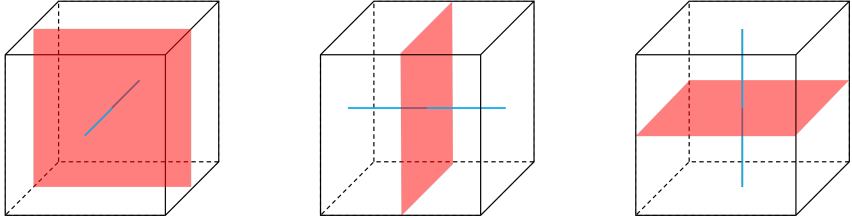


Figure 5.1: Elementary logical operators in the $d = 3 + 1$ toric code. The blue lines are string operators for charges, and the red planes are membrane operators for fluxes. Each pair of string and membrane operators is equivalent to a pair of Pauli matrices X and Z . Operators in different pairs commute.

an algebra of dimension 4, spanned as a vector space by $1, X, Y$ and Z . There are three independent pairs of string and membrane operators, so

$$\dim(A_0) = 4^3 = 64 = \text{GSD}^2,$$

and thus $\text{GSD} = 8$. In general, the new method of calculation aims to describe A_0 as a redundant, formal algebra A of operators quotiented by certain physically justified relations. The $d = 3 + 1$ toric code is too simple to have any non-trivial relation of operators, and more complicated examples will be discussed later in this chapter. Once this quotienting procedure is completed, the GSD is obtained from $\text{GSD}^2 = \dim(A_0)$. Due to its focus on the algebra of logical operators instead of the ground space, I call this method of calculation the *operator algebra approach*.

In what follows, I begin in Section 5.1 by reviewing Ising cage-net. In Section 5.2, I introduce the operator algebra approach by studying the simple example of the chiral Ising anyon model. The underlying mathematics of the this approach is the theory of semisimple algebras, and I discuss the structure of semisimple algebras in Section 5.3. More mathematical details are given in Appendix 5.8. The construction of Ising cage-net involves p-loop condensation, and I study boson condensation in the operator algebra approach in Section 5.4 with the example of a condensation transition in the doubled Ising string-net model. I then use the operator algebra approach in Section 5.5 to study a more complicated $d = 2 + 1$ topological order, the one-foliated Ising cage-net model. This model is closely related to Ising cage-net but is still in $d = 2 + 1$, so the consistency of the operator algebra approach can be checked by anyon counting. I also present another method of computing the GSD within the operator algebra approach via a Cartan subalgebra. In Section 5.6, I put all of these tools together and compute the GSD of Ising cage-net in two ways. The correctness of the result (5.1) is further confirmed with traditional lattice calculation for the smallest system size. Finally in Section 5.7, I discuss the possibility of viewing the operator algebra approach as more than just a trick for calculating the GSD. The framework of the this approach is so natural that it has the potential to provide

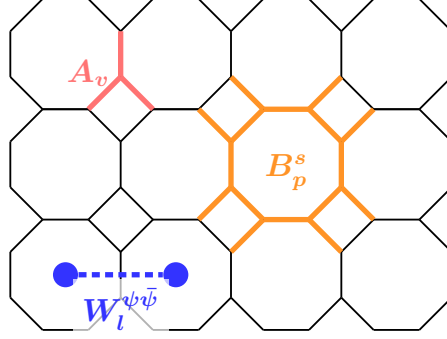


Figure 5.2: A square-octagon lattice. A vertex term A_v and a plaquette term B_p^s are shown. The string operator $W_l^{\psi\bar{\psi}}$ creates a $\psi\bar{\psi}$ excitation on each of the two plaquettes bordering the edge l .

a characterization of fracton models. However, some key parts of the framework are missing and need to be filled in before such potential can be realized.

The results in this chapter are based on Ref. [30].

5.1 Motivating example: The Ising cage-net model

In this section, I review the basic properties of Ising cage-net that are necessary for the GSD calculation later [17]. The building block of Ising cage-net is the doubled Ising string-net model (“doubled Ising” for short) [54]. Doubled Ising can be realized on any $d = 2$ trivalent lattice. Here, a square-octagon lattice (Fig. 5.2) is chosen for the purpose of constructing Ising cage-net later. On each edge of the lattice, there is a local Hilbert space of dimension 3, with orthonormal basis vectors $|0\rangle$, $|1\rangle$ and $|2\rangle$. The labels $\{0, 1, 2\}$ are understood as values of “strings” located at the edges. The model also comes with a set of symbols $(\delta_{ijk}, d_s, F_{klm}^{ijm})$, where all indices take values in $\{0, 1, 2\}$. For example, $\delta_{ijk} = 1$ if $ijk = 000, 011, 022, 112$ or their permutations, and $\delta_{ijk} = 0$ otherwise.

The Hamiltonian consists of a vertex term A_v for each vertex v and a plaquette term B_p for each plaquette p . The vertex term is

$$A_v \left| \begin{array}{c} j \\ i \quad k \end{array} \right\rangle = \delta_{ijk} \left| \begin{array}{c} j \\ i \quad k \end{array} \right\rangle,$$

which allows certain ways for the strings to “fuse” at a vertex at low energy. The plaquette term is

$$B_p = \frac{\sum_s d_s B_p^s}{\sum_s d_s^2},$$

where the operator B_p^s involves the symbols F_{klm}^{ijm} and essentially acts by fusing an s -loop into the plaquette p ; the precise definition of B_p^s is not important here. The

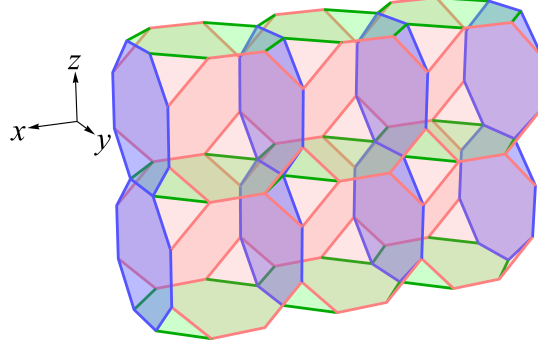


Figure 5.3: A truncated cubic lattice constructed from intersecting layers of the square-octagon lattice.

full Hamiltonian is then

$$H = - \sum_v A_v - \sum_p B_p. \quad (5.2)$$

This is a commuting projector Hamiltonian when restricted to the low-energy subspace where $A_v = 1$ for all v . It has anyons $1, \sigma, \bar{\sigma}, \psi, \bar{\psi}, \sigma\bar{\psi}, \psi\bar{\sigma}, \sigma\bar{\sigma}$ and $\psi\bar{\psi}$, where $\bar{\psi}$ is the time-reversal of ψ but otherwise unrelated to ψ , and similarly for $\bar{\sigma}$. In fact, doubled Ising can be viewed as the chiral Ising anyon model [55] (more discussions in Section 5.2) which has anyons $1, \sigma$ and ψ , stacked with its time-reversal which has anyons $1, \bar{\sigma}$ and $\bar{\psi}$, hence the name “doubled” Ising. The fusion rules for σ and ψ are $\sigma \times \sigma = 1 + \psi$, $\sigma \times \psi = \sigma$, $\psi \times \psi = 1$; similarly for $\bar{\sigma}$ and $\bar{\psi}$. The R -symbols and string operators of the anyons can be found in Ref. [54], and I mention some important ones here:

1. The braiding of σ with ψ gives a phase -1 , and ψ braids trivially with ψ ; same for $\bar{\sigma}$ and $\bar{\psi}$.
2. The operator $W_l^{\psi\bar{\psi}} = (-1)^{n_1(l)}$ creates a $\psi\bar{\psi}$ excitation on each of the two plaquettes bordering the edge l , where $n_1(l) = 1$ if the state on the edge l is $|1\rangle$, and $n_1(l) = 0$ otherwise (Fig. 5.2). The blue dashed line can be extended into a string operator of $\psi\bar{\psi}$.

As a $d = 2 + 1$ topological order, the GSD of doubled Ising is equal to the number of anyons, so $\text{GSD} = 9$.

The construction of Ising cage-net starts with three stacks of doubled Ising in the x, y and z directions, respectively. The resulting lattice is a truncated cubic lattice (Fig. 5.3). In this lattice, an edge l_μ parallel to the μ direction for $\mu = x, y$ or z is called a *principal edge*. I also distinguish the octagon and square plaquettes, denoting them by p_o and p_s , respectively. On a principal edge l_μ , the operator

$$V_{l_\mu} = W_{l_\mu}^{(\psi\bar{\psi})^\nu} W_{l_\mu}^{(\psi\bar{\psi})^\rho} = (-1)^{n_1^\nu(l_\mu)} (-1)^{n_1^\rho(l_\mu)} \quad (5.3)$$

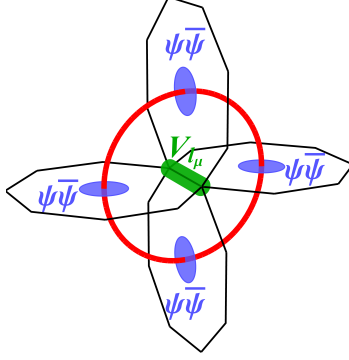


Figure 5.4: A $\psi\bar{\psi}$ p-loop (red) created by the operator V_{l_μ} (green cylinder). The shape of the p-loop is obtained by connecting the $\psi\bar{\psi}$ particles with line segments orthogonal to their hosting plaquettes.

creates a $\psi\bar{\psi}$ particle-loop (“p-loop” for short) around the edge (Fig. 5.4), where μ , ν and ρ are distinct. Here, $a^\mu(i)$ denotes the anyon a in the i th plane orthogonal to the μ direction, and the i label may be omitted when it is clear from context. For example, if $\mu = x$, $\nu = y$ and $\rho = z$, then the $\psi\bar{\psi}$ particles in the p-loop originate from the xz and xy planes. The p-loops can be condensed by the Hamiltonian

$$H_0 - J \sum_{\mu} \sum_{l_{\mu}} V_{l_{\mu}},$$

where H_0 is the Hamiltonian for the decoupled layers of doubled Ising, and $J > 0$ is a large coefficient enforcing the condensation. This reduces the low-energy Hilbert space on each edge to a vector space of dimension 5, spanned by $|00\rangle$, $|02\rangle$, $|20\rangle$, $|22\rangle$ and $|11\rangle$. If perturbation theory is applied with H_0 as the perturbation, then the plaquette terms $B_{p_o}^1$ must be assembled into cube terms

$$B_c = \prod_{p_o \in c} \frac{1}{\sqrt{2}} B_{p_o}^1 \quad (5.4)$$

for each cube c . The resulting Hamiltonian of Ising cage-net is

$$H = - \sum_{v, \mu} A_v^\mu - \sum_{p_s} B_{p_s} - \sum_{p_o} B_{p_o}^2 - \sum_c B_c, \quad (5.5)$$

where A_v^μ is the vertex term at vertex v orthogonal to the μ direction, and $B_{p_o}^2$ is the plaquette term of the 2-loop (not the square of an operator). The terms are shown in Fig. 5.5. This is a commuting projector Hamiltonian when restricted to the low-energy subspace where all vertex terms are satisfied.

In order for an anyon to remain deconfined upon condensation, its string operator must commute with V_{l_μ} . In other words, the anyon must braid trivially with the $\psi\bar{\psi}$ p-loop. For example, a σ planon in an xy plane has a braiding phase -1 with a $\psi\bar{\psi}$

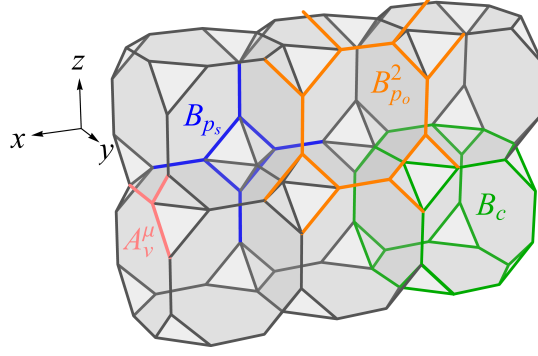


Figure 5.5: Hamiltonian terms of Ising cage-net. The Hamiltonian is given by (5.5).

Mobility	Type	Excitations
Planon	Abelian	$\psi^\mu(i), \bar{\psi}^\mu(i)$
	Non-abelian	$\sigma^\mu(i)\sigma^\mu(j), \bar{\sigma}^\mu(i)\sigma^\mu(j),$ $\sigma^\mu(i)\bar{\sigma}^\mu(j), \bar{\sigma}^\mu(i)\bar{\sigma}^\mu(j)$
Lineon	Abelian	
	Non-abelian	$\sigma^\mu(i)\sigma^\nu(j), \bar{\sigma}^\mu(i)\sigma^\nu(j),$ $\sigma^\mu(i)\bar{\sigma}^\nu(j), \bar{\sigma}^\mu(i)\bar{\sigma}^\nu(j)$

Table 5.1: Elementary excitations in Ising cage-net. The lineon sector requires $\mu \neq \nu$. The lineon $\sigma^x(i)\sigma^y(j)$ moves in the z direction; similarly for the other lineons.

p -loop created by some V_{l_x} or V_{l_y} , and is therefore confined. On the other hand, a σ planon in an xy plane combines with a σ planon in an xz plane to form a lineon that moves in the x direction, and this lineon is deconfined. The deconfined excitations are summarized in Table 5.1.

Although Ising cage-net is exactly solvable, it is not obvious how its GSD can be calculated. In the following sections, I will introduce the operator algebra approach to calculating the GSD, which works for Ising cage-net. I will start with some simple $d = 2 + 1$ topological orders, and work gradually towards Ising cage-net.

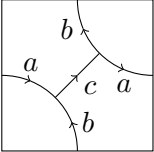
5.2 The chiral Ising anyon model and operator algebra

The chiral Ising anyon model (“chiral Ising” for short) is a well-understood $d = 2 + 1$ topological order [55]. As explained previously, chiral Ising can be used to construct doubled Ising and hence Ising cage-net. In this section, I review chiral Ising and calculate its GSD using the operator algebra approach. While the calculation may seem over-complicated for this simple model, I aim to set up the general formalism and present several useful mathematical statements.

There are three anyons in chiral Ising: 1, σ and ψ . This model can be obtained, for example, by gauging the \mathbb{Z}_2 fermion parity symmetry in a $p + ip$ superconductor.

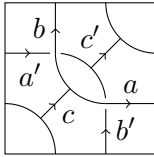
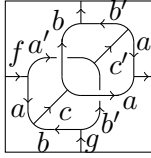
In this context, 1 is the vacuum, σ is the π gauge flux, and ψ is the gauge charge. The fusion rules are $\sigma \times \sigma = 1 + \psi$, $\sigma \times \psi = \sigma$, $\psi \times \psi = 1$. The F - and R -symbols can be found in Ref. [56]. The GSD of a $d = 2 + 1$ topological order is equal to the number of anyons, so chiral Ising has $\text{GSD} = 3$. This is equivalent to saying that the algebra of logical operators is $A_0 = \text{Mat}_3$. Here, Mat_n is the set of all $n \times n$ complex matrices. In the operator algebra approach, I treat A_0 as the more fundamental object, attempt to compute A_0 without knowledge of the ground space \mathcal{H}_0 , and view \mathcal{H}_0 as a representation space of A_0 .

The operator algebra approach starts with a set of logical operators that span the vector space of all logical operators, but are not necessarily linearly independent. For a $d = 2 + 1$ topological order on a torus, these starting operators are chosen to be of the form

$$v(a, b, c) = \begin{array}{|c|} \hline \begin{array}{c} \text{Diagram of } v(a, b, c) \end{array} \\ \hline \end{array}, \quad (5.6)$$


where a, b, c are anyons consistent with the fusion rules (for simplicity I assume no fusion multiplicity). Such an operator is called an *elementary operator*. If $b = 1$ then $a = c$, and I define the short-hand notation $a_x = v(a, 1, a)$; similarly $b_y = v(1, b, b)$.

Of course, an elementary operator acts on the ground space \mathcal{H}_0 and has a matrix representation, but the discussion here does not rely on such a representation. Instead, the operators are viewed as abstract objects. Let A be the complex vector space over the elementary operators, with formal addition and formal scalar multiplication. The vector space A also has an operation called multiplication, defined for a pair of elementary operators by stacking one on top of the other and reducing the diagram to a sum of elementary operators using F - and R -symbols:

$$\begin{aligned} v(a, b, c)v(a', b', c') &= \begin{array}{|c|} \hline \begin{array}{c} \text{Diagram of } v(a, b, c)v(a', b', c') \end{array} \\ \hline \end{array} \\ &= \sum_{f, g} \sqrt{\frac{d_f d_g}{d_a d_{a'} d_b d_{b'}}} \begin{array}{|c|} \hline \begin{array}{c} \text{Diagram of } v(f, g, h) \end{array} \\ \hline \end{array} \\ &= \sum_{f, g, h} \lambda(f, g, h) v(f, g, h), \end{aligned}$$



with some coefficients $\lambda(f, g, h)$. Here f, g and h are some anyons, and d_a is the quantum dimension of a . Going from the first line to the second line, the anyon a is fused with a' into f , and b with b' into g ; going from the second line to the third

line, I used F - and R -moves to transform the diagrams into elementary operators. In principle, $\lambda(f, g, h)$ can be computed for a general anyon theory, but only some simple cases are needed in this thesis. For example, in chiral Ising,

$$\psi_x \psi_y = v(\psi, 1, \psi) v(1, \psi, \psi) = -v(\psi, \psi, 1),$$

where the minus sign comes from $R_1^{\psi, \psi} = -1$. The multiplication has an identity $1 = v(1, 1, 1)$. The set A is called an *algebra*, which is a complex vector space equipped with multiplication and a multiplicative identity (Definition 18 in Appendix 5.8 explains this concept more rigorously). If one views the elements of A as operators on \mathcal{H}_0 , then the addition, scalar multiplication and multiplication are the usual matrix operations. However, I emphasize again that A is considered in the operator algebra approach as a structure in its own right and should not be interpreted as a matrix algebra acting on a Hilbert space just yet.

In chiral Ising, there are 10 elementary operators:

$$\begin{aligned} &v(1, 1, 1), \quad v(\psi, 1, \psi), \quad v(1, \psi, \psi), \quad v(\psi, \psi, 1), \quad v(\sigma, 1, \sigma), \\ &v(1, \sigma, \sigma), \quad v(\sigma, \psi, \sigma), \quad v(\psi, \sigma, \sigma), \quad v(\sigma, \sigma, 1), \quad v(\sigma, \sigma, \psi). \end{aligned}$$

Thus $\dim(A) = 10$. However, by prior knowledge, the algebra of logical operators should be $A_0 = \text{Mat}_3$ with $\dim(A_0) = 9$, so A is too large. This means that A has some redundancy which should be reduced by modding out certain relations. Such redundancy reduction turns out to be equivalent to acting on A by a projector P , which kills the subspace $(1 - P)A$ and preserves its complement PA .

Before discussing where the relations come from, I first answer a question: How does one know whether sufficiently many relations have been found so that PA is small enough? For a topological or fracton model, its algebra of logical operators should be Mat_n for some n . Conversely, a matrix algebra Mat_n has the property that no more redundancy can be modded out (Definition 20 and Lemma 21). Therefore, the redundancy reduction stops if and only if PA is a matrix algebra.

Furthermore, all of the algebras in the physical models in this chapter have the additional property of being so-called semisimple.

Definition 10. An algebra A is *semisimple* if it can be written as a direct sum

$$A = A_1 \oplus \cdots \oplus A_m, \tag{5.7}$$

where each A_i is a matrix algebra.

The redundancy reduction amounts to finding an appropriate projector P that kills all but one A_i , and then the true algebra of logical operators is this A_i . The kernel of P consists of operators that are identified with 0, so the projection essentially takes a “quotient” of A (see details in Appendix 5.8).

The decomposition (5.7) of a semisimple algebra A can be derived systematically, but for the case of chiral Ising in this section, I first write down the result:

$$A = \text{Mat}_3 \oplus \text{Mat}_1. \quad (5.8)$$

A systematic derivation can be found in Section 5.3. In this decomposition,

$$\begin{aligned} \text{Mat}_3 &= \text{span}\{1 + \psi_x, 1 + \psi_y, 1 + r, \sigma_x, \sigma_y, \\ &\quad v(\sigma, \psi, \sigma), v(\psi, \sigma, \sigma), v(\sigma, \sigma, 1), v(\sigma, \sigma, \psi)\}, \\ \text{Mat}_1 &= \text{span}\{1 - r\}, \end{aligned}$$

where

$$r = \frac{1}{2} (1 + \psi_x + \psi_y - \psi_x \psi_y).$$

The 9 spanning elements of Mat_3 are not very important, but the element r will be useful throughout this chapter.

Given the decomposition (5.8), clearly the projector P should be defined such that $PA = \text{Mat}_3$. However, without the prior knowledge that $A_0 = \text{Mat}_3$, this choice of P needs to be justified. To do so, note that A is obtained only using fusion rules, F -symbols and R -symbols, while further information such as the topology of the torus has not been fully utilized. Indeed, one can put a contractible σ -loop “around the corners” of the torus, reduce it to a sum of elementary operators on the one hand, and demand that it be equal to the quantum dimension $\sqrt{2}$ of σ on the other hand. Using red lines for σ -strings and blue lines for ψ -strings, the reduction to elementary operators is performed as follows:

$$\begin{aligned} \frac{1}{\sqrt{2}} \left[\text{Diagram: square with red arcs at corners} \right] &= \frac{1}{\sqrt{2}} \left[\text{Diagram: square with red lines forming a cross} \right] = \frac{1}{\sqrt{2}} \sum_{a,b} \sqrt{\frac{d_a d_b}{d_\sigma^4}} \left[\text{Diagram: square with red cross and labels } a, b \right] \\ &= \frac{1}{2\sqrt{2}} \left(\begin{array}{cccc} \left[\text{Diagram: square with red circle} \right] & + & \left[\text{Diagram: square with red circle and blue horizontal line} \right] & + & \left[\text{Diagram: square with red circle and blue vertical line} \right] & + & \left[\text{Diagram: square with red circle and blue cross} \right] \end{array} \right) \\ &= \frac{1}{2\sqrt{2}} \left(\begin{array}{cccc} \left[\text{Diagram: square with red circle} \right] & + & \left[\text{Diagram: square with red circle and blue horizontal line} \right] & + & \left[\text{Diagram: square with red circle and blue vertical line} \right] & + & \left[\text{Diagram: square with red circle and blue cross and blue arc} \right] \end{array} \right) \\ &= \frac{1}{2\sqrt{2}} \left(\sqrt{2} + \sqrt{2}\psi_x + \sqrt{2}\psi_y + \sqrt{2}v(\psi, \psi, 1) \right) \\ &= \frac{1}{2} (1 + \psi_x + \psi_y - \psi_x \psi_y) \\ &= r, \end{aligned} \quad (5.9)$$

where I moved the $\sqrt{2}$ to the denominator. In this calculation, I first moved the σ -strings close together, and then fused the parallel σ -strings to obtain four outcomes (second line). The result is demanding $r = 1$. In other words, $1 - r$ is identified with 0 by the projector $P = (1 + r)/2$, which precisely kills $1 - r$. The same calculation can be repeated for a 1-loop or a ψ -loop “around the corners”, but the results are tautological relations. Only non-abelian anyons can give non-trivial relations.

To conclude this section, I summarize the operator algebra approach as follows:

Protocol 11. Take a topological or fracton model.

1. Choose a set of logical operators that span the space of all logical operators but are not necessarily linearly independent.
2. Reduce the redundancy of these logical operators with F - and R -moves as much as possible. Then take the formal algebra A over the remaining operators, which is a semisimple algebra. In a $d = 2 + 1$ topological order, if the operators are taken to be $v(a, b, c)$ as in (5.6), then these operators have no such redundancy and there is no need for this step.
3. Find relations in A by physical argument. In a $d = 2 + 1$ topological order, the relations come from loops of (non-abelian) anyons “around the corners”. As will be shown in Section 5.6, the relations in Ising cage-net come from cage structures of non-abelian strings. Then mod out the relations by acting with the corresponding projector P . If PA is a matrix algebra, then the true algebra of logical operators is $A_0 = PA$. In Section 5.3, I will discuss a quick way to find P .

5.3 Structure of semisimple algebra

The correctness of the decomposition (5.8) can be checked by hand, but this is far from systematic. It is also unclear so far how relations can be converted to projectors in general. In this section, I resolve these two issues by discussing the structure of a semisimple algebra, and give an efficient method for computing projectors. Several statements in this section will be used in the calculations in later sections.

In the decomposition (5.7) of a semisimple algebra A , each component A_i has its own multiplicative identity P_i , called a primitive central projector of A .

Definition 12. An element $x \in A$ is *central* if $[x, y] = 0$ for all $y \in A$. The set of all central elements of A is the *center* of A , written as $Z(A)$. A central element $x \in Z(A)$ is a *central projector* if $x^2 = x$. A central projector x is *primitive* if $xy = 0$ or x for all central projector $y \in A$.

The primitive central projectors P_i have the property that every central projector Q

can be written as

$$Q = \sum_i \lambda_i P_i,$$

where $\lambda_i = 0$ or 1 . If A is represented as block-diagonal matrices, then a central projector is the identity of several blocks, and a primitive central projector occupies exactly one block. A central projector Q behaves like a projector in the usual sense when acting on A by left multiplication (which is equivalent to right multiplication and conjugation since Q is central).

In principle, given a basis $\{v_\alpha\}$ of A and structure constants $f_{\alpha\beta}^\gamma$ defined by

$$v_\alpha v_\beta = \sum_\gamma f_{\alpha\beta}^\gamma v_\gamma, \quad (5.10)$$

the central projectors are the solutions to the equations

$$\begin{aligned} [x, v_\alpha] &= 0 \text{ for all } \alpha, \\ x^2 &= x. \end{aligned} \quad (5.11)$$

If the solutions are $\{Q_k\}$, then the primitive ones form the subset $\{P_i\} \subset \{Q_k\}$ of maximal size such that $P_i P_j = 0$ for all $i \neq j$. The decomposition (5.7) then follows where $A_i = P_i A$.

Next, I discuss the conversion of relations into projectors. In this chapter, all relations obtained from physical argument happen to be central in A . It also happens that a simply linear rescaling is enough to convert all the relations into central projectors. For example, in chiral Ising, $1 - r$ is rescaled into $(1 - r)/2$. Given relations Q_1, \dots, Q_m where each Q_k is a central projector, the overall projector is

$$P = (1 - Q_1) \cdots (1 - Q_m). \quad (5.12)$$

Such a projector can also be constructed without the assumption that Q_k is central, and this construction is discussed in Appendix 5.8.

As promised, I now apply the procedure above to chiral Ising. The primitive central projectors are found to be

$$P_1 = \frac{1}{2}(1 + r), \quad P_2 = \frac{1}{2}(1 - r).$$

By (5.12) with $Q = P_2$, the algebra of logical operators is

$$PA = (1 - P_2)A = P_1 A = \text{Mat}_3,$$

which is the desired matrix algebra.

In the rest of this chapter, (5.12) will be used constantly for computing projectors.

5.4 The doubled Ising anyon model and condensation

Ising cage-net is constructed via p-loop condensation, an type of Bose-Einstein condensation. In this section, I explain condensation in the operator algebra approach by studying an example of a condensation transition in doubled Ising.

As explained in Section 5.1, doubled Ising is a stack of two copies of chiral Ising, whose anyons are $1, \sigma, \psi$ and $1, \bar{\sigma}, \bar{\psi}$, respectively. Now consider condensing the boson $\psi\bar{\psi}$. For an anyon to remain deconfined upon condensation, it must braid trivially with $\psi\bar{\psi}$. Such anyons are $1 = \psi\bar{\psi}, \psi = \bar{\psi}$ and $\sigma\bar{\sigma}$. Furthermore, $\sigma\bar{\sigma}$ is no longer a simple particle, but instead “splits” into two anyons $\sigma\bar{\sigma} = e + m$. To understand the splitting, note that $\sigma\bar{\sigma}$ is the fusion product of two Majorana modes and hence a (complex) fermion mode. The parity p of this fermion mode can be 0 (unfilled) or 1 (filled), and braiding with either σ or $\bar{\sigma}$ switches the value of p . Therefore, p is not a good quantum number in doubled Ising. However, if $\psi\bar{\psi}$ is condensed then both σ and $\bar{\sigma}$ are confined, so p becomes a good quantum number that distinguishes the unfilled fermion mode (anyon e) from the filled (anyon m). The resulting topological order is the toric code [57].

It turns out that the operator algebra approach provides a nice description of condensation and, in particular, the splitting of anyons. To begin with, I follow Steps 1 and 2 of Protocol 11 to obtain a semisimple algebra A with $\dim(A) = 100$. Since doubled Ising is two copies of chiral Ising, the decomposition of A is

$$A = (\text{Mat}_3 \oplus \text{Mat}_1)^{\otimes 2} = \text{Mat}_9 \oplus \text{Mat}_3 \oplus \text{Mat}_3 \oplus \text{Mat}_1. \quad (5.13)$$

The quantum dimensions of σ and $\bar{\sigma}$ produce two relations $r = 1$ and $\bar{r} = 1$, where

$$\begin{aligned} r &= \frac{1}{2} (1 + \psi_x + \psi_y - \psi_x \psi_y), \\ \bar{r} &= \frac{1}{2} (1 + \bar{\psi}_x + \bar{\psi}_y - \bar{\psi}_x \bar{\psi}_y). \end{aligned}$$

By (5.12), these relations give rise to a projector

$$P = \frac{1}{4} (1 + r)(1 + \bar{r}),$$

and $PA = \text{Mat}_9$ is the correct algebra of logical operators of doubled Ising. Of course, $\sigma\bar{\sigma}$ is also a non-abelian anyon, and it gives another relation $r\bar{r} = 1$, but this relation is already implied by $r = 1 = \bar{r}$.

Upon condensation of $\psi\bar{\psi}$, the operators $\psi_x\bar{\psi}_x$ and $\psi_y\bar{\psi}_y$ should be identified with 1. Let M be the subalgebra of A generated by $\psi_x\bar{\psi}_x$ and $\psi_y\bar{\psi}_y$, which is an *abelian* subalgebra, meaning that $[x, y] = 0$ for all $x, y \in M$. The logical operators that remain “deconfined” are those that commute with M . Such deconfined operators form the *commutant* of M , which is a semisimple subalgebra of A defined as

$$M' = \{x \in A : [x, y] = 0 \text{ for all } y \in M\}.$$

Since M is abelian, $M \subset M'$. The commutant M' is spanned by elementary operators $v(a, b, c)$ where a and b take values in $\{1, \psi, \bar{\psi}, \psi\bar{\psi}, \sigma\bar{\sigma}\}$. A straightforward calculation shows that $\dim(M') = 28$. By analyzing the primitive central projectors of M' using (5.11), M' can be decomposed as

$$M' = (\text{Mat}_3 \oplus 3\text{Mat}_2) \oplus 3\text{Mat}_1 \oplus 3\text{Mat}_1 \oplus \text{Mat}_1,$$

where 3Mat_2 means $\text{Mat}_2 \oplus \text{Mat}_2 \oplus \text{Mat}_2$, etc. Here, the summands are ordered in correspondence with the summands in (5.13), i.e., $(\text{Mat}_3 \oplus 3\text{Mat}_2)$ is a subalgebra of the Mat_9 in (5.13), the first 3Mat_1 is a subalgebra of the first Mat_3 in (5.13), etc.

The next step is to mod out all known relations. First, the quantum dimension of $\sigma\bar{\sigma}$ demands $r\bar{r} = 1$. By (5.12), this gives a projector

$$P_{12} = \frac{1}{2}(1 + r\bar{r}).$$

The notation P_{12} is chosen for consistency with similar notations in Section 5.5. Now note that

$$P_{12}A = \text{Mat}_9 \oplus \text{Mat}_1,$$

since r and \bar{r} both act as $+1$ on Mat_9 , and both act as -1 on Mat_1 . Therefore, when restricted to M' , the action of P_{12} gives

$$P_{12}M' = (\text{Mat}_3 \oplus 3\text{Mat}_2) \oplus \text{Mat}_1. \quad (5.14)$$

Second, the condensation of $\psi\bar{\psi}$ demands $\psi_x\bar{\psi}_x = 1$ and $\psi_y\bar{\psi}_y = 1$. Again by (5.12), these two relations give a projector

$$P_c = \frac{1}{4}(1 + \psi_x\bar{\psi}_x)(1 + \psi_y\bar{\psi}_y),$$

where the subscript “c” stands for “condensation”. The total projector is $P = P_c P_{12}$. The goal now is to understand the action of P_c on the two components of $P_{12}M'$ in (5.14), namely $(\text{Mat}_3 \oplus 3\text{Mat}_2)$ and Mat_1 . The latter is straightforward: Mat_1 is spanned by $(1 - r)(1 - \bar{r})$, and explicit calculation shows that

$$P_c(1 - r)(1 - \bar{r}) = (1 - r)(1 - \bar{r}).$$

Therefore, Mat_1 is in PM' . On the other hand, let $Q_0 = (1 + r)(1 + \bar{r})/4$ be the central projector that projects A onto Mat_9 . Since both P_c and Q_0 are central projectors, so is $P_c Q_0$, and I claim that $P_c Q_0$ is also primitive. This can be derived from the following lemma:

Lemma 13. Let B be a matrix algebra, N an abelian subalgebra of B , and N' the commutant of N . Then $Z(N') = N$.

It is easy to see that $N \subset Z(N')$, and Lemma 13 says that the two are actually equal. Strictly speaking, N must satisfy another condition, and Lemma 23 in Appendix 5.8 explains this point more rigorously. Lemma 13 with $B = Q_0A$ and $N = Q_0M$ implies that $Z(Q_0M')$ is generated by $\psi_x\bar{\psi}_xQ_0$ and $\psi_y\bar{\psi}_yQ_0$. It is then straightforward to use the prescription in Section 5.3 to find the primitive projectors from the central elements, and indeed P_cQ_0 is one of them. Therefore, P_cQ_0M' is a matrix algebra, and it is either Mat_3 or one of the three copies of Mat_2 . To determine P_cQ_0M' , note that for any operator $x \in A$, the operator xQ_0 can be represented as a 9×9 matrix $\rho_9(xQ_0)$, or $\rho_9(x)$ for short. The subscript l in ρ_l indicates the matrix dimension. A systematic way to determine this representation ρ_9 can be found in Appendix 5.8, but here I will start with a 3×3 matrix representation ρ_3 of operators in chiral Ising:

$$\begin{aligned} \rho_3(\psi_x) &= \begin{pmatrix} 1 & & \\ & 1 & \\ & & -1 \end{pmatrix}, \quad \rho_3(\sigma_x) = \begin{pmatrix} 0 & \sqrt{2} & 0 \\ \sqrt{2} & 0 & 0 \\ 0 & 0 & 0 \end{pmatrix}, \\ \rho_3(\psi_y) &= \begin{pmatrix} 1 & & \\ & -1 & \\ & & 1 \end{pmatrix}, \quad \rho_3(\sigma_y) = \begin{pmatrix} 0 & 0 & \sqrt{2} \\ 0 & 0 & 0 \\ \sqrt{2} & 0 & 0 \end{pmatrix}. \end{aligned} \quad (5.15)$$

The correctness of this representation can be confirmed by hand or by following the discussion in Appendix 5.8. The operators in Mat_9 can be obtained by tensoring the matrices above. In particular, $\rho_9(Q_0)$ is the 9×9 identity matrix, and $\rho_9(P_cQ_0)$ is a diagonal matrix

$$\rho_9(P_cQ_0) = \text{diag}(1, 0, 0, 0, 1, 0, 0, 0, 1). \quad (5.16)$$

It follows that $P_cQ_0M' = \text{Mat}_3$ since $\text{tr}(\rho_9(P_cQ_0)) = 3$. To summarize,

$$PM' = \text{Mat}_3 \oplus \text{Mat}_1, \quad (5.17)$$

where the projector P accounts the condensation of $\psi\bar{\psi}$ as well as relations due to deconfined anyons.

The bottom line of (5.17) is that even after modding out all the relations, the result is still not a matrix algebra. However, the correct algebra of logical operators must be a matrix algebra, so something needs to be done to PM' . For this purpose, I visualize PM' as block-diagonal matrices embedded in Mat_4 :

$$PM' = \begin{array}{|c|} \hline \begin{array}{|c|} \hline \text{shaded} \\ \hline \end{array} \\ \hline \begin{array}{|c|} \hline \text{shaded} \\ \hline \end{array} \\ \hline \end{array}. \quad (5.18)$$

Here is an important observation: The splitting of $\sigma\bar{\sigma}$ precisely “fills the blanks” in (5.18) to turn $\text{Mat}_3 \oplus \text{Mat}_1$ into Mat_4 .

To justify this observation, I now work out a 4×4 matrix representation ρ_4 of, say, e_x and compare it with the known result from the toric code. By (5.16), the Mat_3 block of an element $x \in PM'$ is obtained by taking rows and columns 1, 5 and 9 from $\rho_9(x)$. On the other hand, the Mat_1 block of $x \in PM'$ is determined by its action on the generator $(1-r)(1-\bar{r})$ of Mat_1 . For example,

$$\begin{aligned}\psi_x(1-r)(1-\bar{r}) &= -(1-r)(1-\bar{r}), \\ \sigma_x \bar{\sigma}_x(1-r)(1-\bar{r}) &= 0.\end{aligned}$$

By this method, the ρ_4 representations of some operators in PM' are found to be

$$\begin{aligned}\rho_4(\psi_x) &= \begin{pmatrix} 1 & & & \\ & 1 & & \\ & & -1 & \\ & & & -1 \end{pmatrix}, & \rho_4(\sigma_x \bar{\sigma}_x) &= \begin{pmatrix} 0 & 2 & 0 & 0 \\ 2 & 0 & 0 & 0 \\ 0 & 0 & 0 & 0 \\ 0 & 0 & 0 & 0 \end{pmatrix}, \\ \rho_4(\psi_y) &= \begin{pmatrix} 1 & & & \\ & -1 & & \\ & & 1 & \\ & & & -1 \end{pmatrix}, & \rho_4(\sigma_y \bar{\sigma}_y) &= \begin{pmatrix} 0 & 0 & 2 & 0 \\ 0 & 0 & 0 & 0 \\ 2 & 0 & 0 & 0 \\ 0 & 0 & 0 & 0 \end{pmatrix}.\end{aligned}$$

By physical argument, $\rho_4(e_x)$ satisfies the equations

$$\begin{aligned}\rho_4(e_x)^\dagger &= \rho_4(e_x), \\ (1 + \rho_4(\psi_x))\rho_4(e_x) &= \rho_4(\sigma_x \bar{\sigma}_x), \\ \rho_4(e_x)\rho_4(\psi_y) &= -\rho_4(\psi_y)\rho_4(e_x), \\ \rho_4(e_x)^2 &= 1.\end{aligned}$$

Line 1 says that e is its own antiparticle; line 2 comes from the fusion rules $\psi \times e = m$ and $\sigma \bar{\sigma} = e + m$; line 3 says that e and ψ braid with a -1 phase; line 4 comes from the fusion rule of e . The most general solution is

$$\rho_4(e_x) = \begin{pmatrix} 0 & 1 & & \\ 1 & 0 & & \\ & & 0 & e^{i\theta} \\ & & e^{-i\theta} & 0 \end{pmatrix}.$$

As expected, $\rho_4(e_x)$ has entries $e^{\pm i\theta}$ in the ‘‘blank’’ areas of (5.18). There is no way to fix θ , since conjugation by

$$U = \begin{pmatrix} 1 & & & \\ & 1 & & \\ & & 1 & \\ & & & e^{i\phi} \end{pmatrix}$$

acts trivially on $\text{Mat}_3 \oplus \text{Mat}_1$ but non-trivially on Mat_4 , mapping θ to $\theta \pm \phi$. Without loss of generality, I choose $\theta = 0$. This gives

$$\rho_4(e_x) = \begin{pmatrix} 0 & 1 & & \\ 1 & 0 & & \\ & & 0 & 1 \\ & & 1 & 0 \end{pmatrix}, \quad \rho_4(m_x) = \begin{pmatrix} 0 & 1 & & \\ 1 & 0 & & \\ & & 0 & -1 \\ & & -1 & 0 \end{pmatrix}.$$

With the additional requirement that $\rho_4(e_y)$ commute with $\rho_4(e_x)$, the same method also gives

$$\rho_4(e_y) = \begin{pmatrix} 0 & 0 & 1 & 0 \\ 0 & 0 & 0 & 1 \\ 1 & 0 & 0 & 0 \\ 0 & 1 & 0 & 0 \end{pmatrix}, \quad \rho_4(m_y) = \begin{pmatrix} 0 & 0 & 1 & 0 \\ 0 & 0 & 0 & -1 \\ 1 & 0 & 0 & 0 \\ 0 & -1 & 0 & 0 \end{pmatrix}.$$

One may confirm that these indeed obey the algebra of logical operators of the toric code. Moreover, they generate matrices such as

$$\begin{pmatrix} 0 & 0 & 0 & 1 \\ 0 & 0 & 0 & 0 \\ 0 & 0 & 0 & 0 \\ 0 & 0 & 0 & 0 \end{pmatrix} = \frac{1}{4} \rho_4(\sigma_x \bar{\sigma}_x) [\rho_4(e_y) - \rho_4(m_y)],$$

and hence all other matrices with entries in the “blank” areas of (5.18).

To conclude this section, I summarize condensation in the operator algebra approach as follows:

Protocol 14. Let A be the semisimple algebra of a topological or fractonic order, and suppose that $\{a\}$ is a set of bosons to be condensed.

1. Define M as the subalgebra of logical operators of $\{a\}$. If $\{a\}$ can be condensed simultaneously, then M is always abelian.
2. Let M' be the commutant of M . Construct a projector P based on the condensation condition of $\{a\}$, relations due to deconfined anyons as well as relations from other physical arguments. As will be explained in Section 5.6, the “other physical arguments” for Ising cage-net come from the cage terms of the Hamiltonian (5.5). Then take the algebra PM' .
3. If the semisimple algebra

$$PM' = \text{Mat}_{d_1} \oplus \cdots \oplus \text{Mat}_{d_m}$$

has more than one component, then certain operators must split. The result of the splitting is a matrix algebra

$$A_0 = \text{Mat}_{d_1 + \cdots + d_m},$$

which is obtained by “filling the blanks” in the matrix representation of PM' . The correctness of this operation can be confirmed manually for all the models in $d = 2 + 1$ in this chapter, and I conjecture that the operation is also correct for all topological or fracton models.

5.5 The one-foliated Ising cage-net model and Cartan subalgebra

I discuss one more $d = 2 + 1$ topological order in this section before going to Ising cage-net in Section 5.6. In particular, I present another method of computing the GSD within the operator algebra approach using a Cartan subalgebra, which turns out to be very convenient when applied to Ising cage-net.

The model of interest in this section is called the one-foliated Ising cage-net model (“1-F Ising” for short), which is constructed as follows: Take a stack of $2L$ copies of chiral Ising, and condense the boson $\Psi = \psi(1) \times \cdots \times \psi(2L)$, where $\psi(k)$ is the ψ particle from the k th layer. The chirality of these copies of chiral Ising does not affect the GSD. The condensation of doubled Ising into the toric code in Section 5.4 is a special case of this construction with $L = 1$.

In the $L \rightarrow \infty$ limit, 1-F Ising can be viewed as a fracton model, whose partially mobile excitations are planons. It is related to Ising cage-net as follows: In Ising cage-net, let S_x be a set of principal edges l_x related to each other by translation in the z direction (green edges in Fig. 5.6). Then the operator

$$\prod_{l_x \in S_x} V_{l_x}, \quad (5.19)$$

where V_{l_x} is a condensation operator defined in (5.3), creates a pair of $\psi\bar{\psi}$ anyons in each xy plane. Therefore, Ψ in the xy plane is part of the condensate in Ising cage-net. The same holds for Ψ in the yz and zx planes. In this sense, 1-F Ising is a “one-foliated” version of Ising cage-net, while Ising cage-net is “three-foliated”.

GSD from anyon counting

Since the 1-F Ising is a $d = 2 + 1$ topological order, its GSD can be obtained by counting anyons. In order for an anyon to be deconfined upon condensation, it must contain an even number of σ 's so that it braids trivially with $\Psi = \psi_1 \times \cdots \times \psi_{2L}$. Additionally, ψ can be attached to any layer where there is no σ , since this does not affect the braiding with Ψ . The condensation of Ψ identifies some pairs of anyons with each other, which reduces the number of distinct anyons. Finally, the particle $\Sigma = \sigma(1) \times \cdots \times \sigma(2L)$ splits into two simple anyons $\Sigma = e + m$ since the overall fermion parity of Σ is a good quantum number. Another way to see this is to note that $\Sigma \times \Sigma = 1 + \Psi + \cdots$, and the presence of two identity channels implies that Σ splits into two particles. These conditions constrain the label $a(1) \times \cdots \times a(2L)$ of an anyon.

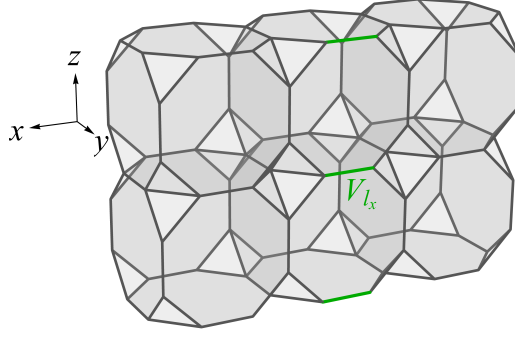


Figure 5.6: 1-F Ising obtained from layers of doubled Ising on a square-octagon lattice, similar to the construction of Ising cage-net. Each plane is a layer of doubled Ising. The product of V_{l_x} on the green edges (the set S_x in (5.19)) creates a pair of $\psi\bar{\psi}$ in each xy plane. If the Ψ particles created this way are condensed, then the system becomes 1-F Ising together with decoupled layers of doubled Ising in the yz and zx planes.

I now count the number of anyons. If σ is attached to $2k$ layers i_1, \dots, i_{2k} , where $k = 0, \dots, L-1$, then there are $2L - 2k$ places left to attach ψ . It would then seem that there are 2^{2L-2k} inequivalent ways to attach ψ to the layers. However, the condensation condition $\Psi = 1$ reduces the number of distinct labellings by a factor of 2. Therefore, there are $\binom{2L}{2k} 2^{2L-2k-1}$ inequivalent ways to place σ 's in $2k$ layers and attach 1's or ψ 's to the remaining layers. The case where $k = L$ needs to be considered separately. In this case, the anyon of interest is Σ , which splits into e and m . Thus the total number of anyons in the theory (equal to the GSD) is

$$\text{GSD} = \sum_{k=0}^{L-1} \binom{2L}{2k} 2^{2L-2k-1} + 2,$$

where the $+2$ accounts for the $k = L$ case. By the binomial theorem,

$$(1+x)^{2L} + (1-x)^{2L} = 2 \sum_{k=0}^L \binom{2L}{2k} x^{2L-2k}.$$

Thus the GSD simplifies to

$$\begin{aligned} \text{GSD} &= \sum_{k=0}^L \binom{2L}{2k} 2^{2L-2k-1} + 2 - \frac{1}{2} \\ &= \frac{1}{4}(1+2)^{2L} + \frac{1}{4}(1-2)^{2L} + \frac{3}{2} \\ &= \frac{1}{4}(9^L + 7). \end{aligned} \tag{5.20}$$

Since the GSD is not strictly exponential in L , the model is not foliated.

GSD from Cartan subalgebra

I now try to reproduce (5.20) using the operator algebra approach. Protocol 14 is based on the full algebra of 1-F Ising, but I delay this calculation to the end of this section. Instead, here I compute the GSD using a so-called Cartan subalgebra.

Definition 15. A subalgebra C of an algebra A is a *Cartan subalgebra* if it is abelian and maximal. Abelian means that $[x, y] = 0$ for all $x, y \in C$; maximal means that if any subalgebra $C' \subset A$ is abelian and $C \subset C'$, then $C' = C$.

Note that this definition is not rigorous mathematically. There is another condition on C which I did not mention, and this condition holds for the choice of C that will be used later. Definition 25 in Appendix 5.8 explains this extra condition. A Cartan subalgebra is related to the GSD by the following lemma:

Lemma 16. Let A_0 be a matrix algebra, and $C_0 \subset A_0$ a Cartan subalgebra. Then $\dim(C_0)^2 = \dim(A_0)$. In particular, if A_0 is the algebra of logical operators, then $\text{GSD} = \dim(C_0)$.

To understand this lemma with an example, let C_0 be the set of diagonal matrices in A_0 . The lemma is obvious in this case.

For $2L$ copies of chiral Ising with semisimple algebra

$$A = (\text{Mat}_3 \oplus \text{Mat}_1)^{\otimes 2L},$$

there is a convenient choice of a Cartan subalgebra C , which is spanned by the elementary operators with no σ . To compute the GSD, I want to understand the transition from C to C_0 . The approach is similar to Steps 1 and 2 of Protocol 14, although these steps are adapted to the context of Cartan subalgebras. Let M be the subalgebra of A generated by Ψ_x and Ψ_y (the condensate). The commutant M' of M has central projectors

$$P_c = \frac{1}{4}(1 + \Psi_x)(1 + \Psi_y)$$

due to condensation, and

$$P_{ij} = \frac{1}{2}(1 + r(i)r(j))$$

due to deconfined anyons $\sigma(i)\sigma(j)$, where $1 \leq i < j \leq 2L$ and

$$r(i) = \frac{1}{2}(1 + \psi_x(i) + \psi_y(i) - \psi_x(i)\psi_y(i)).$$

Although there are also non-abelian anyons with more than two σ 's and possibly ψ 's, for the purpose of constructing projectors, it suffices to only consider pairs of σ 's. For example, the relation due to $\sigma(1)\sigma(2)\sigma(3)\sigma(4)$ is $r(1)r(2)r(3)r(4) = 1$, but this is already implied by $r(1)r(2) = 1$ and $r(3)r(4) = 1$.

From this point on, I will focus only on the Cartan subalgebra. Importantly, in this specific case $C \subset M'$, and the central projectors P_c and P_{ij} all map C to C since they also contain no σ . Meanwhile, it can be argued physically that splitting does not enlarge the Cartan subalgebra. This is because the braiding of Σ with, for example, $\psi(1)$ gives a -1 phase and thus the same holds for the anyons e and m split from Σ . Therefore, the entirety of C_0 can be obtained by projection on C . In other words, the Cartan subalgebra is given by $C_0 = PC$, where

$$P = P_c \prod_{i < j} P_{ij}. \quad (5.21)$$

Since P is a projector, the GSD can be obtained from the equation

$$\text{GSD} = \dim(PC) = \text{tr}(P).$$

I emphasize that the underlying vector space here is C , and that the trace here is the trace of the action of P on C .

To find $\text{tr}(P)$, note that the projector P can be written in principle as

$$P = \sum_{a,b} \mu(a,b) v(a,b, a \times b), \quad (5.22)$$

where neither a nor b contains any σ (hence $a \times b$ is unique), and $\mu(a,b)$ are some coefficients. Observe also that when $v(c,d, c \times d) \in C$ is multiplied by $v(a,b, a \times b)$ in (5.22), the result

$$\pm v(a \times c, b \times d, a \times b \times c \times d)$$

is never proportional to $v(c,d, c \times d)$ unless $a = b = 1$. This means that $v(1,1,1)$ is the only term in (5.22) that contributes to $\text{tr}(P)$. Therefore, for the purpose of computing the GSD, it suffices to find the coefficient $\mu(1,1)$ by expanding (5.21). First, I use $r(i)^2 = 1$ to derive

$$\begin{aligned} \prod_{i < j} P_{ij} &= \frac{1}{2^{2L-1}} \sum_{k=0}^L \prod_{i_1 < \dots < i_{2k}} r(i_1) \cdots r(i_{2k}) \\ &= \frac{1}{2^{2L}} \left[\prod_{i=1}^{2L} (1 + r(i)) + \prod_{i=1}^{2L} (1 - r(i)) \right]. \end{aligned} \quad (5.23)$$

The first line is a sum of all products of an even number of $r(i)$'s; the second line can be interpreted as forcing the $r(i)$'s to be all $+1$ or all -1 , which is a consequence of forcing each pair of the $r(i)$'s to be both $+1$ or both -1 due to $\{P_{ij}\}$. Thus

$$P = \frac{1}{4} (1 + \Psi_x + \Psi_y + \Psi_x \Psi_y) \times \frac{1}{2^{2L}} \left[\prod_{i=1}^{2L} (1 + r(i)) + \prod_{i=1}^{2L} (1 - r(i)) \right].$$

Now since

$$\begin{aligned} 1 + r(i) &= \frac{3}{2} + \frac{1}{2}\psi_x(i) + \frac{1}{2}\psi_y(i) - \frac{1}{2}\psi_x(i)\psi_y(i), \\ 1 - r(i) &= \frac{1}{2} - \frac{1}{2}\psi_x(i) - \frac{1}{2}\psi_y(i) + \frac{1}{2}\psi_x(i)\psi_y(i), \end{aligned}$$

the only four terms in the expansion of $\prod_i(1 + r(i))$ that can combine with one of $1, \Psi_x, \Psi_y$ and $\Psi_x\Psi_y$ to contribute to $\mu(1, 1)$ are

$$\left(\frac{3}{2}\right)^{2L}, \prod_i \left(\frac{1}{2}\psi_x(i)\right), \prod_i \left(\frac{1}{2}\psi_y(i)\right) \text{ and } \prod_i \left(-\frac{1}{2}\psi_x(i)\psi_y(i)\right).$$

Summing these up, the total contribution of the $\prod_i(1 + r(i))$ part of P to $\mu(1, 1)$ is $(9^L + 3)/2^{4L+2}$. Similarly, the contribution of the $\prod_i(1 - r(i))$ part is $4/2^{4L+2}$. Combining these together, the GSD is

$$\text{GSD} = \text{tr}(P) = 2^{4L}\mu(1, 1) = \frac{1}{4}(9^L + 7),$$

where I used the fact that $\dim(C) = 2^{4L}$.

This calculation is almost entirely combinatorial and straightforward. However, it is also highly specific to simple examples such as Ising, because it relies on a nice Cartan subalgebra which is fixed by the central projectors and cannot be enlarged by splitting due to physical arguments.

GSD from full algebra

Finally for the discussion of 1-F Ising, I compute its GSD using Protocol 14. Let M be the subalgebra of A generated by Ψ_x and Ψ_y , and M' the commutant of M . The goal is to find PM' where P is given by (5.21). I will not try to decompose M' into matrix algebras like I did for doubled Ising in Section 5.4, since it turns out that most of the components of A are killed by the central projectors P_{ij} , just like the two copies of Mat_3 in (5.13). Instead, I first discuss the action of P_{ij} on A , and then apply P_c . To start with,

$$\prod_{i < j} P_{ij} A = B_0 \oplus B_1,$$

where $B_0 = \text{Mat}_{9^L}$ and $B_1 = \text{Mat}_1$. This is because $\{P_{ij}\}$ forces the $r(i)$'s to be all +1 or all -1. As a result,

$$\prod_{i < j} P_{ij} M' \subset B_0 \oplus B_1,$$

so the next step is to find the action of P_c on $(B_0 \oplus B_1) \cap M'$.

For the $B_1 \cap M'$ part, clearly $B_1 \subset Z(A)$ since B_1 is a 1×1 block and therefore commutes with everything. Thus $B_1 \cap M' = B_1$. Each of $\psi_x(i)$ and $\psi_y(i)$ acts on B_1 as -1 , so P_c preserves B_1 . The conclusion is that $P_c(B_1 \cap M') = \text{Mat}_1$.

For the $B_0 \cap M'$ part, I repeat what I did in Section 5.4 for $\text{Mat}_3 \oplus 3\text{Mat}_2$, and use a matrix representation of P_c to determine its action. Let

$$Q_0 = \frac{1}{2^{2L}} \prod_i (1 + r(i))$$

be the central projector that projects onto B_0 . By Lemma 13, the central projector $P_c Q_0$ is primitive, and hence the algebra $P_c Q_0 M'$ is a matrix algebra. On B_0 , the action of operators such as P_c has representation ρ_{9^L} . Thus $P_c Q_0 M' = \text{Mat}_n$ where $n = \text{tr}(\rho_{9^L}(P_c Q_0))$. To find n , I use the fact that

$$\begin{aligned} n &= \dim(\text{eigenspace } \rho_{9^L}(P_c) = 1) \\ &= \dim(\text{eigenspace } \rho_{9^L}(\Psi_x) = \rho_{9^L}(\Psi_y) = +1). \end{aligned}$$

Let D_{2L}^{st} , where s, t can be $+$ or $-$, be the dimension of the common eigenspace $\{w\}$ of $\rho_{9^L}(\Psi_x)$ and $\rho_{9^L}(\Psi_y)$ where $\rho_{9^L}(\Psi_x)w = sw$ and $\rho_{9^L}(\Psi_y)w = tw$ (i.e., $\pm w$). Using the representation ρ_3 of ψ_x and ψ_y in (5.15), it can be shown that

$$\begin{aligned} D_{2L}^{++} &= \frac{1}{4} (9^L + 3), \\ D_{2L}^{+-} &= D_{2L}^{-+} = D_{2L}^{--} = \frac{1}{4} (9^L - 1). \end{aligned} \tag{5.24}$$

I now explain the calculation of D_{2L}^{+-} as an example. Let $\{u_1, u_2, u_3\}$ be the standard basis for \mathbb{C}^3 , and

$$w = u_1^{\otimes k_1} \otimes u_2^{\otimes k_2} \otimes u_3^{\otimes k_3}.$$

By (5.15), in order for $\rho_{9^L}(\Psi_x)w = +w$ and $\rho_{9^L}(\Psi_y)w = -w$, it must be the case that k_3 is odd, k_2 is even, and hence k_1 is odd. The number of such combinations of (k_1, k_2, k_3) satisfying $k_1 + k_2 + k_3 = 2L$ can be found using the multinomial theorem:

$$\begin{aligned} D_{2L}^{+-} &= \frac{1}{4} [(1 + 1 + 1)^{2L} - (1 + 1 - 1)^{2L} \\ &\quad + (1 - 1 + 1)^{2L} - (1 - 1 - 1)^{2L}] \\ &= \frac{1}{4} (9^L - 1). \end{aligned}$$

Using (5.24),

$$\text{tr}(\rho_{9^L}(P_c Q_0)) = D_{2L}^{++} = \frac{1}{4} (9^L + 3).$$

Although here I only made use of D_{2L}^{++} , the other D 's will be used in Section 5.6.

The $B_0 \cap M'$ and $B_1 \cap M'$ parts together imply that

$$PM' = \text{Mat}_{(9^L+3)/4} \oplus \text{Mat}_1.$$

This is a semisimple algebra. Just like the situation in Section 5.4 for condensation in doubled Ising, one can also find matrix representations of e_x, m_x, e_y and m_y and

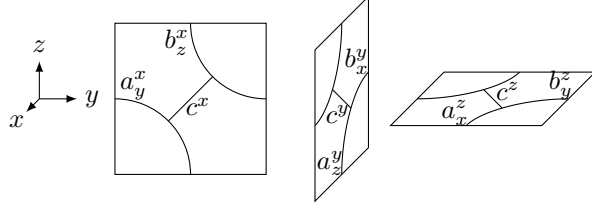


Figure 5.7: Constituents $v^x(a_y^x, b_z^x, c_x^x)$, $v^y(a_z^y, b_x^y, c_y^y)$ and $v^z(a_x^z, b_y^z, c_z^z)$ of an elementary operator in Ising cage-net. Arrows are omitted since in Ising cage-net, every particle is its own antiparticle.

confirm that they have non-zero entries in the “blank” areas of PM' , but I omit this calculation here. By Protocol 14, the semisimple algebra turns into a matrix algebra

$$A_0 = \text{Mat}_{(9^L+7)/4},$$

and $\text{GSD} = (9^L + 7) / 4$ as expected.

5.6 Tackling the Ising cage-net model

In this section, I compute the GSD of Ising cage-net, first using a Cartan subalgebra, and then using the full algebra.

Consider a system where L_x , L_y and L_z layers of doubled Ising are stacked in the x , y and z directions, respectively. The elementary operators here are products of the $d = 2 + 1$ elementary operators $v^x(a_y^x, b_z^x, c_x^x)$ in the yz planes, $v^y(a_z^y, b_x^y, c_y^y)$ in the zx planes, and $v^z(a_x^z, b_y^z, c_z^z)$ in the xy planes (Fig. 5.7). I also define notations such as $\psi_y^x(i)$ for the string operator of ψ from the i th plane orthogonal to the x direction (i.e., a yz plane) traversing the y direction. To obtain Ising cage-net from the decoupled layers, $\psi\bar{\psi}$ p-loops should be condensed as explained in Section 5.1. Since the operator algebra approach uses logical operators on the ground space, the condensation operators V_{l_μ} defined in (5.3) should be combined into logical operators (of the decoupled layers). An example of such a logical operator is shown in Fig. 5.8 (a), which looks like a “net” orthogonal to the z direction. I call the operator a Ψ -net and denote it by Ψ^z . Explicitly, if T^z is a set of principal edges l_z related to each other by translation in the x and y directions (red edges in Fig. 5.9), then

$$\Psi^z = \prod_{l_z \in T^z} V_{l_z} = \prod_{i=1}^{L_x} (\psi\bar{\psi})_y^x(i) \prod_{j=1}^{L_y} (\psi\bar{\psi})_x^y(j). \quad (5.25)$$

Different choices of T^z at different xy planes give the same Ψ^z when acting on the ground space. Similarly, net-shaped operators Ψ^x and Ψ^y can be defined.

If in the net shape of Fig. 5.8 (a), all $\psi\bar{\psi}$'s are replaced by $\sigma\bar{\sigma}$'s, then the result is an operator which I call a Σ -net, or Σ^z in this specific case. Upon condensation, each

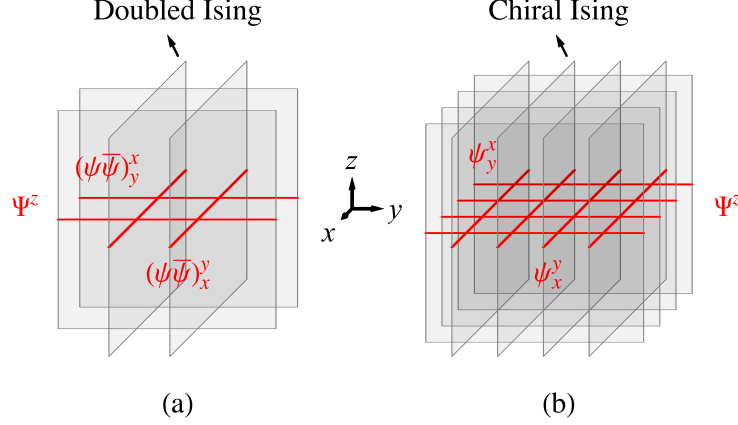


Figure 5.8: Net-shaped logical operator Ψ^z defined in (5.25), which is to be condensed in Ising cage-net. In (a), each plane is a layer of doubled Ising, and the red strings are $(\psi\bar{\psi})_y^x(i)$ and $(\psi\bar{\psi})_x^y(j)$. In (b), equivalently, each plane is a layer of chiral Ising, and the red strings are $\psi_y^x(i)$ and $\psi_x^y(j)$.

Σ^α splits into two operators $\Sigma^\alpha = e^\alpha + m^\alpha$ of the same net shape. In the case of Σ^z , the operators e^z and m^z are distinguished by the parity p^z of the fermion mode

$$\prod_{i=1}^{L_x} (\sigma\bar{\sigma})^x(i) \prod_{j=1}^{L_y} (\sigma\bar{\sigma})^y(j),$$

which is a good quantum number. This is because anyons such as $\sigma^x(i)$ which can change p^z by braiding with Σ^z are confined.

The semisimple algebra of the decoupled layers is

$$A = (\text{Mat}_3 \oplus \text{Mat}_1)^{\otimes 2(L_x + L_y + L_z)}.$$

Besides the condensation condition, there should also be relations due to deconfined excitations. Since Ising cage-net has deconfined fractons, lineons and planons, it is not obvious where exactly the relations come from. For this reason, I return to the Hamiltonian (5.5) and construct the relations from the Hamiltonian terms.

First, the Hamiltonian (5.5) contains the doubled Ising plaquette terms $B_p^0 = 1$ and B_p^2 , so a ground state must satisfy the projector

$$\frac{1}{2} (1 + B_p^2) = \frac{1}{2} (B_p^1)^2. \quad (5.26)$$

In the string-net model of doubled Ising, a 1-loop on a (smallest) plaquette can be viewed as a σ -loop or, equivalently, a $\bar{\sigma}$ -loop. Here, (5.26) is interpreted as creating a loop of $\sigma\bar{\sigma}$ at a plaquette. Suppose that this plaquette term is placed “around the

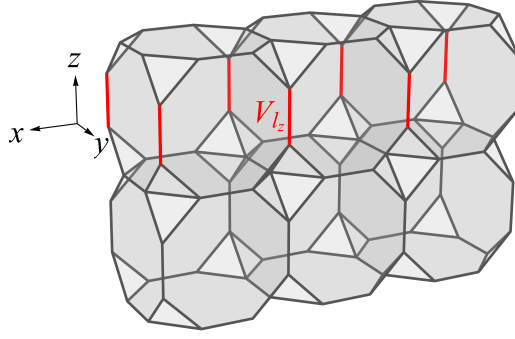


Figure 5.9: Action on the lattice degrees of freedom of the operator Ψ^z , which is to be condensed in Ising cage-net. The product of V_{l_z} on the red edges (the set T^z in (5.25)) is the net-shaped logical operator Ψ^z shown in Fig. 5.8 (a). Note that (5.25) shown here is a logical operator, whereas (5.19) shown in Fig. 5.6 creates excitations.

corner edges” like

$$\frac{1}{2} (B_p^1)^2 = \text{[Diagram of a square with rounded corners]} .$$

In each layer i orthogonal to the α direction, this configuration yields a relation

$$r^\alpha(i) \bar{r}^\alpha(i) = 1, \quad (5.27)$$

where, for example,

$$r^x(i) = \frac{1}{2} (1 + \psi_y^x(i) + \psi_z^x(i) - \psi_y^x(i) \psi_z^x(i)),$$

and similarly for $\bar{r}^\alpha(i)$.

Second, a cage term B_c can also be placed “around the corner edges” (Fig. 5.10). This term involves 1-loops in the xy , yz and zx planes. In the setup of Fig. 5.10, the 1-loops can be brought closer together by enlarging the cube c to size $L_x \times L_y \times 1$. The result is a flat, degenerate cuboid, some of whose edges coincide with each other. This enlargement is allowed since the 1-loops can be deformed individually in each layer of doubled Ising and the enlarged cage term commutes with the condensation terms V_{l_μ} . I now simplify this large cage term. The red strings give

$$\text{[Diagram of a square with red strings forming a cross-like structure]} = 2r^z(i)r^z(i+1),$$

where the two 1-loops are in different xy planes but drawn in the same plane for illustration, and the degenerate cuboid is drawn as a large yet non-degenerate one.

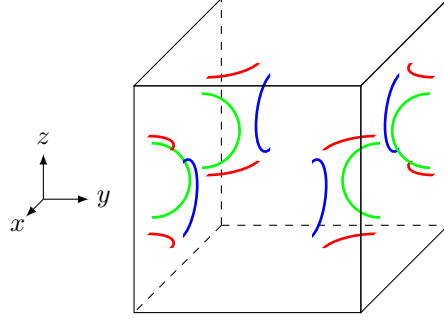
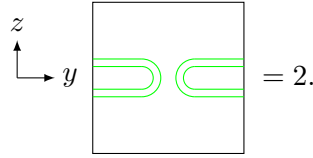


Figure 5.10: Cage term B_c of Ising cage-net placed “around the corner edges”. The red, green and blue strings are 1-loops in the xy , yz and zx planes, respectively.

I chose to interpret the two 1-loops as two σ -loops; other interpretations such as one σ -loop and one $\bar{\sigma}$ -loop are all equivalent due to (5.27). The green strings give



Note that this simplification uses only the fusion rules, F -symbols and R -symbols. Similarly, the blue strings also simplify to a constant 2. Therefore, Fig. 5.10 gives a relation $r^z(i)r^z(i+1) = 1$.

In summary, the Hamiltonian (5.5) implies that the product of $r^\alpha(i)$ or $\bar{r}^\alpha(i)$ with any other $r^\alpha(j)$ or $\bar{r}^\alpha(j)$ should be 1, where i and j may or may not be equal. Although the relations are derived explicitly from Hamiltonian terms, they can still be interpreted as due to quantum dimensions of deconfined planons. Therefore, the operator algebra approach still only uses intrinsic properties of the model instead of lattice details. Note that for the purpose of writing down relations, there is no difference between anyons with and without bars. Thus from now on, I view the system as $2L_x$, $2L_y$ and $2L_z$ layers of chiral Ising. The names of operators change accordingly. For example,

$$\Psi^z = \prod_{i=1}^{2L_x} \psi_y^x(i) \prod_{j=1}^{2L_y} \psi_x^y(j),$$

as shown in Figure 5.8 (b). Let M be the subalgebra of A generated by Ψ^x , Ψ^y and Ψ^z , and M' the commutant of M . Inside M' , the relations are enforced by the central projectors

$$P_c = \frac{1}{8}(1 + \Psi^x)(1 + \Psi^y)(1 + \Psi^z) \quad (5.28)$$

due to condensation, and

$$P_{ij}^\alpha = \frac{1}{2}(1 + r^\alpha(i)r^\alpha(j)) \quad (5.29)$$

due to deconfined planons and cage terms. Their product is

$$P = P_c \prod_{\alpha} \prod_{i < j} P_{ij}^{\alpha}. \quad (5.30)$$

With the setup above, the GSD is ready to be computed.

GSD from Cartan subalgebra

Following Section 5.5, I calculate the GSD of Ising cage-net first using a Cartan subalgebra. The semisimple algebra A has a Cartan subalgebra C spanned by the elementary operators with no σ . Just like in Section 5.5, it happens that $C \subset M'$, and that the central projectors P_c and P_{ij}^{α} all map C to C . The Σ -nets also split, but the splitting does not enlarge the Cartan subalgebra. This is because every Σ^{α} (and hence e^{α} and m^{α}) braids non-trivially with some ψ operator. Therefore, the GSD can be obtained from $\text{GSD} = \text{tr}(P)$, where the underlying vector space is C . Again using the argument in Section 5.5, if P is expanded into a linear combination of elementary operators, then only the constant term $\mu_0 = \mu(1, 1, 1, 1, 1, 1)$ (which is called $\mu(1, 1)$ for 1-F Ising) contributes to $\text{tr}(P)$.

The constant μ_0 can be obtained from the expansion of (5.30), which is very similar to the calculation in Section 5.5. To start with,

$$\prod_{i < j} P_{ij}^{\alpha} = \frac{1}{2^{2L_{\alpha}}} \left[\prod_{i=1}^{2L_{\alpha}} (1 + r^{\alpha}(i)) + \prod_{i=1}^{2L_{\alpha}} (1 - r^{\alpha}(i)) \right],$$

as can be shown by the technique in (5.23). Thus the projector simplifies to

$$P = \frac{1}{8} (1 + \Psi^x + \Psi^y + \Psi^z + \Psi^y \Psi^z + \Psi^z \Psi^x + \Psi^x \Psi^y + \Psi^x \Psi^y \Psi^z) \\ \times \prod_{\alpha} \frac{1}{2^{2L_{\alpha}}} \left[\prod_{i=1}^{2L_{\alpha}} (1 + r^{\alpha}(i)) + \prod_{i=1}^{2L_{\alpha}} (1 - r^{\alpha}(i)) \right].$$

The next step is to find the terms in the expansion of $\prod_{\alpha}(\dots)$ that can combine with any one of the eight terms $1, \Psi^x, \dots, \Psi^x \Psi^y \Psi^z$ to yield a constant term. For example, in the expansion of $\prod_i (1 + r^z(i))$, the only four terms that can contribute to μ_0 are

$$\left(\frac{3}{2}\right)^{2L_z}, \quad \prod_i \left(\frac{1}{2} \psi_x^z(i)\right), \quad \prod_i \left(\frac{1}{2} \psi_y^z(i)\right) \quad \text{and} \quad \prod_i \left(-\frac{1}{2} \psi_x^z(i) \psi_y^z(i)\right).$$

Therefore, the projector P can be written as

$$P = \frac{1}{8} (1 + \Psi^x + \Psi^y + \Psi^z + \Psi^y \Psi^z + \Psi^z \Psi^x + \Psi^x \Psi^y + \Psi^x \Psi^y \Psi^z) \\ \times \frac{1}{2^{4L_x}} \left[(9^{L_x} + 1) + 2 \prod_i \psi_y^x(i) + 2 \prod_i \psi_z^x(i) + 2 \prod_i \psi_y^x(i) \psi_z^x(i) \right]$$

$$\begin{aligned} & \times \frac{1}{2^{4L_y}} \left[(9^{L_y} + 1) + 2 \prod_j \psi_z^y(j) + 2 \prod_j \psi_x^y(j) + 2 \prod_j \psi_z^y(j) \psi_x^y(j) \right] \\ & \times \frac{1}{2^{4L_z}} \left[(9^{L_z} + 1) + 2 \prod_k \psi_x^z(k) + 2 \prod_k \psi_y^z(k) + 2 \prod_k \psi_x^z(k) \psi_y^z(k) \right] + \dots, \end{aligned}$$

where “ \dots ” means terms that cannot possibly contribute to μ_0 . Up to permutation of x, y and z , the pairing of the terms works as follows:

$$\begin{aligned} 1 & \iff (9^{L_x} + 1) \times (9^{L_y} + 1) \times (9^{L_z} + 1), \\ \Psi^z & \iff (9^{L_z} + 1) \times 2 \prod_i \psi_y^x(i) \times 2 \prod_j \psi_x^y(j), \\ \Psi^x \Psi^y & \iff 2 \prod_i \psi_z^x(i) \times 2 \prod_j \psi_z^y(j) \times 2 \prod_k \psi_x^z(k) \psi_y^z(k), \\ \Psi^x \Psi^y \Psi^z & \iff 2 \prod_i \psi_y^x(i) \psi_z^x(i) \times 2 \prod_j \psi_z^y(j) \psi_x^y(j) \times 2 \prod_k \psi_x^z(k) \psi_y^z(k), \end{aligned}$$

where “ \iff ” indicates the pairing. Combining these together, the GSD is

$$\begin{aligned} \text{GSD} &= 2^{4(L_x+L_y+L_z)} \mu_0 \\ &= \frac{1}{8} [(9^{L_x} + 1) (9^{L_y} + 1) (9^{L_z} + 1) \\ &\quad + 4 (9^{L_x} + 1) + 4 (9^{L_y} + 1) + 4 (9^{L_z} + 1) \\ &\quad + 8 + 8 + 8 + 8] \\ &= \frac{1}{8} (E_3 + E_2 + 5E_1 + 45), \end{aligned}$$

where $E_3 = 9^{L_x+L_y+L_z}$, $E_2 = 9^{L_x+L_y} + 9^{L_y+L_z} + 9^{L_z+L_x}$, and $E_1 = 9^{L_x} + 9^{L_y} + 9^{L_z}$. At the end of this section, I will confirm this result with a traditional string-net or cage-net method for the smallest system size $L_x = L_y = L_z = 1$.

GSD from full algebra

I now calculate the GSD of Ising cage-net using Protocol 14. Just like the situation in 1-F Ising, the central projectors P_{ij}^α defined in (5.29) kill most of the components of the semisimple algebra M' . This is because for each α , projection by P_{ij}^α forces the $r^\alpha(i)$'s to be all +1 or all -1. The remaining algebra is

$$\prod_\alpha \prod_{i < j} P_{ij}^\alpha A = (B_0^x \oplus B_1^x) \otimes (B_0^y \oplus B_1^y) \otimes (B_0^z \oplus B_1^z),$$

where $B_0^\alpha = \text{Mat}_{9^{L_\alpha}}$ and $B_1^\alpha = \text{Mat}_1$. Define central projectors

$$Q_{s_x s_y s_z} = \prod_\alpha \left[\frac{1}{2^{2L_\alpha}} \prod_{i=1}^{2L_\alpha} (1 + (-1)^{s_\alpha} r^\alpha(i)) \right],$$

where $s_\alpha = 0$ or 1 , which project onto the components

$$B_{s_x s_y s_z} = \bigotimes_{\alpha} B_{s_\alpha}^\alpha.$$

The next step is to find the action of P_c defined in (5.28) on

$$\left[\bigotimes_{\alpha} (B_0^\alpha \oplus B_1^\alpha) \right] \cap M'.$$

This intersection has eight components, namely $B_{000} \cap M'$ and so on. Up to permutation of x , y and z , there are four cases, and I discuss them in ascending order of difficulty:

1. On $B_{111} \cap M' = B_{111}$, every $\psi_\beta^\alpha(i)$ acts as -1 , so $P_c Q_{111} M' = B_{111} = \text{Mat}_1$.
2. On $B_{110} \cap M'$, each of $\psi_y^x(i)$, $\psi_z^x(i)$, $\psi_z^y(j)$ and $\psi_x^y(j)$ acts as -1 , while each of $\psi_x^z(k)$ and $\psi_y^z(k)$ has the representation ρ_3 given by (5.15). By Lemma 13, the central projector $P_c Q_{110}$ is primitive. The matrix algebra $P_c Q_{110} M'$ can be determined from the representation ρ_l of $\text{Mat}_1 \otimes \text{Mat}_1 \otimes \text{Mat}_{9^{L_z}}$, where $l = 9^{L_z}$. More precisely, let $\{w\}$ be the common eigenspace such that $\rho_l(\Psi^\alpha)w = +w$ for all α . Now $\rho_l(\Psi^z)w = +w$ is already true because $\psi_y^x(i) = -1$ and $\psi_x^y(j) = -1$. To ensure $\rho_l(\Psi^x)w = +w$, for example, I require

$$\left[\bigotimes_k \rho_3[\psi_y^z(k)] \right] w = +w, \quad (5.31)$$

since $\psi_z^y(j) = -1$. Similarly, I also require

$$\left[\bigotimes_k \rho_3[\psi_x^z(k)] \right] w = +w. \quad (5.32)$$

The dimension of the eigenspace that satisfies (5.31) and (5.32) is precisely $D_{2L_z}^{++}$ defined in (5.24). Therefore, $P_c Q_{110} M' = \text{Mat}_{(9^{L_z}+3)/4}$.

3. On $B_{001} \cap M'$, each of $\psi_x^z(k)$ and $\psi_y^z(k)$ acts as -1 , while each of $\psi_y^x(i)$, $\psi_z^x(i)$, $\psi_z^y(j)$ and $\psi_x^y(j)$ has the representation ρ_3 . The matrix algebra $P_c Q_{001} M'$ can be determined from the common eigenspace $\{w\}$ such that $\rho_l(\Psi^\alpha)w = +w$ in the representation ρ_l of $\text{Mat}_{9^{L_x}} \otimes \text{Mat}_{9^{L_y}} \otimes \text{Mat}_1$, where $l = 9^{L_x+L_y}$. The equations $\rho_l(\Psi^x)w = \rho_l(\Psi^y)w = +w$ and $\psi_x^z(k) = \psi_y^z(k) = -1$ imply that

$$\left[\bigotimes_i \rho_3[\psi_z^x(i)] \right] w = \left[\bigotimes_j \rho_3[\psi_z^y(j)] \right] w = +w.$$

Meanwhile, the equation $\rho_l(\Psi^z)w = +w$ implies two possibilities

$$\left[\bigotimes_i \rho_3[\psi_y^x(i)] \right] w = \left[\bigotimes_j \rho_3[\psi_x^y(j)] \right] w = \pm w. \quad (5.33)$$

The solutions to (5.33) with $+w$ form a subspace of dimension $D_{2L_x}^{++} D_{2L_y}^{++}$. On the other hand, the solutions to (5.33) with $-w$ form a subspace of dimension $D_{2L_x}^{+-} D_{2L_y}^{+-}$. Overall, $P_c Q_{001} M' = \text{Mat}_{(9^{L_x+L_y+9^{L_x+9^{L_y+5}}})/8}$.

4. On $B_{000} \cap M'$, all $\psi_\beta^\alpha(i)$ operators have the representation ρ_3 . The matrix algebra $P_c Q_{000} M'$ can be determined from the common eigenspace $\{w\}$ such that $\rho_l(\Psi^\alpha)w = +w$ in the representation ρ_l of $\text{Mat}_{9^{L_x}} \otimes \text{Mat}_{9^{L_y}} \otimes \text{Mat}_{9^{L_z}}$, where $l = 9^{L_x+L_y+L_z}$. This gives the equations

$$\left[\bigotimes_j \rho_3[\psi_z^y(j)] \right] w = \left[\bigotimes_k \rho_3[\psi_y^z(k)] \right] w = \pm w, \quad (5.34)$$

$$\left[\bigotimes_k \rho_3[\psi_x^z(k)] \right] w = \left[\bigotimes_i \rho_3[\psi_z^x(i)] \right] w = \pm w, \quad (5.35)$$

$$\left[\bigotimes_i \rho_3[\psi_y^x(i)] \right] w = \left[\bigotimes_j \rho_3[\psi_x^y(j)] \right] w = \pm w. \quad (5.36)$$

Depending on the choice of $\pm w$ in these equations, there are eight possibilities. For example, with $-w$ in (5.34) and (5.35) and $+w$ in (5.36), the contribution to the dimension of the common eigenspace is $D_{2L_x}^{+-} D_{2L_y}^{+-} D_{2L_z}^{--}$. The total dimension accounting for all eight possibilities is

$$\begin{aligned} \dim(\{w\}) &= D_{2L_x}^{++} D_{2L_y}^{++} D_{2L_z}^{++} + \left(D_{2L_x}^{-+} D_{2L_y}^{+-} D_{2L_z}^{++} + \text{perm.} \right) \\ &\quad + \left(D_{2L_x}^{+-} D_{2L_y}^{-+} D_{2L_z}^{--} + \text{perm.} \right) + D_{2L_x}^{--} D_{2L_y}^{--} D_{2L_z}^{--} \\ &= \frac{1}{8}(E_3 + E_1 + 4), \end{aligned}$$

where ‘‘perm.’’ means permutations of x , y and z . Since $D_{2L}^{+-} = D_{2L}^{-+}$, only cyclic permutations are included. Therefore, $P_c Q_{000} M' = \text{Mat}_{(E_3+E_1+4)/8}$.

Summarizing all four cases,

$$\begin{aligned} PM' &= \text{Mat}_{(E_3+E_1+4)/8} \oplus \left(\text{Mat}_{(9^{L_x+L_y+9^{L_x+9^{L_y+5}}})/8} \oplus \text{perm.} \right) \\ &\quad \oplus \left(\text{Mat}_{(9^{L_z+3})/4} \oplus \text{perm.} \right) \oplus \text{Mat}_1. \end{aligned}$$

Using Protocol 14 with the conjecture of ‘‘filling the blanks’’, PM' is enlarged to a simple algebra, and $\text{GSD} = (E_3 + E_2 + 5E_1 + 45)/8$. At the end of this section, I will confirm this result with a traditional string-net or cage-net method for the smallest system size $L_x = L_y = L_z = 1$.

GSD for the minimal system size

To support the GSD formula (5.1) obtained from the operator algebra approach, I conclude this section by calculating the GSD of Ising cage-net for the smallest system

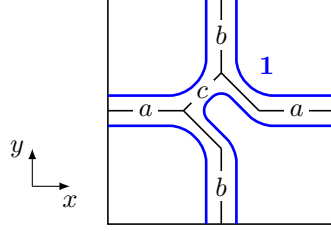


Figure 5.11: A minimal trivalent lattice, a state vector $|abc\rangle$, and the plaquette term B_p^1 (the blue 1-loop).

size $L_x = L_y = L_z = 1$ using the Hamiltonian (5.5) and a traditional string-net or cage-net method. The result $\text{GSD} = 144$ agrees with (5.1).

I start with doubled Ising on a minimal trivalent lattice (Fig. 5.11). State vectors are written as $|abc\rangle$, where $a, b, c = 0, 1$ or 2 . The subspace of the Hilbert space that satisfies the vertex terms A_v has dimension 10. It is spanned by

$$\begin{aligned}
 w_1 &= |101\rangle, \quad w_2 = |011\rangle, \quad w_3 = |110\rangle, \\
 w_4 &= |121\rangle, \quad w_5 = |211\rangle, \quad w_6 = |112\rangle, \\
 w_7 &= \frac{1}{2} |000\rangle + \frac{1}{2} |202\rangle + \frac{1}{2} |022\rangle - \frac{1}{2} |220\rangle, \\
 w_8 &= \frac{1}{2} |000\rangle - \frac{1}{2} |202\rangle + \frac{1}{2} |022\rangle + \frac{1}{2} |220\rangle, \\
 w_9 &= \frac{1}{2} |000\rangle + \frac{1}{2} |202\rangle - \frac{1}{2} |022\rangle + \frac{1}{2} |220\rangle, \\
 w_{10} &= -\frac{1}{2} |000\rangle + \frac{1}{2} |202\rangle + \frac{1}{2} |022\rangle + \frac{1}{2} |220\rangle.
 \end{aligned} \tag{5.37}$$

The only nontrivial plaquette term is B_p^1 (blue loop in Fig. 5.11), which is a 1-loop that traverses each edge twice. It can also be viewed as a σ -loop (or equivalently, a $\bar{\sigma}$ -loop) placed “around the corners”. It can be shown with the method of (5.9) that $B_p^1 = \sqrt{2} r$, whose eigenvalues are $\pm\sqrt{2}$. By direct calculation,

$$\begin{aligned}
 B_p^1 w_i &= +\sqrt{2} w_i \text{ for } i = 1, \dots, 9, \\
 B_p^1 w_{10} &= -\sqrt{2} w_{10}.
 \end{aligned}$$

The details of this calculation are not important and are omitted. The point here is that the ground space of the minimal doubled Ising is spanned by w_1, \dots, w_9 .

The minimal Ising cage-net is obtained by condensing $\psi\bar{\psi}$ p-loops in three copies of minimal doubled Ising which are pairwise orthogonal. The states in, for example, the doubled Ising perpendicular to the z direction are labelled by $|a_x^z b_y^z c^z\rangle$, where a_x^z is on the edge in the x direction, etc. The Hamiltonian consists of condensation operators V_μ , vertex terms A_v and a single cube term B_c , but with an important caveat: Here B_c acts on a “degenerate” cube, whose opposite faces are identified. For

example, the upper and lower faces of B_c are both proportional to

$$r^z = \frac{1}{2}(1 + \psi_x^z + \psi_y^z - \psi_x^z \psi_y^z).$$

Since $(r^z)^2 = 1$, the product of these two faces is a constant. Thus B_c is a constant and can be ignored.

The Hilbert space that satisfies all vertex terms is spanned by $w_i^x \otimes w_j^y \otimes w_k^z$, where w_i^α are given by (5.37) and $i, j, k = 1, \dots, 10$. By (5.3), a state that remains in the low-energy subspace upon condensation must satisfy

$$(a_x^z, b_x^y), (a_y^x, b_y^z), (a_z^y, b_z^x) = (1, 1) \text{ or contain no } 1. \quad (5.38)$$

Therefore, I now count the number of states $w_i^x \otimes w_j^y \otimes w_k^z$ that satisfy (5.38). Up to permutation of x, y and z , there are four cases:

1. If none of the a 's or b 's (and hence c 's) is 1, then the states are $w_i^x \otimes w_j^y \otimes w_k^z$ where $i, j, k = 7, 8, 9$ or 10 . There are $4 \times 4 \times 4 = 64$ possibilities.
2. If $(a_x^z, b_x^y) = (1, 1)$ and neither (a_x^z, b_x^y) nor (a_y^x, b_y^z) contains 1, then $i = 2$ or 5 , $j = 1$ or 4 , and $k = 7, 8, 9$ or 10 . There are $2 \times 2 \times 4 = 16$ possibilities.
3. If $(a_x^z, b_x^y), (a_y^x, b_y^z) = (1, 1)$ and (a_z^y, b_z^x) contains no 1, then $i = 1$ or 4 , $j = 2$ or 5 , and $k = 3$ or 6 . There are $2 \times 2 \times 2 = 8$ possibilities.
4. If all a 's and b 's are 1, then $i, j, k = 3$ or 6 . There are $2 \times 2 \times 2 = 8$ possibilities.

Summarizing these cases,

$$\text{GSD} = 64 + 3 \times 16 + 3 \times 8 + 8 = 144,$$

where the factors of 3 account for permutations of x, y and z . This agrees with (5.1).

5.7 Trick or treat?

With the GSD formula (5.1) derived, the main physical property of Ising cage-net for the purpose of this thesis has been established, namely the absence of a foliation structure. However, the derivation of (5.1) uses the unconventional method that is the operator algebra approach, and it is worth an extra section in this chapter to discuss this method. Is the operator algebra approach simply a trick of calculation? Or is there deeper significance in it?

If the operator algebra approach is viewed as a trick, then the key part of the trick is the semisimple algebra A . The whole calculation uses A as an intermediate step, because it is spanned by naturally chosen elementary operators, and can be mapped to the algebra A_0 of logical operators by modding out physically justified relations. However, Protocol 14 suggests that A has its own significance: When studying the

condensation of $\psi\bar{\psi}$ in doubled Ising in Section 5.4, both of the components Mat_9 and Mat_1 of A are important since they both intersect non-trivially with M' . If one focused only on the matrix algebra Mat_9 of doubled Ising, then the Mat_1 would be missed. Therefore, condensation naturally and necessarily involves A . In another perspective, when constructing A , only the relations due to fusion rules, F -symbols and R -symbols are considered. It is in the map from A to A_0 that the relations due to deconfined anyons are further enforced. Now when bosons are condensed, confinement of certain anyons reduces the number of relations coming from anyons, but does not invalidate any of the fusion rules, F -symbols or R -symbols – if they involve confined anyons then they do not affect M or M' anyway. In this sense, the relations have a “hierarchy”, with relations due to deconfined anyons being “less essential” than those due to fusion rules, F -symbols and R -symbols.

In light of the importance of the semisimple algebra A , I would like to point out an inconsistency in the treatment of Ising cage-net in this chapter: I started with the semisimple algebra A of the decoupled layers, but only ended up with the **simple** algebra A_0 of Ising cage-net. The fact that A and A_0 are defined for different systems is just a matter of notation. However, Ising cage-net should have its own semisimple algebra \tilde{A} , which can be obtained in principle from Protocol 11. Since Ising cage-net is a non-abelian fracton model, \tilde{A} is expected not to be simple. The point here is that the condensation procedure in Protocol 14 gives the correct GSD but not \tilde{A} . I conjecture that the correct \tilde{A} after condensation is constructed as follows:

Protocol 17. Let A be the semisimple algebra of a topological or fractonic order, and suppose that $\{a\}$ is a set of bosons to be condensed.

1. Define M as the subalgebra of logical operators of $\{a\}$. If $\{a\}$ can be condensed simultaneously, then M is always abelian.
2. Let M' be the commutant of M , and S the set of deconfined anyons. Construct a projector P_c based on the condensation condition of $\{a\}$, as well as a projector P_s for each deconfined anyon $s \in S$. Then for each subset $R \subset S$, let

$$P_R = \prod_{s \in R} P_s \prod_{s \notin R} (1 - P_s).$$

The M' can be decomposed as

$$M' = \bigoplus_{R \subset S} P_R M'.$$

Intuitively, this is the best decomposition of M' possible given the information of the deconfined anyons. Depending on the choice of R , it may be the case that $P_R M' = 0$. For example, consider doubled Ising where nothing is condensed. The

choice $R = \{\sigma, \bar{\sigma}\}$ leads to $P_R M' = 0$ because it enforces the self-contradicting relations $r = 1$, $\bar{r} = 1$ and $r\bar{r} = -1$.

3. If the semisimple algebra

$$P_R M' = \text{Mat}_{d_1} \oplus \cdots \oplus \text{Mat}_{d_m}$$

has more than one component, then certain operators must split. The result of the splitting is a matrix algebra

$$A_R = \text{Mat}_{d_1 + \cdots + d_m},$$

which is obtained by “filling the blanks” in the matrix representation of $P_R M'$. The semisimple algebra after condensation is

$$\tilde{A} = \bigoplus_{R \subset S} A_R.$$

This makes the components of \tilde{A} **precisely** determined by deconfined anyons, in agreement with Protocol 11.

This conjectured protocol directly connects the semisimple algebras before and after condensation. For example, the semisimple algebra of 1-F Ising is

$$\tilde{A} = \left[\bigoplus_{n=0}^{L-1} \binom{2L}{n} \text{Mat}_{t_n} \right] \oplus \frac{1}{2} \binom{2L}{L} \text{Mat}_{t_L},$$

where $t_n = [3^n + 3^{2L-n} + 6 \times (-1)^n] / 4$. This decomposition can be derived using either Protocol 11 or Protocol 17.

Protocol 17 again suggests that the operator algebra approach may provide a characterization of fracton models. Indeed, the approach is set up naturally for fracton models: It does not care about spatial dimension, and treats logical operators of fully mobile particles, partially mobile particles and even extended excitations (such as membrane operators for loop excitations) on equal ground. However, the operator algebra approach should not be viewed merely as an **abstract** semisimple algebra mod some relations. For example, consider two copies of the toric code (Fig. 5.12). The ground space of each copy is two qubits, say qubits 1 and 2 for the first copy, and qubits 3 and 4 for the second copy. Qubit i has logical operators X_i and Z_i which are Pauli matrices. If the operators X_1 and X_2 are condensed, then only the second copy of the toric code remains. Now suppose, instead, that the operators X_1 and X_4 are condensed. On the one hand, this is unphysical, since enforcing $X_1 = X_4 = 1$ leads to an unstable ground space with infinite degeneracy. This degeneracy is not robust, and can be lifted by local perturbations. An example of such local perturbations is Pauli X 's on the horizontal edges of the first lattice and the vertical edges of the

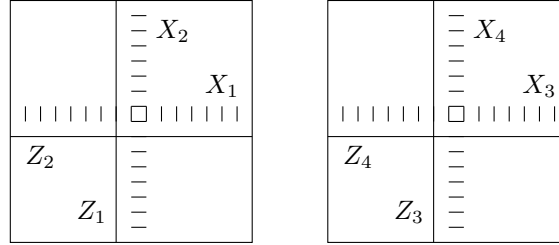


Figure 5.12: Two copies of the toric code and their logical operators. I use the setup of Ref. [58] on a square lattice, which is not drawn explicitly.

second lattice. The result is the trivial topological order. On the other hand, if U is the (non-local) unitary that swaps qubits 2 and 4, then

$$UX_1U^\dagger = X_1, UX_2U^\dagger = X_4.$$

Thus from a purely abstract perspective, the pair of operators (X_1, X_2) is the same as the pair of operators (X_1, X_4) . In other words, Protocol 14 (or 17) describes the condensation of certain operators assuming that the process is physical, but it does not clarify which operators can be condensed physically. Therefore, more information in the semisimple algebra A , especially regarding locality, must be specified in order to set up the mathematical structure in a physical way.

To help with this effort, I ask the following questions:

1. In a general fracton model, where do the relations in the semisimple algebra A come from? In Ising cage-net, the relations are obtained from the Hamiltonian, and they demand that a loop of a planon $\sigma^\alpha(i)\sigma^\alpha(j)$ be equal to its quantum dimension. Alternatively, the action of a cage term B_c can be viewed as lineon operators on the edges of a cube. However, if the relations are interpreted from a lineon perspective, then it is unclear what analog of “quantum dimension” should be assigned to the other side of the relation, because lineons cannot form contractible loops. For another example, in a $d = 3 + 1$ gauge theory, a point charge can form contractible loops in the xy , yz and zx planes, giving three relations. Is this a general feature that depends on some notion of “codimension” of an elementary operator?
2. Does the conjecture of “filling the blanks” in Protocols 14 and 17 hold for condensation transitions in general? Can the operation of “filling the blanks” be characterized more abstractly, perhaps by some universal property?
3. How can the process of gauging, the opposite of condensation [59], be understood in this approach?

4. How about foliation and generalized foliation (see Chapter 6)? What is an appropriate notion of RG here?
5. Can the notion of locality be incorporated into the various algebras? Equivalently, how can the algebras be decorated such that certain bases are preferred?
6. Is it possible to do reverse engineering, i.e., start with a matrix algebra written as a quotient of a semisimple algebra with some notion of locality, and construct a corresponding lattice model? Or even construct the spatial manifold without specifying it separately from the algebraic data?

As explained in the example of Fig. 5.12, I expect Question 5 concerning locality to be the most difficult and crucial one. The operator algebra approach currently only uses basic structures and theorems in noncommutative algebra. Given that topological orders are characterized by modular tensor categories, if the operator algebra approach characterizes fractonic orders in some sense, then it must involve mathematical tools that are at least as sophisticated. If an appropriate language that incorporates locality exists, then the operator algebra approach becomes a real treat. If not, then a trick is not too bad, either.

5.8 Appendix: Supplementary mathematics

This appendix is for some mathematics that is supplementary to the main text of this chapter.

Some definitions and theorems

In the first part of this appendix, I write down some definitions and theorems that are glossed over in the main text. They can also be found in mathematics textbooks such as Ref. [60].

Definition 18. An *algebra* is a complex vector space A equipped with associative multiplication and a multiplicative identity 1 , such that

$$\begin{aligned}(x + y)z &= xz + yz, \\ z(x + y) &= zx + zy, \\ (\lambda x)(\mu y) &= (\lambda\mu)(xy),\end{aligned}$$

for all $x, y, z \in A$, and $\lambda, \mu \in \mathbb{C}$. An *involution* is an antilinear map $x \mapsto x^*$ on A such that $1^* = 1$, $x^{**} = x$ and $(xy)^* = y^*x^*$ for all $x, y \in A$. The involution is *positive* if $x^*x \neq 0$ for all $x \neq 0$.

For a semisimple algebra A in $d = 2 + 1$, the involution is defined on elementary operators by replacing anyons a, b, c with their respective antiparticles a^*, b^*, c^* , and extended to A antilinearly, i.e., $(\lambda x)^* = \lambda^*x^*$ where $\lambda \in \mathbb{C}$, $x \in A$ and λ^* is the

complex conjugate of λ . In the examples in this chapter, all anyons are self-dual, so the involution acts trivially on the elementary operators. For chiral Ising, it can be shown by explicit calculation that this map is indeed an involution and is positive. Note that this check is performed manually on elementary operators for the definition of involution, and on an arbitrary operator for positivity. One cannot trivialize this check by identifying the operators with block-diagonal matrices, which would require Theorem 22. Although the check is tedious, I do not know an easier method.

In an algebra, the structures that can be quotiented out are called ideals.

Definition 19. A subset $I \subset A$ is an *ideal* if I is a subspace of the vector space A , and $rx \in I$, $xr \in I$ for all $r \in I$, $x \in A$. In the presence of an involution, an ideal $I \subset A$ is *involutive* if it is closed under the involution.

Basically, an involutive ideal is a set of elements that can be identified with 0 consistently, since if r is identified with 0 then so are r^* , rx and xr for all $x \in A$. If I is an involutive ideal, then the quotient algebra A/I is defined in the same way as for quotients of vector spaces. If A is finite dimensional, then A/I is also an algebra with positive involution (positivity is a consequence of Theorem 22). When A is reduced to A_0 in Section 5.2, the ideal I in the quotient $A_0 = A/I$ is generated from certain physically justified relations. Here, if $\Omega \subset A$ is a subset, for example $\Omega = \{\omega_1, \omega_2\}$, then the ideal generated by Ω is written as

$$\langle \omega_1, \omega_2 \rangle_{\text{id}, A} = \{x_1 \omega_1 y_1 + x_2 \omega_2 y_2 : x_i, y_i \in A\},$$

where the subscript A indicates the overall algebra. The ideal generated by Ω is the smallest ideal of A containing Ω , as one must multiply ω_i on both the left and the right, and then take linear combinations to make it an ideal. In all of the physical examples in this chapter, such ideals happen to be involutive. When it is clear from the context, I will drop the word “involutive” and simply say “ideal”.

The fact that matrix algebras have no non-trivial ideal is summarized as follows:

Definition 20. An algebra A_0 is *simple* if its only (not necessarily involutive) ideals are $\{0\}$ and A_0 itself.

Lemma 21. A finite dimensional algebra is simple if and only if it is a matrix algebra.

Note that the notions of simplicity and semisimplicity (Definition 10) do not rely on an involution. The following theorem relates semisimple algebras to algebras with positive involution:

Theorem 22. Let A be a finite dimensional algebra with positive involution. Then A is semisimple, and can be written in the form of (5.7) where the involution acts as Hermitian conjugation of matrices.

This is why positivity of the involution is important, and the theorem fails if the involution is not positive. The ideals of a semisimple algebra (5.7) are of the form $A_{i_1} \oplus \cdots \oplus A_{i_k}$ where $1 \leq i_1 < \cdots < i_k \leq m$. In other words, an ideal I of A is obtained simply by throwing away some of the summands in (5.7) and keeping the rest. To make the quotient A/I simple, precisely one A_i should be thrown away and the rest should be put into the ideal I , and A/I is isomorphic to this A_i .

To generate an ideal from relations, the general method uses the primitive central projectors $\{P_i\}$. Consider an ideal $I = \langle \{x_k\} \rangle_{\text{id}, A}$ where $\{x_k\}$ is a set of generic elements. Define a set

$$S = \{i : P_i x_k \neq 0 \text{ for some } k\}.$$

Then it can be shown that

$$I = \bigoplus_{i \in S} A_i, \quad A/I = \bigoplus_{i \notin S} A_i = \left(\sum_{i \notin S} P_i \right) A.$$

The proof is straightforward, and the idea is that if x_k has a non-trivial component in some A_i , then the entirety of A_i must be in I . This statement can be viewed as a more general version of (5.12).

Next, I present a more rigorous version of Lemma 13:

Lemma 23. Let B be a finite dimensional simple algebra with positive involution, $N \subset B$ an abelian, involutive subalgebra of B , and N' the commutant of N . Then $Z(N') = N$.

This lemma follows from the so-called von Neumann Bicommutant Theorem:

Theorem 24. Let B , N and N' be as in Lemma 23, and N'' the commutant of N' . Then $N'' = N$.

The theorem implies that $N'' = N \subset Z(N') \subset N''$, so $N = Z(N')$.

When discussing Definition 15, I mentioned that a Cartan subalgebra must satisfy an extra condition. Here is a rigorous definition of a Cartan subalgebra:

Definition 25. A subalgebra C of an algebra A is a *Cartan subalgebra* if it is abelian, diagonalizable and maximal. Diagonalizable means that every $x \in C$ is diagonalizable in its (faithful) matrix representation; maximal means that if any subalgebra $C' \subset A$ is abelian and diagonalizable and $C \subset C'$, then $C' = C$.

Diagonalizability can also be characterized intrinsically: $x \in A$ is diagonalizable if and only if its minimal polynomial has distinct linear factors [61]. This statement can be used to show that the Cartan subalgebras chosen for 1-F Ising in Section 5.5 and Ising cage-net in Section 5.6 are indeed diagonalizable, since their generators all

satisfy the polynomial $t^2 - 1 = (t + 1)(t - 1)$, which has distinct linear factors $t + 1$ and $t - 1$. Diagonalizability is needed for Lemma 16 to hold since, for example, the subalgebra of Mat_4 consisting of elements of the form

$$\begin{pmatrix} a & 0 & b & c \\ & a & d & e \\ & & a & 0 \\ & & & a \end{pmatrix}$$

is abelian, contains elements that are not diagonalizable, and has dimension 5.

Matrix representation of simple algebra

In the second part of this appendix, I answer the following question: Given a finite dimensional simple algebra A_0 with positive involution, how can a matrix representation of A_0 be constructed? Of course, there exists an isomorphism $\rho_n : A_0 \rightarrow \text{Mat}_n$ for some n , such that the involution on A_0 maps to Hermitian conjugation on Mat_n . However, the goal here is to determine ρ_n while only assuming knowledge of the structure constants $f_{\alpha\beta}^\gamma$ with respect to some basis $\{v_\alpha\}$, as defined in (5.10), as well as the action of the involution. The answer to this question leads to the representation (5.15) of chiral Ising operators without prior knowledge.

The construction of ρ_n involves several claims without proof, and the proofs can be found in Ref. [60]. I begin by solving the following set of linear and quadratic equations in the variables $\xi_\alpha, \lambda_\alpha \in \mathbb{C}$:

$$\begin{aligned} \xi^* &= \xi, \\ \xi^2 &= 1, \\ \xi v_\alpha \xi &= \lambda_\alpha \xi \text{ for all } \alpha, \end{aligned} \tag{5.39}$$

where $\xi = \sum_\alpha \xi_\alpha v_\alpha$. I claim that (5.39) always has solutions. In fact, if $n > 1$ then there are many solutions, in which case I choose one solution. The element ξ can be viewed as the elementary matrix whose only non-zero entry is the $(1, 1)$ entry, which is 1. The variables λ_α are of no use anymore.

Let V be the vector space spanned by $\{v_\alpha \xi\}$. I claim that $\dim(V) = n$ even though V is defined as the span of n^2 elements. Clearly V is closed under left multiplication by A_0 , and indeed it is the vector space that affords the representation ρ_n of A_0 . Practically, one may reduce the overcomplete set $\{v_\alpha \xi\}$ to obtain a basis for V . The final part of the construction is to find an inner product $\langle x, y \rangle$ for all $x, y \in V$, which then defines Hermitian conjugation of matrices. By the definition of V , there exist $a, b \in A_0$ (not unique) such that $x = a\xi$, $y = b\xi$. By (5.39),

$$x^* y = \xi a^* b \xi = \lambda \xi$$

for some $\lambda \in \mathbb{C}$. Since $\xi \neq 0$, this λ does not depend on the choice of a and b . I then define $\langle x, y \rangle = \lambda$, and I claim that this is an inner product.

The Hermitian conjugation derived from this inner product is compatible with the involution on A_0 . This is because for all $z \in A_0$ and $x, y \in V$,

$$\langle x, z^*y \rangle \xi = x^*z^*y\xi = (zx)^*y\xi = \langle zx, y \rangle \xi = \langle x, z^\dagger y \rangle \xi,$$

which implies that $z^* = z^\dagger$. Therefore, the action of A_0 on V by left multiplication serves as a representation ρ_n .

GENERALIZED FOLIATION

In the final chapter of this thesis, I resolve the problem concerning the definition of phase for Ising cage-net, which is not foliated as shown in Chapter 5. The solution turns out to be a generalized version of the foliation RG that is both physically intuitive and, to some extent, inevitable.

One way to see the inevitability of this generalization is by phrasing the original foliation RG purely in terms of quantum circuits. Consider the foliation RG for the X-cube model, which acts as a finite-depth circuit and uses $d = 2 + 1$ toric codes as resource layers [19]. Being a topological order, a resource layer cannot itself be created with a finite-depth circuit from a product state. However, it is well-known that the layer can be created with a linear-depth circuit [62], one whose depth is bounded by the linear system size. Therefore, the original foliation RG is unnatural: It allows for a finite-depth circuit acting on the bulk of the system, together with a linear-depth circuit acting only on the ancilla qubits in a product state. A more natural definition is to allow the linear-depth circuit to act arbitrarily within a planar region on both the ancilla qubits and the bulk.

Alternatively, a toric code resource layer of the X-cube model can also be removed by condensing a boson in the layer. This corresponds to condensing a bosonic planon in the X-cube model. The planon is special in the sense that it can be viewed as part of a $d = 2 + 1$ model that is decoupled from the $d = 3 + 1$ bulk. To be more general, the RG should allow the condensation of arbitrary bosonic planons.

In light of the above, there are two natural ways to extend the foliation RG: linear-depth circuits and planon condensation. In this chapter, I show that both approaches lead to generalized foliated RG schemes applicable to Ising cage-net. In fact, the two approaches are closely related, since partial application of the linear-depth circuit for Ising cage-net leads to a gapped boundary which condenses the appropriate planons and separates a doubled Ising ground state from an Ising cage-net ground state. In Section 6.1, I study the generalized foliation RG on Ising cage-net via condensation. In Section 6.2, I review the linear-depth circuit that creates doubled Ising from a product state. This circuit serves as a preparation for Section 6.3, where I explain the generalized foliation RG on Ising cage-net via planar linear-depth circuit. To conclude this chapter and hence the entire thesis, I show in Section 6.4 that the generalized foliation RG does not work for most CS_∞ theories.

The results in this chapter are based on Ref. [31].

6.1 Generalized foliation via condensation

The first way to apply the generalized foliation RG on Ising cage-net is via planon condensation. Specifically, consider condensing the boson $\psi\bar{\psi}$ in the plane $z = 0$. This changes the set of fractional excitations of the model (Table 5.1) by identifying some excitations and confining others. More precisely:

1. Since $\psi\bar{\psi}$ is a fracton dipole, fractons between the planes $z = 0$ and $z = 1$ are identified with the corresponding fractons between the planes $z = -1$ and $z = 0$.
2. The planons ψ and $\bar{\psi}$ in the plane $z = 0$ are identified.
3. The planon $\sigma\bar{\sigma}$ in the plane $z = 0$ splits into two abelian bosonic planons e and m with a -1 mutual statistic.
4. The lineons in the plane $z = 0$ are all confined.

Thus the fractional excitations that remain in the plane $z = 0$ are e , m and $\psi = \bar{\psi}$. By further condensing e or m , no fractional excitation is left in the plane $z = 0$. The remaining fractional excitations are exactly those of Ising cage-net with a smaller system size $(L_x, L_y, L_z - 1)$. In particular, the fractons between the planes $z = 0$ and $z = 1$, now identified with the fractons between the planes $z = -1$ and $z = 0$, become the new fractons between the planes $z = -1$ and $z = 1$. Therefore, the generalized foliation RG is able to shrink the system size of Ising cage-net.

Conversely, the generalized foliation RG is also able to grow the system size of Ising cage-net. For this purpose, it is convenient to view Ising cage-net as obtained by gauging the planar \mathbb{Z}_2 symmetries of a subsystem symmetry enriched topological (SSET) model protected by such symmetries [63]. The condensation of planons is equivalent to breaking the planar symmetries in the appropriate planes. To reverse this process and increase the system size, planar states with said symmetries are added to the system and then the symmetries are gauged.

6.2 The doubled Ising anyon model and linear-depth circuit

The planar linear depth circuit for Ising cage-net is built upon the linear depth circuit that creates doubled Ising from a product state, and I review the latter in this section [62]. The goal is to start from a product state on a minimal trivalent lattice (Fig. 5.11), enlarge the lattice plaquette by plaquette, and eventually obtain a ground state wavefunction of doubled Ising. I work with a square-octagon lattice (Fig. 5.2) for the convenience of discussing Ising cage-net in Section 6.3.

The sewing gate

I begin by defining a useful quantum gate in a general string-net model, called the *sewing gate*. It is written as G_p , labelled by a plaquette p (the *target plaquette*) and

an edge of p (the *control edge*, not displayed explicitly). To understand the action of G_p intuitively, consider a state on the lattice such that the control edge is in the state $|s'\rangle$ while the other edges are in a string-net ground state, where s' is a string label. The gate is of the form $G_p = \sum_s G_p^s$, where the sum is over all string labels, and G_p^s is given by

$$\begin{aligned}
 G_p^s \left| \begin{array}{c} \bar{t}_2 \quad \bar{t}_3 \\ \bar{t}_2 \quad t_2 \quad b \quad \bar{t}_3 \quad \bar{t}_3 \\ a \quad \quad \quad c \\ \bar{t}_1 \quad t_1^* \quad t_4 \quad \bar{t}_4 \\ t_1 \quad \quad \quad t_4 \end{array} \right\rangle &= \delta_{ss'} \left| \begin{array}{c} \bar{t}_2 \quad \bar{t}_3 \\ \bar{t}_2 \quad t_2 \quad b \quad \bar{t}_3 \quad \bar{t}_3 \\ a \quad \quad \quad c \\ \bar{t}_1 \quad t_1^* \quad t_4 \quad \bar{t}_4 \\ t_1 \quad \quad \quad 0 \quad \quad t_4 \end{array} \right\rangle \\
 &= \delta_{ss'} \sum_{\substack{\alpha\beta\gamma\delta \\ \epsilon\zeta\eta}} F_{ss^*\alpha}^{t_1 t_1^* 0} F_{s\alpha^*\beta}^{\bar{t}_1 a t_1} F_{s\beta^*\gamma}^{\bar{t}_2 t_2 a^*} F_{s\gamma^*\delta}^{\bar{t}_2 b t_2^*} F_{s\delta^*\epsilon}^{\bar{t}_3 t_3 b^*} F_{s\epsilon^*\zeta}^{\bar{t}_3 c t_3^*} F_{s\zeta^*\eta}^{\bar{t}_4 t_4 c^*} \left| \begin{array}{c} \bar{t}_2 \quad \bar{t}_3 \\ \bar{t}_2 \quad t_2 \quad b \quad \bar{t}_3 \quad \bar{t}_3 \\ \alpha \quad \quad \quad \delta \quad \quad \quad \epsilon \\ \beta \quad \quad \quad \gamma \quad \quad \quad \zeta \\ \bar{t}_1 \quad t_1^* \quad t_4 \quad \bar{t}_4 \\ t_1 \quad \quad \quad t_4 \end{array} \right\rangle.
 \end{aligned} \tag{6.1}$$

Here, the red edge is the control edge, while the black edges are in a string-net ground state. The action of G_p^s is non-zero only if $s' = s$, in which case it “extends” the s -string into an s -loop. Equivalently, G_p^s first sets $|s'\rangle$ to $|0\rangle$ and then applies the plaquette operator B_p^s . This is a generalization of the controlled NOT (CNOT) gate to string-net models. Many equations in this chapter such as (6.1) are derived using graphical method, a standard yet often complicated arithmetic in string-net models. I demonstrate the details of the graphical calculation in (6.1) below:

$$\begin{aligned}
 &\left| \begin{array}{c} \bar{t}_2 \quad \bar{t}_3 \\ \bar{t}_2 \quad t_2 \quad b \quad \bar{t}_3 \quad \bar{t}_3 \\ a \quad \quad \quad c \\ \bar{t}_1 \quad t_1^* \quad t_4 \quad \bar{t}_4 \\ t_1 \quad \quad \quad 0 \quad \quad t_4 \end{array} \right\rangle = \sum_{\alpha} F_{ss^*\alpha}^{t_1 t_1^* 0} \left| \begin{array}{c} \bar{t}_2 \quad \bar{t}_3 \\ \bar{t}_2 \quad t_2 \quad b \quad \bar{t}_3 \quad \bar{t}_3 \\ a \quad \quad \quad c \\ \bar{t}_1 \quad t_1^* \quad t_4 \quad \bar{t}_4 \\ t_1 \quad \quad \quad s \quad \quad t_4 \end{array} \right\rangle \\
 &= \sum_{\alpha\beta} F_{ss^*\alpha}^{t_1 t_1^* 0} F_{s\alpha^*\beta}^{\bar{t}_1 a t_1} \left| \begin{array}{c} \bar{t}_2 \quad \bar{t}_3 \\ \bar{t}_2 \quad t_2 \quad b \quad \bar{t}_3 \quad \bar{t}_3 \\ \beta \quad \quad \quad c \\ \bar{t}_1 \quad \alpha \quad t_4 \quad \bar{t}_4 \\ t_1 \quad \quad \quad t_4 \end{array} \right\rangle = \sum_{\alpha\beta\gamma} F_{ss^*\alpha}^{t_1 t_1^* 0} F_{s\alpha^*\beta}^{\bar{t}_1 a t_1} F_{s\beta^*\gamma}^{\bar{t}_2 t_2 a^*} \left| \begin{array}{c} \bar{t}_2 \quad \bar{t}_3 \\ \bar{t}_2 \quad t_2 \quad b \quad \bar{t}_3 \quad \bar{t}_3 \\ \beta \quad \quad \quad \delta \quad \quad \quad \epsilon \\ \gamma \quad \quad \quad \zeta \\ \bar{t}_1 \quad \alpha \quad t_4 \quad \bar{t}_4 \\ t_1 \quad \quad \quad t_4 \end{array} \right\rangle \\
 &= (\text{repeat similar steps across the vertices of the plaquette}) \\
 &= \sum_{\substack{\alpha\beta\gamma\delta \\ \epsilon\zeta\eta}} F_{ss^*\alpha}^{t_1 t_1^* 0} F_{s\alpha^*\beta}^{\bar{t}_1 a t_1} F_{s\beta^*\gamma}^{\bar{t}_2 t_2 a^*} F_{s\gamma^*\delta}^{\bar{t}_2 b t_2^*} F_{s\delta^*\epsilon}^{\bar{t}_3 t_3 b^*} F_{s\epsilon^*\zeta}^{\bar{t}_3 c t_3^*} F_{s\zeta^*\eta}^{\bar{t}_4 t_4 c^*} \left| \begin{array}{c} \bar{t}_2 \quad \bar{t}_3 \\ \bar{t}_2 \quad t_2 \quad b \quad \bar{t}_3 \quad \bar{t}_3 \\ \alpha \quad \quad \quad \delta \quad \quad \quad \epsilon \\ \beta \quad \quad \quad \gamma \quad \quad \quad \zeta \\ \bar{t}_1 \quad t_1^* \quad t_4 \quad \bar{t}_4 \\ t_1 \quad \quad \quad t_4 \end{array} \right\rangle.
 \end{aligned}$$

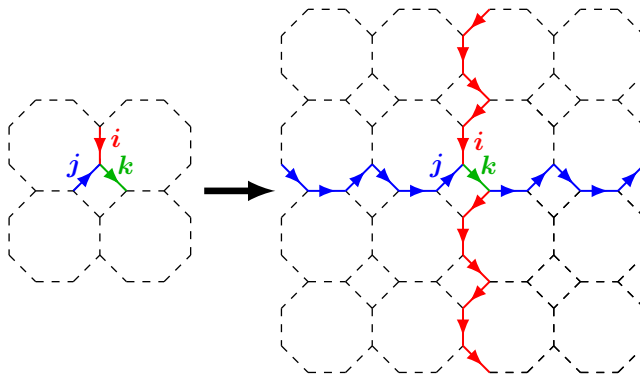


Figure 6.1: The starting steps in the linear depth circuit for doubled Ising. A ground state of doubled Ising on a minimal lattice is extended along non-contractible loops.

In each step, edges are manipulated using F -moves. From now on, I will not show any more graphical calculations explicitly, as they are all similar to the calculation above. An important corollary of (6.1) is that the sewing gate G_p turns a product state projector into a string-net plaquette term. More precisely, let

$$P = \sum_{ss'} \frac{d_s d_{s'}}{D} |s\rangle \langle s'| \quad (6.2)$$

be a projector on the control edge, where $D = \sum_s d_s^2$ is the total quantum dimension. As can be shown by graphical calculation, G_p acts on P by conjugation as

$$G_p P G_p^\dagger = B_p, \quad (6.3)$$

so P is mapped to a plaquette term. Therefore, G_p “sews” a decoupled control edge into a string-net ground state by creating a plaquette term that involves the control edge, and hence its name. In fact, G_p is not unitary on the entire string-net Hilbert space, but is isometric on the subspace of states in (6.1). The latter is enough for the purpose of constructing linear-depth circuits in this chapter. It is in this sense that (6.3) is an action of G_p by conjugation. Furthermore, two sewing gates commute if neither acts on the other’s control edge. Similarly, a sewing gate commutes with any plaquette term B_p that does not act on its control edge.

The circuit for doubled Ising

The sewing gate is a key part of the linear depth circuit that creates a ground state of doubled Ising (5.2) from a product state, which I describe now. The focus here is on states rather than Hamiltonians, so some of the gates in the circuit are only defined as isometries on certain subspaces. To start with, take a ground state $|ijk\rangle$ of doubled Ising on a minimal trivalent lattice, such as one of w_1, \dots, w_9 in (5.37), and put the state on three edges sharing a vertex (Fig. 6.1). Apart from these three

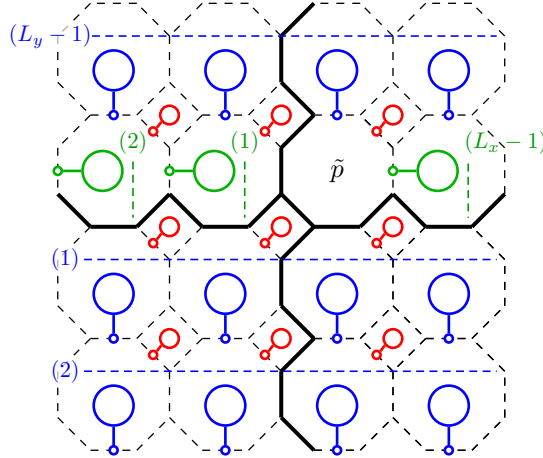


Figure 6.2: Adding plaquette term constraints with sewing gates. Initially, the edges on the solid black lines are in a ground state of doubled Ising on a minimal trivalent lattice, while the other edges are set to the state $|\psi\rangle$ in (6.4). Small circles indicate control edges of sewing gates, and large circles indicate target plaquettes. First, the red gates are applied in a single step. Next, the blue gates are applied row by row, from row 1 to row $(L_y - 1)$. Finally, the green gates are applied from column 1 to column $(L_x - 1)$ in row L_y . No plaquette term is generated for the last plaquette \tilde{p} .

edges, all other edges of the lattice are set to

$$|\psi\rangle = \sum_s \frac{d_s}{\sqrt{D}} |s\rangle, \quad (6.4)$$

an eigenstate of the projector P in (6.2). Then copy the states $|i\rangle$ and $|j\rangle$ along non-contractible loops using gates of the form $\sum_s |s\rangle |s\rangle \langle\psi| \langle s|$. By definition of the state $|ijk\rangle$, the copying process yields a state $|\Phi\rangle$ which satisfies a maximal plaquette term B_{mp} , where the subscript “mp” stands for “maximal plaquette”. This maximal plaquette takes the shape of the blue loop in Fig. 5.11.

Continuing from the state $|\Phi\rangle$, plaquette terms can be added with sewing gates. This is shown in Fig. 6.2, where a sewing gate is represented by a small circle (indicating the control edge) connected to a large circle (indicating the target plaquette). Since the focus here is the state, “adding a term” really means transforming the state such that it satisfies the constraint enforced by the term. First, since the square plaquettes are all disjoint, the red sewing gates can be applied in a single step. Next, the blue gates are applied to the octagon plaquettes row by row, from row 1 to row $(L_y - 1)$. Since two gates from adjacent rows do not commute, the blue gates must be applied sequentially. Finally, the green gates are applied to the octagon plaquettes from column 1 to column $(L_x - 1)$ in row L_y , also sequentially for a similar reason.

The depth of the circuit in Fig. 6.2 is clearly linear in the system size. Furthermore, the state $|\Phi\rangle$ and the gates acting on it all respect the vertex terms. However, the

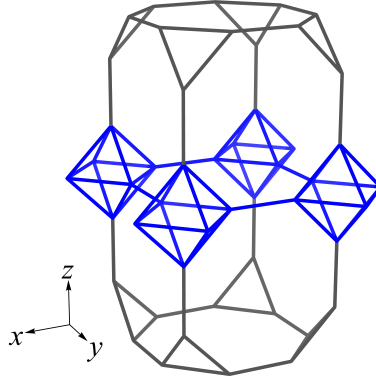


Figure 6.3: Insertion of an xy plane bisecting a cube in the original lattice. Each intersection point of the inserted plane with the z principal edges is expanded into an octahedron to preserve the trivalent structure.

last plaquette \tilde{p} has no plaquette term of its own. Since none of the edges of \tilde{p} is in the state $|\psi\rangle$, the sewing gate cannot be applied to \tilde{p} in the usual way. Despite the absence of a plaquette term, the circuit in Fig. 6.2 still correctly maps $|\Phi\rangle$ to a doubled Ising ground state. This is because when all the plaquette terms except for $B_{\tilde{p}}$ are satisfied, enforcing $B_{\tilde{p}}$ is equivalent to enforcing B_{mp} on the maximal plaquette. None of the sewing gates in Fig. 6.2 has its control edge on the solid black lines, so the circuit commutes with B_{mp} . Since $|\Phi\rangle$ satisfies B_{mp} , so does its image under the circuit.

6.3 Generalized foliation via planar linear-depth circuit

In this section, I explain the planar linear-depth circuit which implements the generalized foliation RG on Ising cage-net. The circuit inserts a doubled Ising ground state into an Ising cage-net ground state and thus increases the system size of Ising cage-net in the z direction. This section is structured similarly to Section 6.2: I first define a gate that grows a cage, and then discuss the full circuit.

Growing a cage

Just as a single sewing gate G_p grows a plaquette, a certain combination G_c of sewing gates grows a cage in Ising cage-net. Consider a truncated cubic lattice in an Ising cage-net ground state, and suppose that an xy plane is inserted into the lattice which bisects a cube (Fig. 6.3). At each point where the inserted plane intersects with a z principal edge, an octahedron is added to preserve the trivalent structure. Each edge of the octahedra carries a Hilbert space of dimension 3, spanned by $|0\rangle$, $|1\rangle$ and $|2\rangle$, and is set to $|0\rangle$ for now. Each principal edge (i.e., one in the x or y direction) of the octagon carries a Hilbert space of dimension 5, spanned by $|00\rangle$, $|02\rangle$, $|20\rangle$, $|22\rangle$ and $|11\rangle$, and is set to $|00\rangle$ for now. The latter Hilbert space is chosen to comply

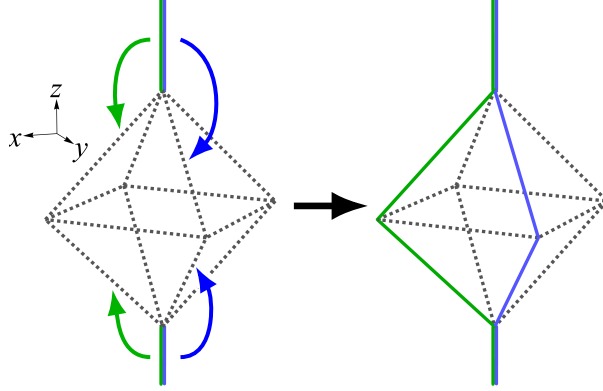


Figure 6.4: Extending the state on a bisected z principal edge to some edges of the octahedron. A dotted black edge is in the state $|00\rangle$ if it is a principal edge, and $|0\rangle$ otherwise. The resulting state satisfies the vertex terms in the xz and yz planes.

with the condensation operator V_{l_μ} given by (5.3). Indeed, all gates in the circuit for Ising cage-net commute with V_{l_μ} .

In the first step of the gate G_c , states on the bisected z principal edges are extended to some edges of the octahedra (Fig. 6.4). This is achieved by gates of the form

$$\sum_{xy} |xy\rangle \langle xy| \otimes |x\rangle \langle 0| \quad \text{or} \quad \sum_{xy} |xy\rangle \langle xy| \otimes |y\rangle \langle 0|,$$

where the first component of the tensor product is the identity on a z principal edge, and the second component acts on an edge of an octahedron. The resulting state satisfies the vertex terms in the xz and yz planes.

In the second step, plaquette terms are added to the square plaquettes by sewing gates. More precisely, in each square plaquette there exists an edge in the state $|0\rangle$ after the first step of G_c (Fig. 6.4). This state $|0\rangle$ is now mapped to $|\psi\rangle$ given by (6.4) and then the edge is used as the control edge of the sewing gate.

In the third and final step, the cage term as well as plaquette terms on the octagon plaquettes are added through a non-trivial process which I explain now. Of the two cubes in Fig. 6.3, I focus on the top one. First, take a state $|00\rangle$ on a principal edge of the bottom face p_b and map it to $|\psi\rangle \otimes |0\rangle$, where $|\psi\rangle$ is given by (6.4). In the current context, the first component of a tensor product of two states or operators is always associated with the xy plane, and the second component is associated with the xz or yz plane. Although $|\psi\rangle \otimes |0\rangle$ does not satisfy the condensation term V_{l_μ} given by (5.3), it is eventually mapped to a state that does. Now as shown in Fig. 6.5 (a), with the state $|\psi\rangle \otimes |0\rangle$ as the control edge, apply to the top face p_t and the bottom face p_b the modified sewing gate

$$\tilde{G} = \sum_s \frac{1}{d_s} G_{p_b}^s B_{p_t}^s.$$

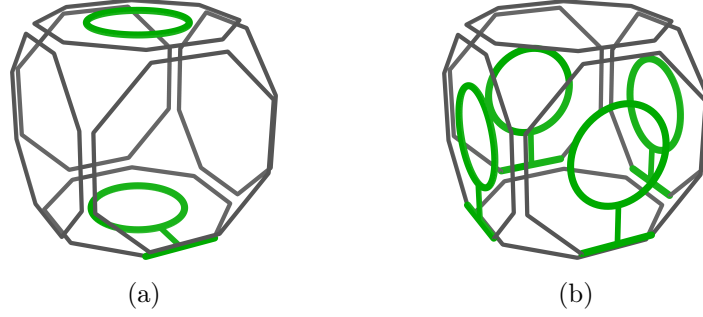


Figure 6.5: Growing a cage. As shown in subfigure (a), plaquette terms are added to the top and bottom faces by sewing gates with an edge of the bottom face as the control edge. Then as shown in subfigure (b), plaquette terms are added to the side faces by sewing gates with edges of the side faces as the control edges.

Intuitively, \tilde{G} is a sum of gates that draw s -loops on p_t and p_b simultaneously. The label s is on an edge of p_b , so the s -string is grown into a loop on p_b by G_{p_b} , whereas a full s -loop is created on p_t by B_{p_t} . By graphical calculation, \tilde{G} acts on the control edge projector as

$$\tilde{G} |\psi\rangle \langle\psi| \tilde{G}^\dagger = \frac{1}{4} (1 + B_{p_b}^1 B_{p_t}^1 + B_{p_b}^2 B_{p_t}^2). \quad (6.5)$$

This should be viewed as enforcing two terms $B_{p_b}^1 B_{p_t}^1$ and $B_{p_b}^2 B_{p_t}^2$ since the terms commute. The next step is to draw loops on the side faces. Take the state $|\xi\rangle \otimes |0\rangle$ on each principal edge of the bottom face p_b , where $|\xi\rangle$ is a superposition of the states $|0\rangle$, $|1\rangle$ and $|2\rangle$, and apply the map

$$f : |s0\rangle \mapsto \begin{cases} |s\rangle \otimes \frac{1}{\sqrt{2}}(|0\rangle + |2\rangle), & \text{if } s = 0 \text{ or } 2, \\ |11\rangle, & \text{if } s = 1. \end{cases} \quad (6.6)$$

The rationale behind the map f will be explained soon. For now, it is clear that f yields a state that satisfies the condensation operator V_{l_μ} . As shown in Fig. 6.5 (b), sewing gates are then applied to the side faces with edges of the side faces as the control edges. As a result, plaquette terms are thus added to the side faces but not in a standard way, since the states in the xz and yz planes are not the standard $|\psi\rangle$ and thus (6.3) cannot be invoked. Therefore, I now explicitly calculate the action of $G_p \circ f$ on the $B_{p_b}^1$ term in (6.5). I drop the $B_{p_t}^1$ factor since it is unaffected. For each string label s , define a projector $P^s = |s\rangle \langle s|$. Graphical calculation shows that G_p^s (a component of G_p) in (6.1) satisfies

$$G_p^s |s\rangle \langle s'| G_p^{s'\dagger} = P^s \left(\sum_k \frac{d_k}{d_s d_{s'}} B_p^k \right) P^{s'}. \quad (6.7)$$

For convenience of calculation, I also write

$$B_p^1 = (P^0 + P^2) B_p^1 P^1 + P^1 B_p^1 (P^0 + P^2),$$

which breaks the domain and target of B_p^1 into two pieces each. Let p_v be a side face, where the subscript “v” stands for “vertical”. The action of $G_{p_v} \circ f$ is

$$\begin{aligned}
& G_{p_v} f [B_{p_b}^1 \otimes (|0\rangle \langle 0|)] f^\dagger G_{p_v}^\dagger \\
&= \frac{1}{\sqrt{2}} G_{p_v} [(P^0 + P^2) B_{p_b}^1 P^1 \otimes (|0\rangle \langle 1| + |2\rangle \langle 1|)] G_{p_v}^\dagger \\
&\quad + \frac{1}{\sqrt{2}} G_{p_v} [P^1 B_{p_b}^1 (P^0 + P^2) \otimes (|1\rangle \langle 0| + |1\rangle \langle 2|)] G_{p_v}^\dagger \\
&= \frac{1}{\sqrt{2}} [(P^0 + P^2) B_{p_b}^1 P^1] \otimes [(P^0 + P^2) B_{p_v}^1 P^1] \\
&\quad + \frac{1}{\sqrt{2}} [P^1 B_{p_b}^1 (P^0 + P^2)] \otimes [P^1 B_{p_v}^1 (P^0 + P^2)],
\end{aligned} \tag{6.8}$$

where I used (6.7) to obtain the last equality. As can be seen from the pattern of the projectors P^s , (6.8) commutes with the condensation operator V_{l_μ} . With this property understood, I hide the projectors in (6.8) and write

$$G_{p_v} f [B_{p_b}^1 \otimes (|0\rangle \langle 0|)] f^\dagger G_{p_v}^\dagger = \frac{1}{\sqrt{2}} B_{p_b}^1 B_{p_v}^1.$$

Similarly, $G_p \circ f$ maps the $B_{p_b}^2$ term in (6.5) to

$$G_{p_v} f [B_{p_b}^2 \otimes (|0\rangle \langle 0|)] f^\dagger G_{p_v}^\dagger = \frac{1}{2} B_{p_b}^2 (1 + B_{p_v}^2). \tag{6.9}$$

This explains the peculiar definition of f in (6.6): If the superposition $(|0\rangle + |2\rangle)/\sqrt{2}$ is replaced by a basis vector $|0\rangle$ or $|2\rangle$, then no $B_{p_v}^2$ term can be generated in (6.9). Note that (6.5) automatically satisfies the constraint $B_{p_t}^2 = 1$, since the top face p_t is already in an Ising cage-net ground state. Therefore, a ground state of the enlarged Ising cage-net should be in the eigenspace of (6.9) with the largest eigenvalue. This is achieved when the plaquette terms $B_{p_b}^2$ and $B_{p_v}^2$ are both satisfied. Thus for the purpose of describing ground states, (6.9) can be rewritten as

$$B_{p_b}^2 \otimes (|0\rangle \langle 0|) \mapsto B_{p_b}^2 + B_{p_v}^2.$$

By applying $G_p \circ f$ to all side faces, the operator (6.5) is mapped to

$$\sum_{p_o} B_{p_o}^2 + B_c,$$

where B_c is the cube term given by (5.4). This is not exactly the image of (6.5) under $G_p \circ f$ but nevertheless describes the correct ground states. All terms associated with the new cube are hence generated successfully.

The circuit for Ising cage-net

The planar linear-depth circuit that performs the generalized foliation RG on Ising cage-net is designed in close analogy with the circuit that creates doubled Ising in

Section 6.2. Just as the latter circuit starts with one of the states w_1, \dots, w_9 in (5.37), the former circuit requires a suitable starting product state. The choice of the starting state here is more complicated than in the case of doubled Ising, and I address this issue now.

In doubled Ising, the starting state is chosen to satisfy the maximal plaquette term. This is to make sure that after the circuit is applied, there can be one plaquette (\tilde{p} in Fig. 6.2) without a plaquette term of its own. Similarly, in Ising cage-net, the starting state should satisfy a cage term B_c on a cage that is maximal in the xy plane and has thickness 1 in the z direction (Fig. 5.10). As explained in Section 5.6, this term B_c enforces $r^z(i)r^z(i+1) = 1$. Many notations in the current discussion are defined in Section 5.6. If i is the label for the inserted layer, then the original Ising cage-net ground state can be chosen to satisfy $r^z(i+1) = \pm 1$. The term B_c then enforces

$$r^z(i) = \pm 1, \quad (6.10)$$

where the ± 1 depends on $r^z(i+1)$. Furthermore, the state should also satisfy condensation conditions $\Psi^\alpha = 1$ where, for example, Ψ^z is given by (5.25). Given that the original Ising cage-net ground state already satisfies its condensation conditions, the new conditions simplify to

$$\psi_x^z(i)\bar{\psi}_x^z(i) = 1, \quad \psi_y^z(i)\bar{\psi}_y^z(i) = 1. \quad (6.11)$$

A straightforward calculation shows that (6.10) and (6.11) are solved by w_7, w_8 and w_9 with $+1$ in (6.10), and by w_{10} with -1 in (6.10). Either way, there always exists a state $|ijk\rangle$ on the minimal trivalent lattice that satisfies both the fat cage term B_c and the condensation conditions. The notation $|ijk\rangle$ here is chosen for analogy with Section 6.2, and does not indicate that the state factorizes on the three edges of the minimal trivalent lattice. Now extend the state $|ijk\rangle$ along non-contractible loops of the inserted plane (Fig. 6.1), and set the other added edges to $|0\rangle$ or $|00\rangle$, whichever is appropriate. This is the starting state of the circuit.

Given the starting state, the job of the circuit is to grow cages on top of the inserted layer (Fig. 6.6). First, the circuit grows cages row by row, from row 1 to row $(L_y - 1)$ following the blue arrows. Note that on a side face p_v shared by two adjacent cubes, the sewing gate G_{p_v} only acts once. Next, the circuit grows cages in row L_y , from column 1 to column $(L_x - 1)$ following the green arrows. In the end, all terms in the Ising cage-net Hamiltonian (5.5) are generated except for the cage term at the final, untouched cube. Similar to the situation for doubled Ising, the circuit outputs a correct Ising cage-net ground state despite the absence of a cage term, because this term is implied by the fat cage term which the state is chosen to satisfy from the very beginning. The depth of the circuit is clearly linear in the system size.

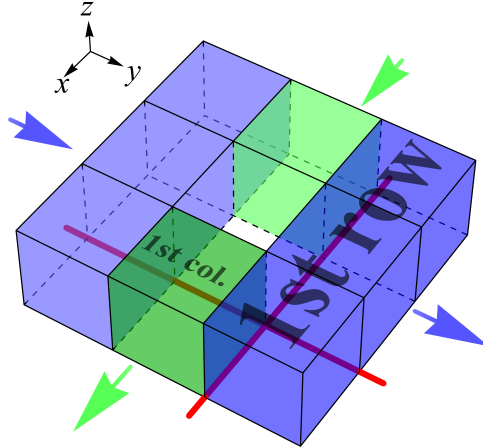


Figure 6.6: Growing cages on top of the layer inserted into Ising cage-net. The red lines indicate the non-trivial part of the starting state. First, cages are grown row by row (blue), from row 1 to row $(L_y - 1)$. Next, cages are grown in row L_y (green), from column 1 to column $(L_x - 1)$. The last cube has no cube term.

6.4 Feasibility for infinite-component Chern-Simons theory

In the final section of this thesis, I try to apply generalized foliation to gapped CS_∞ theories. For simplicity, I focus on K matrices with period $r = 1$ and of the form

$$K(u) = (c_1 u + c_0 + c_1 u^{-1}), \quad (6.12)$$

where c_0 is even, so that exchange statistics are well-defined. It turns out that most CS_∞ theories with such K matrices do not have a generalized foliation structure, at least from the perspective of boson condensation.

The process of finding and condensing bosons relies heavily on the information of braiding statistics. For this reason, I discuss several facts concerning braiding statistics in the polynomial description. Let $x(u)$ be the polynomial representations of the planon x specified by its charge vector. Specifically, if $\{e_i\}$ is the standard basis for the space \mathbb{Z}^N of charge vectors and $x = \sum_k x_k e_k$, then $x(u) = \sum_k x_k u^k$. Note that unlike the K matrix, the charge vector is not periodic but still has a polynomial representation. It can be shown that the braiding statistic $x^T K^{-1} y$ of the planons x and y is equal to the constant term in the series expansion of $x^\dagger(u) K(u)^{-1} y(u)$, where $x^\dagger(u) = x(u^{-1})$. In particular, x is a boson if and only if the constant term θ_0 in the expansion

$$\theta_x(u) = x^\dagger(u) K(u)^{-1} x(u) = \sum_{k=-\infty}^{\infty} \theta_k u^k \quad (6.13)$$

is an even integer. Moreover, the RG is expected to be applicable repeatedly if the theory is assumed to be an RG fixed point. This means that if $x(u)$ is condensed by

the RG, then a translation $u^k x(u)$ of $x(u)$ remains deconfined if $|k|$ is large enough, and thus can also be condensed by the RG. In other words, the coefficient θ_k in (6.13) is an integer. However, as shown in Section 2.4, θ_k decays (a bit more slowly than) exponentially. Therefore, for all sufficiently large $|k|$, the integer θ_k must be 0. The conclusion is that a boson x can be condensed in the RG only if $\theta_x(u)$ has finitely many terms. This is a strong condition on bosons suitable for the generalized foliation RG.

Indeed, in a CS_∞ theory whose K matrix is of the form (6.12), there may not even be a suitable boson to condense. For example, consider $K(u) = (u + 4 + u^{-1})$. Let L (resp. L') be the ring of Laurent polynomials with integer (resp. rational) coefficients. Suppose that x is a boson such that $\theta_x(u)$ has finitely many terms. Since

$$\theta_x(u) = \frac{x^\dagger(u)x(u)}{K(u)}$$

is the ratio of two elements of L and can be computed, for example, by long division, its coefficients θ_k must be rational, i.e., $\theta_x(u) \in L'$. Note that this conclusion fails if $\theta_x(u)$ has infinitely many terms and cannot be computed by long division. Since $K(u)$ is primitive (see definition in Proposition 3), basic ring theory implies that actually $\theta_x(u) \in L$ [35]. In this particular example, $\theta_x(u) \in L$ can be derived using long division and the fact that the leading coefficient of $K(u)$ is $c_1 = 1$, although primitivity is enough in general. Furthermore, $K(u)$ is *irreducible*, meaning that it cannot be factorized into a product of two non-trivial Laurent polynomials in L . By basic ring theory, the ring L has the property that $K(u)$ is irreducible if and only if it is *prime*, meaning that if $K(u)$ divides $x^\dagger(u)x(u)$ (i.e., the ratio $\theta_x(u) \in L$), then it divides $x^\dagger(u)$ or $x(u)$. Using $K(u^{-1}) = K(u)$, it is easy to show that if $K(u)$ divides either $x^\dagger(u)$ or $x(u)$ then it must divide both. However, this means that $x \in K\mathbb{Z}^N$, so the planon is actually trivial.

Even if there are suitable bosons to condense in a CS_∞ theory, the generalized foliation RG may still fail to work. For example, consider $K(u) = (-3u + 10 - 3u^{-1})$. Here, $K(u) = (3 - u)(3 - u^{-1})$ is reducible. By the argument above, up to translation and reflection in the z direction, the only suitable boson is $x(u) = 3 - u$. The braiding statistic of $y = \sum_k y_k e_k$ with x is the constant term of

$$x^\dagger(u)K(u)^{-1}y(u) = \frac{y(u)}{3 - u} = \frac{1}{3}y(u) \sum_{k=0}^{\infty} \left(\frac{u}{3}\right)^k. \quad (6.14)$$

If $y_k = 0$ for all $k \leq 0$, then (6.14) has no constant term. This means that half of the elementary planons e_k , $k \geq 1$, are deconfined upon the condensation of x . These planons satisfy the relations

$$-3e_{k+1} + 10e_k - 3e_{k-1} = 0 \quad (6.15)$$

imposed by the K matrix. Moreover, the condensation of x imposes a new relation

$$9e_1 - 3e_2 = 3e_0 - e_1 = 0. \quad (6.16)$$

All other relations of e_k , $k \geq 1$, can be derived from (6.15) and (6.16). For example, it can be shown that $27e_2 - 9e_3 = 0$, $81e_3 - 27e_4 = 0$, etc. Next, to understand what happens to the other half of the elementary planons, I set $y_k = 0$ for all $k \geq 1$. The braiding statistic is then

$$x^T K^{-1} y = \sum_{k=-\infty}^0 3^{k-1} y_k. \quad (6.17)$$

By (6.15) and the condensation of x , the planon

$$3e_{-1} - e_0 = 9e_0 - 3e_1 = 3(3e_0 - e_1) = 0$$

is trivial. Similarly, all planons of the form $3e_{k-1} - e_k$, $k \leq 0$, are trivial. Therefore without loss of generality, I assume that $y_k = 0, 1$ or 2 for all $k \leq 0$. However, with this assumption, the only non-trivial choice of y_k such that (6.17) is an integer is $y_k = 2$ for all $k \leq 0$. This can be seen using numbers in base 3. The excitation y is thus an extended object. The conclusion is that the condensation of x divides the system into two regions. In the region $z \geq 1$, planons remain deconfined but have new relations; in the region $z \leq 0$, there is only an extended excitation left. The highly inhomogeneous system after condensation contradicts the usual expectation of an RG circuit, which should affect the system only near the support region of the circuit. This contradiction can be traced back to the non-local statistics in the CS_∞ theory. In general, there are two possibilities for a gapped CS_∞ theory whose K matrix is of the form (6.12), $c_1 \neq 0$: Either the theory does not have a suitable boson to condense, or it does but the system becomes highly inhomogeneous in the z direction after condensation of a single boson. Therefore, new notions of phases need to be invented in order to classify CS_∞ theories into fractonic orders.

BIBLIOGRAPHY

- [1] L. Néel, “Magnetic properties of magnetite and titanomagnetite: Curie temperature and magnetic moment determinations”, *J. Geophys. Res.* **68**, 4545 (1963).
- [2] K. G. Wilson, “Renormalization group and critical phenomena. I. Renormalization group and the Kadanoff scaling picture”, *Phys. Rev. B* **4**, 3174 (1971).
- [3] A. Carosso, A. Hasenfratz, and E. T. Neil, “Renormalization group properties of scalar field theory using gradient flow”, arXiv:1811.03182.
- [4] C. Chamon, “Quantum glassiness in strongly correlated clean systems: An example of topological overprotection”, *Phys. Rev. Lett.* **94**, 040402 (2005).
- [5] S. Bravyi, B. Leemhuis, and B. M. Terhal, “Topological order in an exactly solvable 3D spin model”, *Ann. Phys. (N. Y.)* **326**, 839 (2011).
- [6] J. Haah, “Local stabilizer codes in three dimensions without string logical operators”, *Phys. Rev. A* **83**, 042330 (2011).
- [7] J. Haah, “Commuting Pauli Hamiltonians as maps between free modules”, *Commun. Math. Phys.* **324**, 351 (2013).
- [8] F. J. Wegner, “Duality in generalized Ising models and phase transitions without local order parameters”, *J. Math. Phys.* **12**, 2259 (1971).
- [9] S. Vijay, J. Haah, and L. Fu, “Fracton topological order, generalized lattice gauge theory, and duality”, *Phys. Rev. B* **94**, 235157 (2016).
- [10] W. Shirley, K. Slagle, and X. Chen, “Foliated fracton order from gauging subsystem symmetries”, *SciPost Phys.* **6**, 041 (2019).
- [11] T. Devakul, W. Shirley, and J. Wang, “Strong planar subsystem symmetry-protected topological phases and their dual fracton orders”, *Phys. Rev. Res.* **2**, 012059 (2020).
- [12] M. Pretko, “Subdimensional particle structure of higher rank $U(1)$ spin liquids”, *Phys. Rev. B* **95**, 115139 (2017).
- [13] M. Pretko, “Generalized electromagnetism of subdimensional particles: A spin liquid story”, *Phys. Rev. B* **96**, 035119 (2017).
- [14] D. Bulmash and M. Barkeshli, “Higgs mechanism in higher-rank symmetric $U(1)$ gauge theories”, *Phys. Rev. B* **97**, 235112 (2018).
- [15] H. Ma, M. Hermele, and X. Chen, “Fracton topological order from the Higgs and partial-confinement mechanisms of rank-two gauge theory”, *Phys. Rev. B* **98**, 035111 (2018).
- [16] H. Ma, E. Lake, X. Chen, and M. Hermele, “Fracton topological order via coupled layers”, *Phys. Rev. B* **95**, 245126 (2017).
- [17] A. Prem, S.-J. Huang, H. Song, and M. Hermele, “Cage-net fracton models”, *Phys. Rev. X* **9**, 021010 (2019).

- [18] D. Aasen, D. Bulmash, A. Prem, K. Slagle, and D. J. Williamson, “Topological defect networks for fractons of all types”, *Phys. Rev. Res.* **2**, 043165 (2020).
- [19] W. Shirley, K. Slagle, Z. Wang, and X. Chen, “Fracton models on general three-dimensional manifolds”, *Phys. Rev. X* **8**, 031051 (2018).
- [20] G. Vidal, “Entanglement renormalization”, *Phys. Rev. Lett.* **99**, 220405 (2007).
- [21] W. Shirley, K. Slagle, and X. Chen, “Fractional excitations in foliated fracton phases”, *Ann. Phys. (N. Y.)* **410**, 167922 (2019).
- [22] T. Wang, W. Shirley, and X. Chen, “Foliated fracton order in the Majorana checkerboard model”, *Phys. Rev. B* **100**, 085127 (2019).
- [23] W. Shirley, K. Slagle, and X. Chen, “Foliated fracton order in the checkerboard model”, *Phys. Rev. B* **99**, 115123 (2019).
- [24] W. Shirley, K. Slagle, and X. Chen, “Twisted foliated fracton phases”, *Phys. Rev. B* **102**, 115103 (2020).
- [25] E. Witten, “Quantum field theory and the Jones polynomial”, *Commun. Math. Phys.* **121**, 351 (1989).
- [26] X. Chen, H. T. Lam, and X. Ma, “Ground state degeneracy of infinite-component Chern-Simons-Maxwell theories”, arXiv:2306.00291,
- [27] C. Wall, “Quadratic forms on finite groups, and related topics”, *Topology* **2**, 281 (1963).
- [28] X. Ma, W. Shirley, M. Cheng, M. Levin, J. McGreevy, and X. Chen, “Fractonic order in infinite-component Chern-Simons gauge theories”, *Phys. Rev. B* **105**, 195124 (2022),
- [29] X. Chen, H. T. Lam, and X. Ma, “Gapless infinite-component Chern-Simons-Maxwell theories”, arXiv:2211.10458,
- [30] X. Ma, A. Malladi, Z. Wang, Z. Wang, and X. Chen, “Ground state degeneracy of the Ising cage-net model”, *Phys. Rev. B* **107**, 085123 (2023),
- [31] Z. Wang, X. Ma, D. T. Stephen, M. Hermele, and X. Chen, “Renormalization of Ising cage-net model and generalized foliation”, arXiv:2301.00103,
- [32] X.-G. Wen, “Topological orders in rigid states”, *Int. J. Mod. Phys. B* **04**, 239 (1990).
- [33] R. C. Daileda, “Algebraic integers on the unit circle”, *J. Number Theory* **118**, 189 (2006).
- [34] L. Kronecker, “Zwei Sätze über Gleichungen mit ganzzahligen Coefficienten.”, *J. Reine Angew. Math.* **1857**, 173 (1857).
- [35] P. Cohn, *Classic algebra* (Wiley, 2000).
- [36] A. Polyakov, “Quark confinement and topology of gauge theories”, *Nucl. Phys. B* **120**, 429 (1977).
- [37] X.-G. Wen and A. Zee, “Tunneling in double-layered quantum Hall systems”, *Phys. Rev. B* **47**, 2265 (1993).

- [38] A. Kitaev, “Anyons in an exactly solved model and beyond”, Ann. Phys. (N. Y.) **321**, January Special Issue, 2 (2006).
- [39] L. Wang and Z. Wang, “In and around abelian anyon models”, J. Phys. A **53**, 505203 (2020).
- [40] X. Qiu, R. Joynt, and A. MacDonald, “Phases of the multiple quantum well in a strong magnetic field: Possibility of irrational charge”, Phys. Rev. B **40**, 11943 (1989).
- [41] X. Qiu, R. Joynt, and A. H. MacDonald, “Phase transitions in a multiple quantum well in strong magnetic fields”, Phys. Rev. B **42**, 1339 (1990).
- [42] J. D. Naud, L. P. Pryadko, and S. L. Sondhi, “Fractional quantum Hall effect in infinite-layer systems”, Phys. Rev. Lett. **85**, 5408 (2000).
- [43] J. Naud, L. P. Pryadko, and S. Sondhi, “Notes on infinite layer quantum Hall systems”, Nucl. Phys. B **594**, 713 (2001).
- [44] T. Farrelly, “A review of quantum cellular automata”, Quantum **4**, 368 (2020).
- [45] V. Kalmeyer and R. B. Laughlin, “Equivalence of the resonating-valence-bond and fractional quantum Hall states”, Phys. Rev. Lett. **59**, 2095 (1987).
- [46] M. B. Hastings and X.-G. Wen, “Quasiadiabatic continuation of quantum states: The stability of topological ground-state degeneracy and emergent gauge invariance”, Phys. Rev. B **72**, 045141 (2005).
- [47] J. Sullivan, A. Dua, and M. Cheng, “Fractonic topological phases from coupled wires”, Phys. Rev. Res. **3**, 023123 (2021).
- [48] J. Sullivan, A. Dua, and M. Cheng, “Weak symmetry breaking and topological order in a 3D compressible quantum liquid”, arXiv:2109.13267.
- [49] A. H. MacDonald, “Staging transitions in multiple-quantum-well systems”, Phys. Rev. B **37**, 4792 (1988).
- [50] D. Gaiotto, A. Kapustin, N. Seiberg, and B. Willett, “Generalized global symmetries”, J. High Energy Phys. **2015** (2015).
- [51] X.-G. Wen, “Classifying gauge anomalies through symmetry-protected trivial orders and classifying gravitational anomalies through topological orders”, Phys. Rev. D **88**, 045013 (2013).
- [52] M. Abramowitz and I. Stegun, *Handbook of mathematical functions, with formulas, graphs, and mathematical tables* (Dover, 1965).
- [53] C. Knapp, M. Zaletel, D. E. Liu, M. Cheng, P. Bonderson, and C. Nayak, “The nature and correction of diabatic errors in anyon braiding”, Phys. Rev. X **6**, 041003 (2016).
- [54] M. A. Levin and X.-G. Wen, “String-net condensation: A physical mechanism for topological phases”, Phys. Rev. B **71**, 045110 (2005).
- [55] D. A. Ivanov, “Non-abelian statistics of half-quantum vortices in p -wave superconductors”, Phys. Rev. Lett. **86**, 268 (2001).

- [56] P. H. Bonderson, *Non-abelian anyons and interferometry* (California Institute of Technology, 2012).
- [57] F. J. Burnell, S. H. Simon, and J. K. Slingerland, “Phase transitions in topological lattice models via topological symmetry breaking”, *New J. Phys.* **14**, 015004 (2012).
- [58] A. Kitaev, “Fault-tolerant quantum computation by anyons”, *Ann. Phys. (N. Y.)* **303**, 2 (2003).
- [59] A. Davydov, M. Müger, D. Nikshych, and V. Ostrik, “The Witt group of non-degenerate braided fusion categories”, *J. Reine Angew. Math.* **2013**, 135 (2013).
- [60] D. R. Farenick, *Algebras of linear transformations* (Springer, 2000).
- [61] R. A. Horn and C. R. Johnson, *Matrix analysis*, 2nd ed. (Cambridge University Press, 2012).
- [62] Y.-J. Liu, K. Shtengel, A. Smith, and F. Pollmann, “Methods for simulating string-net states and anyons on a digital quantum computer”, *PRX Quantum* **3**, 040315 (2022).
- [63] A. Vadali, Z. Wang, A. Dua, and X. Chen, “Partial condensation and decoration of sub-dimensional excitation”, work in progress.